

1-1-2002

Composite pipe material from PET and coal combustion products

Eric Andrew Hackbarth
Iowa State University

Follow this and additional works at: <https://lib.dr.iastate.edu/rtd>

Recommended Citation

Hackbarth, Eric Andrew, "Composite pipe material from PET and coal combustion products" (2002).
Retrospective Theses and Dissertations. 19866.
<https://lib.dr.iastate.edu/rtd/19866>

This Thesis is brought to you for free and open access by the Iowa State University Capstones, Theses and Dissertations at Iowa State University Digital Repository. It has been accepted for inclusion in Retrospective Theses and Dissertations by an authorized administrator of Iowa State University Digital Repository. For more information, please contact digirep@iastate.edu.

Composite pipe material from PET and coal combustion products

by

Eric Andrew Hackbarth

A thesis submitted to the graduate faculty
in partial fulfillment of the requirements for the degree of
MASTER OF SCIENCE

Major: Civil Engineering
(Civil Engineering Materials)

Program of Study Committee:
David J. White Major Professor
Say K. Ong
Joshua U. Otaigbe

Iowa State University

Ames, Iowa

2002

Copyright © Eric Andrew Hackbarth, 2002. All rights reserved.

Graduate College
Iowa State University

This is to certify that the master's thesis of
Eric Andrew Hackbarth
has met the thesis requirements of Iowa State University

Signatures have been redacted for privacy

TABLE OF CONTENTS

	Page
TABLE OF CONTENTS	iii
LIST OF FIGURES.....	vi
LIST OF TABLES	xii
ACKNOWLEDGEMENTS.....	xiv
ABSTRACT	xv
1 INTRODUCTION.....	1
1.1 Research Program.....	1
1.1.1 Objectives.....	1
1.1.2 Scope.....	2
1.2 Background	2
2 LITERATURE REVIEW	4
2.1 Municipal Solid Waste.....	4
2.2 Plastics	5
2.2.1 PET	5
2.2.2 PET recycling process.....	8
2.2.2.1 PVC contamination.....	9
2.3 Coal Combustion Byproducts	9
2.4 Fiberglass Fibers.....	12
2.5 Polymer Concrete	12
2.5.1 Filler materials.....	13
2.5.2 Polymer binders	15
2.5.3 Polymer concrete processing.....	16
2.5.4 Properties and applications.....	17
2.6 Composite Material from Fly Ash and Recycled Plastics	20
2.6.1 Masonry blocks.....	20
2.6.2 Recycled PET and fly ash in PC.....	21
2.7 Pipes.....	22
2.7.1 Thermoplastic pipe	23

2.7.2	Vitrified clay pipes.....	24
2.7.3	Concrete pipes	25
2.7.3.1	Sulfuric acid attack.....	27
3	EXPERIMENTAL PROCEDURE	29
3.1	Materials	29
3.1.1	Plastic material	29
3.1.2	Filler material	32
3.1.3	Fiberglass fibers.....	36
3.2	Cylinder Specimen Process.....	37
3.2.1	Manufacturing process.....	37
3.2.2	Compressive testing process	40
3.2.3	Splitting tensile test.....	41
3.3	Pipe Specimens.....	44
3.3.1	Manufacturing process.....	44
3.3.2	Testing process	50
3.4	Durability tests	53
3.4.1	Water absorption procedure	53
3.4.2	Acid resistance procedure	54
4	RESULTS	55
4.1	Cylinder Specimens.....	55
4.1.1	Statistical analysis of results.....	55
4.1.2	Compressive strength.....	56
4.1.3	Splitting tensile strength.....	64
4.2	Pipe Specimens.....	72
4.2.1	Ultimate 3-edge bearing strength.....	72
4.2.2	Microstructural observations	80
4.3	Durability Tests	83
4.3.1	Water absorption tests.....	83
4.3.2	Acid tests.....	85
4.4	Viscosity Observation.....	87

5	CONCLUSIONS.....	88
6	RECOMMENDATIONS.....	89
	APPENDIX A: MATERIAL DATA	90
	APPENDIX B: CYLINDER SPECIMEN DATA.....	97
	APPENDIX C: PIPE SPECIMEN DATA	122
	APPENDIX D: DURABILITY DATA.....	142
	REFERENCES	149

LIST OF FIGURES

	Page
Figure 2.1 Reaction of terephthalic acid and ethylene glycol to form PET	7
Figure 2.2 Ames fly ash and ISU CFB bottom ash	10
Figure 2.3 Leading Fly Ash Uses	11
Figure 2.4 Leading bottom ash uses	12
Figure 2.5 Classification of polymer binders	15
Figure 2.6 Change in strength with temperature	18
Figure 2.7 Change in modulus with temperature	19
Figure 2.8 Concrete corrosion of the inner surface of the sewage conduit due to the activities of sulfur oxidizing bacteria	28
Figure 3.1 Three experimental PET processing levels	30
Figure 3.2 First stage in reducing the volume of PET from curbside recycling programs	31
Figure 3.3 Chipper shredder	31
Figure 3.5 6 mm and 13 mm fiberglass fibers	36
Figure 3.6 (a) Composite flowing into mold, (b) cylinder specimens cooled	39
Figure 3.7 Compression test for cylinder specimens	41
Figure 3.8 (a) Splitting tension test setup, (b) specimen failing	44
Figure 3.9 Preheating molds in oven.....	45
Figure 3.10 Electric melting pot used to melt PET.....	46
Figure 3.11 Melted composite material.....	46
Figure 3.12 Melted composite material with fiberglass	47
Figure 3.13 Centering the pipe with the wooden spacers.....	48
Figure 3.14 (a) Pipe specimens cooling, (b) pipe specimen.....	50
Figure 3.15 Pipe testing.....	52
Figure 4.1 Cylinder specimens' compressive strength vs. filler material plot for different filler materials with, 13 mm long fiberglass fibers, 3% fiberglass by weight with 50/50 PET to filler ratio by weight	59

Figure 4.2 Cylinder specimens' compressive strength vs. filler material plot for different filler materials with, 13 mm long fiberglass fibers, 3% fiberglass by weight with 50/50 PET to filler ratio by weight	59
Figure 4.3 Cylinder specimens' compressive strength vs. PET to filler ratio	60
Figure 4.4 Cylinder specimens' compressive strength vs. percentage of 6 mm fiberglass.....	61
Figure 4.5 Cylinder specimens' compressive strength vs. percentage of 13 mm..... fiberglass.....	62
Figure 4.6 Cylinder specimens' compressive strength vs. form of PET.....	63
Figure 4.7 Cylinder specimens' compressive strength vs. maximum particle size plot	64
Figure 4.8 Cylinder specimens' splitting tensile strength vs. filler material plot for different filler materials with, 13 mm long fiberglass fibers, 3% fiberglass by weight with 50/50 PET to filler ratio by weight	66
Figure 4.9 Cylinder specimens' splitting tensile strength vs. filler material plot for different filler materials with, 13 mm long fiberglass fibers, 3% fiberglass by weight with 50/50 PET to filler ratio by weight	66
Figure 4.10 Cylinder specimens' splitting tensile strength vs. PET to filler ratio.....	67
Figure 4.11 Cylinder specimens' splitting tensile strength vs. percentage of 6 mm fiberglass fibers	68
Figure 4.12 Cylinder specimens' splitting tensile strength vs. percentage of 13 mm fiberglass fibers	69
Figure 4.13 Cylinder specimens' splitting tensile strength vs. form of PET.....	70
Figure 4.14 Cylinder specimens' splitting tensile strength vs. maximum particle size	71
Figure 4.15 Composite material with no fiberglass	71
Figure 4.16 Cylinder specimens made from UNI FB with 3% fiberglass by weight tested in splitting tension	72
Figure 4.17 Pipe specimens ultimate 3-edge bearing strength vs. filler material for different filler materials, 13 mm long fiberglass fiber, and 3% fiberglass by weight with 50/50 PET ratio by weight	73

Figure 4.18 Pipe specimens ultimate 3-edge bearing strength vs. filler material for different filler materials, 13 mm long fiberglass fiber, and 3% fiberglass by weight with 50/50 PET ratio by weight	74
Figure 4.19 Pipe specimens ultimate 3-edge bearing strength vs. PET to filler ratio.....	75
Figure 4.20 Pipe specimen #18 with 4% fiberglass content.....	76
Figure 4.21 Pipe specimens ultimate 3-edge bearing strength vs. percent of fiberglass.....	76
Figure 4.22 Pipe specimens ultimate 3-edge bearing strength vs. form of PET.....	77
Figure 4.23 (a) Ends of pipes expanding due to the moisture in the air, (b) dusting	78
Figure 4.24 Pipe specimens ultimate 3-edge bearing strength vs. maximum particle size.....	79
Figure 4.25 (a) Crushed pipe composite material, (b) pipe made from recycled composite pipe material.....	79
Figure 4.26 Pipe specimens ultimate 3-edge bearing strength vs. recycled material	80
Figure 4.27 Bonding between the fiberglass fibers and the composite.....	81
Figure 4.28 Diagram of pipe failure.....	82
Figure 4.29 Pipe failure plane.....	82
Figure 4.30 ISU CFB bottom ash water absorption.....	83
Figure 4.31 Water absorption test specimens	85
Figure 4.32 Sulfuric acid test.....	86
Figure A.1 Fly ash particle distribution curves.....	91
Figure A.2 Bottom ash particle and UNI fluidized bed ash distribution curves.....	91
Figure A.3 Non-coal combustion byproducts particle distribution curves.....	92
Figure A.4 Particle distribution curves for the three forms of PET.....	92
Figure A.5 X-ray diffractogram and mineral identification for Ames fly ash	93
Figure A.6 X-ray diffractogram and mineral identification for UNI fluidized bed ash.....	93
Figure A.7 X-ray diffractogram and mineral identification for ISU CFB bottom ash	94
Figure A.8 X-ray diffractogram and mineral identification for ISU CFB fly ash.....	94
Figure A.9 X-ray diffractogram and mineral identification for stoker bottom ash	95
Figure A.10 X-ray diffractogram and mineral identification for stoker fly ash	95
Figure A.11 X-ray diffractogram and mineral identification for Sump.....	96

Figure A.12 X-ray diffractogram and mineral identification for Lime.....	96
Figure B.1 Stress vs. strain plot for P.C. fly ash.....	103
Figure B.2 Stress vs. strain plot for UNI fluidized bed ash.....	103
Figure B.3 Stress vs. strain plot for Ames fly ash, 13 mm long fiberglass fibers, no fiberglass, with 50/50 PET to filler ratio by weight.....	104
Figure B.4 Stress vs. strain plot for Ames fly ash	104
Figure B.5 Stress vs. strain plot for Ames fly ash, 13 mm long fiberglass fibers, 3% fiberglass by weight with 45/55 PET to filler ratio by weight.....	105
Figure B.6 Stress vs. strain plot for Ames fly ash, 13 mm long fiberglass fibers, 3% fiberglass by weight with 40/60 PET to filler ratio by weight.....	105
Figure B.7 Stress vs. strain plot for Ames fly ash, 13 mm long fiberglass fibers, 3% fiberglass by weight with 35/65 PET to filler ratio by weight.....	106
Figure B.8 Stress vs. strain plot for Ames fly ash, 13 mm long fiberglass fibers, 1% fiberglass by weight with 50/50 PET to filler ratio by weight.....	106
Figure B.9 Stress vs. strain plot for Ames fly ash, 13 mm long fiberglass fibers, 2% fiberglass by weight with 50/50 PET to filler ratio by weight.....	107
Figure B.10 Stress vs. strain plot for Ames fly ash, 13 mm long fiberglass fibers, 4% fiberglass by weight with 50/50 PET to filler ratio by weight.....	107
Figure B.11 Stress vs. strain plot for ISU CFB fly ash	108
Figure B.12 Stress vs. strain plot for ISU Stoker bottom ash.....	108
Figure B.13 Stress vs. strain plot for Ames fly ash, 6 mm long fiberglass fibers, 3% fiberglass by weight with 50/50 PET to filler ratio by weight.....	109
Figure B.14 Stress vs. Strain plot for Ames fly ash, 6 mm long fiberglass fibers, 4% fiberglass by weight with 50/50 PET to filler ratio by weight.....	109
Figure B.15 Stress vs. strain plot for Ames fly ash, 6 mm long fiberglass fibers, 5% fiberglass by weight with 50/50 PET to filler ratio by weight.....	110
Figure B.16 Stress vs. strain plot for Ames fly ash, 6 mm long fiberglass fibers, 6% fiberglass by weight with 50/50 PET to filler ratio by weight.....	110
Figure B.17 Stress vs. strain plot for Ames fly ash, 13 mm long fiberglass fibers, 3% fiberglass by weight with 50/50 PET to filler ratio by weight, “dirty” PET	111

Figure B.18 Stress vs. strain plot for Ames fly ash, 13 mm long fiberglass fibers, 3% fiberglass by weight with 50/50 PET to filler ratio by weight, “clean” PET	111
Figure B.19 Stress vs. strain plot for PET plastic	112
Figure B.20 Stress vs. strain plot for lime	112
Figure B.21 Stress vs. strain plot for ISU CFB bottom ash, 13 mm long fiberglass fibers, 3% fiberglass by weight with 50/50 PET to filler ratio by weight, maximum particle size 4.75 mm.....	113
Figure B.22 Stress vs. strain plot for ISU CFB bottom ash, 13 mm long fiberglass fibers, 3% fiberglass by weight with 50/50 PET to filler ratio by weight, maximum particle size 0.425 mm.....	113
Figure B.23 Stress vs. strain plot for ISU CFB bottom ash, 13 mm long fiberglass fibers, 3% fiberglass by weight with 50/50 PET to filler ratio by weight, maximum particle size 0.150 mm.....	114
Figure B.24 Stress vs. strain plot for sump.....	114
Figure C.1 Pipe specimen # 3, crushing strength vs. strain.....	125
Figure C.2 Pipe specimen # 4, crushing strength vs. strain.....	125
Figure C.3 Pipe specimen # 5, crushing strength vs. strain.....	126
Figure C.4 Pipe specimen # 6, crushing strength vs. strain.....	126
Figure C.5 Pipe specimen # 7, crushing strength vs. strain.....	127
Figure C.6 Pipe specimen # 8, crushing strength vs. strain.....	127
Figure C.7 Pipe specimen # 9, crushing strength vs. strain.....	128
Figure C.8 Pipe specimen # 11, crushing strength vs. strain.....	128
Figure C.9 Pipe specimen # 12, crushing strength vs. strain.....	129
Figure C.10 Pipe specimen # 13, crushing strength vs. strain.....	129
Figure C.11 Pipe specimen # 14, crushing strength vs. strain.....	130
Figure C.12 Pipe specimen # 15, crushing strength vs. strain.....	130
Figure C.13 Pipe specimen # 16, crushing strength vs. strain.....	131
Figure C.14 Pipe specimen # 17, crushing strength vs. strain.....	131
Figure C.15 Pipe specimen # 18, crushing strength vs. strain.....	132
Figure C.16 Pipe specimen # 19, crushing strength vs. strain.....	132

Figure C.17 Pipe specimen # 20, crushing strength vs. strain.....	133
Figure C.18 Pipe specimen # 21, crushing strength vs. strain.....	133
Figure C.19 Pipe specimen # 22, crushing strength vs. strain.....	134
Figure C.20 Pipe specimen # 23, crushing strength vs. strain.....	134
Figure C.21 Pipe specimen # 24, crushing strength vs. strain.....	135
Figure C.22 Pipe specimen # 25, crushing strength vs. strain.....	135
Figure C.23 Pipe specimen # 26 crushing strength vs. strain.....	136
Figure C.24 Pipe specimen # 27 crushing strength vs. strain.....	136
Figure C.25 Pipe specimen # 28 crushing strength vs. strain.....	137
Figure C.26 Pipe specimen # 30 crushing strength vs. strain.....	137
Figure C.27 Piston and inner collapsible mold.....	138
Figure C.28 Outer mold and bottom plate.....	139
Figure C.29 Mold setup.....	140
Figure C.30 Upper and lower bearing strips.....	141

LIST OF TABLES

	Page
Table 2.1 SPI. Voluntary Plastic Container Coding System	6
Table 2.2 Fly Ash Classification Chemical Requirements	10
Table 2.3 Comparison of properties of concretes made with varying binders	19
Table 2.4 Summary of characteristics and applications of polymer concrete	20
Table 2.5 Composition of non-recycled mixed plastic	21
Table 2.6 Common additives in plastic piping material	23
Table 2.7 Common thermoplastic properties and applications	24
Table 2.8 Minimum three-edge bearing strengths for vitrified clay pipe	25
Table 2.9 Nonreinforced concrete pipe requirements	26
Table 2.10 D-load requirements	27
Table 2.11 Reinforce concrete pipe design strength requirements	27
Table 3.1 Chemical analyses of the filler materials by XRF.....	35
Table 3.2 Specific gravity of filler materials.....	36
Table 4.1 Cylinder design mixes with average elastic modulus values.....	57
Table 4.2 Statistical significance between compressive strengths for different fillers.....	58
Table 4.3 Statistical significance between compressive strengths for different fillers.....	65
Table 4.4 Water absorption results.....	84
Table 4.5 Summary of acid test results	86
Table B.1 Cylinder specimen design mixes	98
Table B.2 Cylinder compressive strength data	99
Table B.3 Cylinder splitting tensile strength data.....	115
Table B.4 Treatments for the statistical analysis	118
Table B.5 Statistics results for filler material.....	119
Table B.6 Statistics results for PET to filler ratio	120
Table B.7 Statistics results for form of PET.....	120
Table B.8 Statistics results for length of fiberglass fibers.....	120
Table B.9 Statistics results for percentage of 6 mm fiberglass fibers.....	120
Table B.10 Statistics results for percentage of 13 mm fiberglass fibers.....	121

Table B.11 Statistics results for largest particle size.....	121
Table C.1 Pipe specimen design mixes.....	123
Table C.2 Pipe specimen dimensions.....	124
Table D.1 Water Absorption data.....	143
Table D.2 Specimen dimensions prior to acid tests.....	144
Table D.3 Acid test results for week 1.....	145
Table D.4 Acid test results for week 3.....	146
Table D.5 Acid test results for week 5.....	147
Table D.6 Acid test results for week 7.....	148

ACKNOWLEDGEMENTS

I would like to thank my major professor Dr. David White for the assistance and guidance he has provided throughout my graduate career at Iowa State University, and also for the opportunity to work on this project.

I would also like to thank Dr. Say K. Ong, and Dr. Joshua Otaigbe for being on my research committee and for guidance throughout my master's degree.

The author would like to express his deepest appreciation and gratitude to Sara Somsy, Jeff Hoffman, Zach Thomas, Tyson Rupnow, Ken Hoevelkamp, and Jake Bigelow for their help in preparing specimens. Without their help I would not have been able to manufacture pipe specimens. I would also like to thank Sara for the Auto CAD drawings. Thanks should be given to Dave White and Angie Campbell for help in proof reading the report.

Thanks are extended to the various facilities, companies, and employees who donated materials, equipment, and time to the project, particularly Doug Wood, Scott Schlorholz, and Don Davidson.

Finally, I thank my family for their encouragement, support, and love throughout my pursuit of my master's degree.

ABSTRACT

A pipe specimen was manufactured from a new composite material utilizing postconsumer polyethylene terephthalate (PET) and coal combustion byproducts. The primary objectives of this research were to determine engineering properties and durability of the composite material, and then manufacture a pipe specimen. Engineering properties determined include compressive and splitting tensile strengths, elastic modulus, and ultimate three-edge bearing strength. Tests were conducted to determine the influence of filler type, PET to filler ratio, fiber content, form of PET, and maximum filler particle size. Water absorption and sulfuric acid durability tests were also conducted.

Results indicate engineering properties of the composite material engineering properties were greatly affected by the processing technique. The compressive and tensile strengths were slightly greater than ordinary Portland cement concrete, while the elastic modulus was 7 to 10 times lower. Increasing the filler content increased compressive and splitting tensile strengths. Results also showed that fiberglass fibers increased strength and resist the propagation of shrinkage cracks. Twenty-three of the 26 pipe specimens exhibited greater ultimate 3-edge bearing strengths than are required by ASTM for the 200 and 250 mm diameter vitrified extra strength clay pipes and all classes of nonreinforced concrete pipes.

Further research should focus on developing better processing techniques to produce composite specimens. Further investigation should also be conducted on the influence that filler chemistry has on the durability of the composite material.

1 INTRODUCTION

The purpose of this investigation is to research and develop engineering parameters values for a new pipe product made from composite material consisting of coal combustion byproducts and polyethylene terephthalate (PET) beverage bottles. Use of this material is advantageous because of the environmental benefits from using waste products. The objectives and scope for this investigation along with background information for this research will be discussed in this chapter.

1.1 Research Program

1.1.1 Objectives

The objectives of this research are:

- 1) To determine engineering properties of the composite material;
- 2) To determine the influence of maximum particle size on the composite properties;
- 3) To determine the influence of different filler materials on the composite properties;
- 4) To determine the influence of PET to filler ratio on the composite properties;
- 5) To determine the influence of fiberglass fibers on the composite properties;
- 6) To determine the influence of different forms of PET on the composite properties;
- 7) To evaluate the durability of composite materials; and
- 8) To manufacture a composite pipe specimen and compare engineering properties with other conventional pipes.

1.1.2 Scope

The scope of this research is:

- 1) Manufacture several composite cylinder specimens by varying the type of filler, PET to filler ratio, fiberglass fiber content, form of PET, and maximum particle size;
- 2) Test composite cylinder specimens in axial compression and split cylinder tension;
- 3) Manufacture disc specimens from composite cylinder specimens for durability testing;
- 4) Test the water absorption and sulfuric acid resistance of the disc specimens;
- 5) Manufacture composite pipe specimens with the same wide range of composite mixtures used to produce the cylinder specimens;
- 6) Test pipe specimens for ultimate three-edge bearing strength; and

1.2 Background

The objectives of this research program stem from a previous feasibility studies conducted by White [1, 2]. This work showed that ASTM Class C and Class F fly ash could be combined with postconsumer polyethylene terephthalate (PET) to produce a value-added composite material. The primary focus of the research was concerned with the physio-mechanical properties and microstructure features of the composite material.

The major conclusions of this feasibility research are:

- Fly ash filler increases crystallinity in the PET;
- Compressive strength increased with added fly ash content;
- Compressive strength is 3 to 4 times that of ordinary Portland cement concrete;
- Tensile strengths for the composite varied from 3 to 7 MPa for fly ash contents ranging from 0 to 70 percent with optimum strength at 50 percent;
- Elastic modulus values are 10 times less than ordinary Portland cement concrete;
- Density ranged from 1.28 to 2.03 g/cm³ for fly ash contents of 0 to 70 percent;
- Water absorption values varied from 0 to 0.9%; and
- Future research will focus on real world applications for the composite such as manufacturing a pipe specimen.

2 LITERATURE REVIEW

The purpose of this literature review is to review important subjects related to the composite material. Subjects in order of presentation include: municipal solid waste; plastics; coal combustion byproducts; fiberglass fibers; polymer concrete; fly ash and RPET composites; and pipes.

2.1 Municipal Solid Waste

Managing the generation and disposal of municipal solid waste (MSW) is a problem that society has been facing for many years. The latest annual report by the Environmental Protection Agency (EPA) reported that approximately 209 million metric tons of MSW was generated in the United States in 1999 [3]. This problem will become more evident as population increases and landfill space becomes more scarce. In the eleven-year period from 1988 to 1999, the number of landfills decreased from 7,924 to 2,216, while the average landfill size increased [3]. Society is turning to different means to reduce the amount of MSW disposed in landfills. EPA suggests the following components to reduce MSW, listed in order of preference: (1) source reduction; (2) recycling; and (3) combustion. Out of approximately 209 million metric tons of MSW generated in 1999, 28 percent was recovered, 15 percent was combusted, and 57 percent was disposed of in landfills [3]. The total amount of plastic waste generated in 1999 was 22.2 million metric tons, of which only 1.3 million metric tons was recovered [3].

2.2 Plastics

There are two generic types of plastics: thermoplastics and thermosets. They differ by the physical changes that occur when they are subjected to heating and cooling. The most common generic type is thermoplastics, which is defined as materials that (1) become soft or “plastic” when heated, (2) are molded or shaped with pressure when in the plastic state, and (3) solidify when cooled to retain the mold or shape [4]. This process is reversible and can be repeated since no chemical change occurs. However, repeated heating will eventually cause decomposition of the polymer [4].

The second generic type is thermosets, which is defined as materials that can be softened, molded, and then hardened or “set” when heated once [4]. When reheated, thermosets decompose because they are infusible solids [4]. Unlike thermoplastics, when thermosets harden, an irreversible chemical reaction occurs which is known as cross-linking [4, 5].









Although different types of plastic materials look very similar to each other, they have significantly different properties. In order to help separate the plastics by type, several identification systems have been created [4]. One of these systems is called the Society for the Plastics Industry Voluntary Plastic Container Coding System. Its resin identification includes seven different classifications and codes, which are presented in Table 2.1.

2.2.1 PET

Polyethylene terephthalic (PET) thermoplastic is given the resin code #1. PET is a popular polymer used to package food and non-food products since it is inexpensive, lightweight, shatter resistant, and recyclable. Plastic beverage bottles are constructed from

PET. PET is produced from a solution of terephthalic acid or dimethyl terephthalate and ethylene glycol [4]. This solution is heated, typically with an antimony catalyst [4], and then water or methanol is removed. Figure 2.1 shows the equation for the reaction of terephthalic acid and ethylene glycol.

Table 2.1 SPI. Voluntary Plastic Container Coding System [6]

Full Name	Typical Consumer Products	Resin Code
PET Polyethylene Terephthalate	Bottles: soft drink, honey, liquor, dish detergent, antacid, cold medicine, some oven-safe food trays, and peanut butter jars.	 PETE
HDPE Natural High Density Polyethylene (without color)	Jugs: milk, cider, distilled water and spring water bottles, juice (not clear), rubbing alcohol, and large vinegar. Grocery bags.	 HDPE
HDPE Natural High Density Colored Polyethylene	Bottles: laundry and dish detergent, fabric softener, saline solution, bleach, motor oil and antifreeze.	 HDPE
PVC Polyvinyl Chloride	Bottles: imported mineral water, salad dressing, salad and vegetable oil, floor polish, mouthwash, liquor, some translucent pharmaceutical bottles, bottle liners and cap coating, blister pack "bubble" for batteries, tile and drainage pipes.	 V
LDPE Low Density Polyethylene	Usually appears in flexible film bags for dry cleaning, bread, produce, trash, etc.; also some rigid items such as food storage containers and flexible lids, coating, and recycling bins.	 LDPE
PP Polypropylene	Battery cases, medical containers; oil additive containers, some dairy tubs; cereal box liners; bottle caps; rope and strapping; combs; snack wraps; bags; some yogurt cups and lids for containers (those that do not crack easily when bent).	 PP
PS & HIPS Polystyrene & High Impact PS	Some yogurt cups and tubs, cookie and muffin trays, clear carry-out containers, vitamin bottles, most fast food cutlery, waste baskets, and audio cassette tapes.	 PS
Other Various Items	Plastics other than the six most common or made of multiple layered resins, blends, or different parts (i.e., water cooler bottles, microwavable serving ware, most snack bags, and squeezable bottles for condiments, etc.)	 OTHER

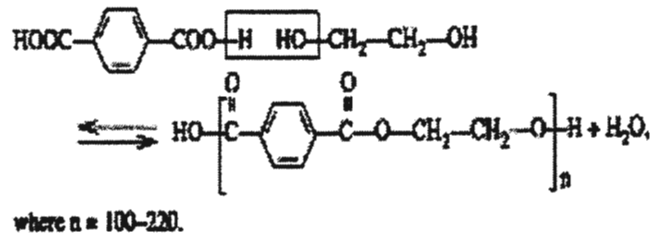


Figure 2.1 Reaction of terephthalic acid and ethylene glycol to form PET [4]

PET has been used as a material to make soft drink bottles since 1977 [4]. Recycling PET began shortly after its introduction due to state laws requiring deposits on beverage containers [4]. Now PET bottles are collected by local curbside recycling programs across the nation. According to the National Association for Plastic Container Recovery (NAPCOR) the total number of pounds of PET bottles and jars available for recycling in the U.S. for the year of 2000 was 3.445 billion [7]. NAPCOR also estimated that the total amount of PET bottles that were recycled and sold in the U.S. was 769 million pounds in 2000 [7]. This produces a gross recycling rate of 22.3% for PET bottles. Recycled polyethylene terephthalate (RPET) is currently being used as material to make fiber for polyester carpet; fabric for clothes, shoes, luggage, and upholstery; fiberfill for sleeping bags and winter coats; industrial strapping, sheet and film; automotive parts, such as bumpers, grilles, and door panels; and new PET containers [7].

PET exists in an amorphous or crystalline state [4, 8]. The normal state of PET is the crystalline state [4]. In this state, the molecules are highly organized and form crystallites [4]. Oriented, crystalline state, PET exhibits better mechanical, barrier, and chemical resistant properties than the unoriented, amorphous state [8]. PET has a melt temperature of 260 °C and a transition temperature of 73 °C [4]. Rapid cooling of melted PET resin from its melt temperature to its transition temperature will produce a polymer in the amorphous state,

while slow cooling will produce a polymer in the crystalline state. PET bottles are produced by blow-molding process, which requires rather pure and slow crystallized PET material [9].

During the reprocessing of PET, contaminants that can catalyze the hydrolysis of PET (Figure 2.1 in the reverse direction) need to be removed. Hydrolysis catalysts are acids or bases, which promote hydrolysis at an elevated temperature but below 205 °C [4]. Once hydrolysis occurs, the reaction is autocatalytic. Degradation of the polymer chain leads to the formation of low molecular weight polymers with carboxylic acid end groups. These acids further catalyze hydrolysis [4].

2.2.2 PET recycling process

The reclaiming process for plastic beverage bottles differs between different recycling facilities. The first process in a typical flotation or hydrocyclone process of reclaiming PET is to sort the plastic by type and color. Next, the sorted PET bottles are sent to a shredder and/or a granulator which reduces the material (PET, HDPE, and aluminum) to 3.2 to 9.5 mm flakes [4]. During the size reduction of the PET, most of the labels are freed from the plastic and removed by air classification. The most expensive part of PET bottles recycling process is the removal of aluminum and paper impurities, and green and brown colors [10]. The flakes are then introduced into an agitated washing tank along with a hot non-foaming detergent solution. The number of wash cycles, detergent recipes, temperature, and the solids concentration in the slurry vary between different recycling facilities. After the wash bath, the flakes are rinsed with water to remove residual wash solution, label, and other materials.

Clean material flakes are then introduced into a flotation tank or a hydrocyclone where the heavy material (PET and aluminum) are separated from the lighter material (HDPE). Heavy material is rinsed and sent to be dried first in a spin dryer and then through hot-air dryers. The last process in the reclaiming of PET is to separate the PET from the aluminum with the aid of an electrostatic separator. The final product is a high purity PET flake.

2.2.2.1 PVC contamination

With the many different custom bottles, polyvinyl chloride (PCV) bottles can be mistaken for PET bottles in the separation process when reclaiming [4, 11]. PVC material severely contaminates PET stock. One improperly sorted PVC bottle can ruin a container with 800 pounds (3.5 kN) of PET flake [11]. This is due to the fact that PVC degrades at a lower temperature than the PET melting point [11]. This degradation forms an acid that breaks down the physical and chemical structure of PET [11]. Another problem with PVC contamination is that as little as 1 parts per million (ppm) of PVC in PET can discolor PET [4].

2.3 Coal Combustion Byproducts

The burning of coal to generate electricity produces a variety of inorganic byproducts, including fly ash and bottom ash. In 2000, the American Coal Ash Association [12] estimated 57.1 million metric tons of fly ash and 15.3 million metric tons of bottom ash were produced. Out of this production of byproducts only 31.9% of fly ash and 29.2% of bottom ash was recycled [12]. The majority of the byproducts end up in sluice ponds or landfills.

Fly ash has a powdery appearance and its particles are spherical in shape. Bottom ash is coarse in appearance. Figure 2.2 shows the contrast in appearance of fly ash and bottom ash. Characteristics of fly ash and bottom ash depend on the type of coal from which they originate and the type of boilers used to burn them.



Figure 2.2 Ames fly ash and ISU CFB bottom ash (100 g shown)

Currently, fly ash is widely used in Portland cement concrete and is becoming more readily accepted as a material in geotechnical applications. The benefits to adding fly ash to Portland cement concrete are: significant strength gain, improved workability, reduced bleeding, reduces heat of hydration, reduced permeability, increased resistance to sulfate attack, increased resistance to alkali-silica reactivity, and lowers cost [13]. American Society for Testing and Materials (ASTM) C 618 [14] classifies fly ash materials that are used as mineral admixtures in concrete. ASTM's chemical requirements for the three classifications can be seen in Table 2.2.

Table 2.2 Fly Ash Classification Chemical Requirements [14]

	Mineral Admixture Class		
	N	F	C
Silicon dioxide (SiO ₂) plus aluminum oxide (Al ₂ O ₃) plus iron oxide (Fe ₂ O ₃) min, %	70	70	50
Sulfur trioxide (SO ₃), max, %	4	5	5
Moisture content, max, %	3	3	3
Loss on ignition, max, %	10	6	6

All these fly ashes have pozzolanic properties. ASTM defines pozzolans as: a siliceous or siliceous and aluminous material which in itself possesses little or no cementitious value but will, in finely divided form and in the presence of moisture, chemically react with calcium hydroxide at ordinary temperatures to form compounds possessing cementitious properties [14]. Fly ash with high calcium content has self-cementation characteristics and is being used in soil stabilization. Fly ash is also used as filler in PVC pipes, polymer concrete, and polymer mortar, as well as in plastic parts used in automobiles. Figure 2.3 shows the leading applications for fly ash and Figure 2.4 shows the leading applications for bottom ash. Bottom ash is also used in Portland cement concrete and geotechnical applications but not to the extent of fly ash.

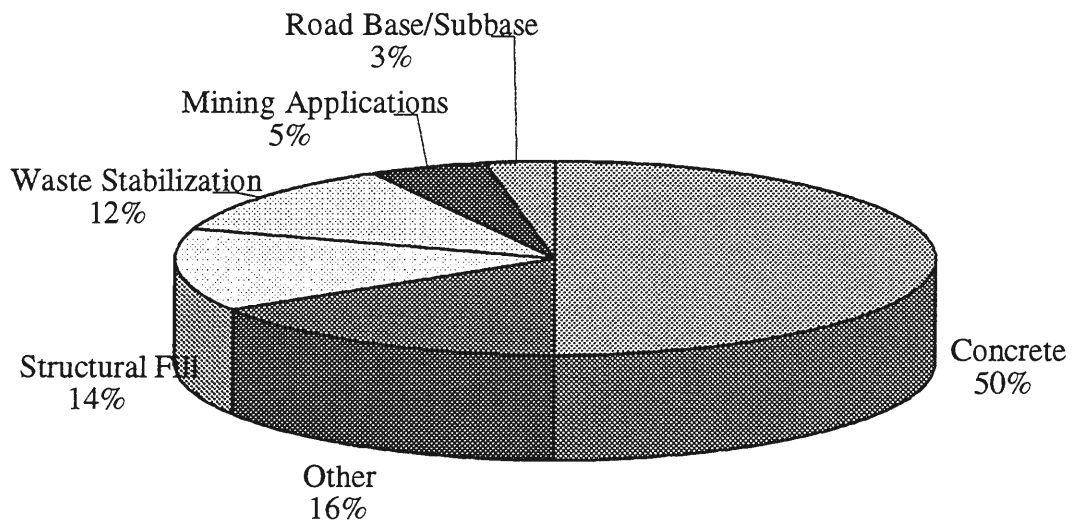


Figure 2.3 Leading Fly Ash Uses [15]

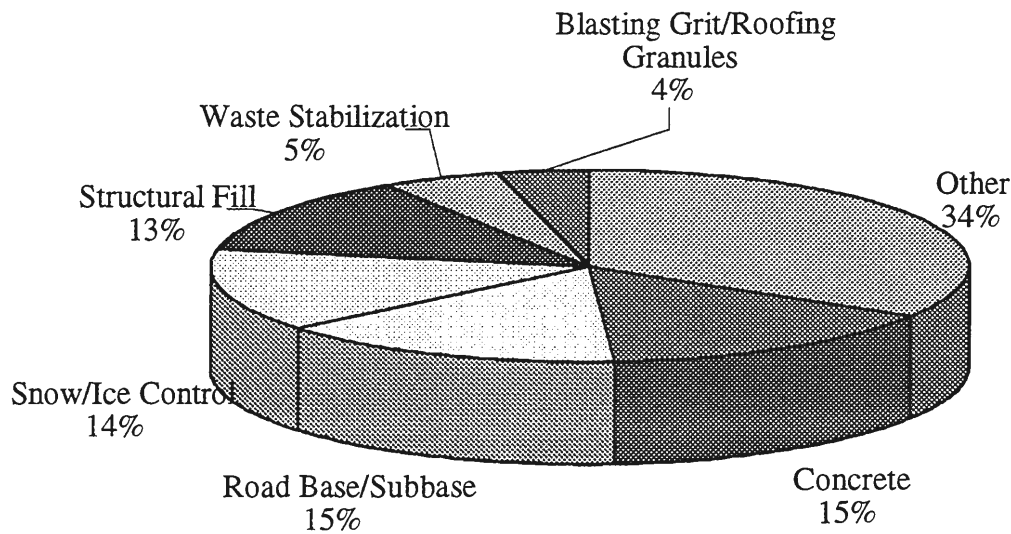


Figure 2.4 Leading bottom ash uses [15]

2.4 Fiberglass Fibers

Fiberglass fibers are added to composites and plastics to improve the engineering properties. Fibers increase tensile and flexural strengths, flexural modulus (stiffness), strength to weight ratio, impact strength (toughness), and temperature range [16]. They also improve creep resistance when loaded and reduce the thermal coefficient of expansion and contraction [16]. The extent to which fiberglass fibers affect composite properties depends on the type of fiber (cross-section and length), fiber content, orientation and interactions at the fiber matrix interface [17].

2.5 Polymer Concrete

Polymers have been used to increase the performance of ordinary Portland cement concrete since the 1920s [18]. Concrete-polymer composites are made by replacing part or all of the cement in conventional concrete or mortar with polymers. Concrete-polymer composites are classified into three processing technologies. The first process is polymer-

modified mortar and concrete. These composites are made by partially replacing and strengthening the cement hydrated binder with polymers. The second process is polymer-impregnated mortar and concrete. These composites are made by forcing polymers into the void spaces of conventional concrete before the composites cure. The third process is polymer mortar (PM) and polymer concrete (PC). Polymer concrete produced with no coarse aggregates is referred to as polymer mortar. In this process the polymer replaces all of the cement in the conventional concrete. The focal point of this literature review will be the third process, PM and PC.

Polymer concrete and polymer mortar are composite materials that are being used in place of Portland cement concrete (PCC). Advantages of PC are that the properties of strength, adhesion, water tightness, chemical resistance, freeze-thaw durability, and abrasion resistance are generally improved to a great extent due to the polymer binder [18]. Disadvantages of PC are its, poor resistance to heat and fire and the fact that its mechanical properties are largely dependent on temperature [18]. Materials used to make PC are similar to the materials used to make Portland cement concrete. The only difference is the binding agent. Portland cement concrete uses Portland cement as the binding agent whereas PC uses polymers to bind the filler materials together. Fillers, which take up the majority of the volume in the composite, are inorganic materials such as coarse aggregates, sand, and fly ash.

2.5.1 Filler materials

Filler materials perform several functions in PC, such as reducing the cost by providing bulk and improving its dimensional stability by reducing shrinkage and thermal expansion [19, 20]. Coarse aggregates (4.75 mm or greater) such as river gravels and

crushed limestone, and fine materials (less than 4.75 mm) such as sands and fly ashes are filler materials used in PC. Filler materials, to a certain extent, prohibit micro-cracks that develop in the composite material. Fly ash is a waste byproduct that is produced from burning coal in power plants. Fly ash improves the workability of fresh composite material due to the spherical shape of the particles [19, 20]. The addition of fly ash gives the mix a better gradation which improves the mechanical properties of the composite.

The mechanical properties of PC can be altered by changing the filler material. Filler materials are selected based upon their strength, soundness, gradation, particle shape, absorption characteristics, and their moisture content. The amount of absorption of the binder has to be kept to a minimum to reduce the cost of the polymer material. Filler materials need low moisture content of less than 0.5% due to the fact that moisture reduces the bonding between the polymer and the aggregates [18]. Size and gradation of the filler are selected depending on the thickness of cover, the type of application, and the type of polymer binder.

Polymer concrete is similar to PCC in that it has significantly low tensile strength compared to its compressive strength [18]. To increase its mechanical properties, reinforcements are typically added. Conventional PCC reinforcements such as mild steel bars, pre-stressed bars, and fiber-reinforced plastic rods are used to reinforce structural members (beams, columns, and roads) [18]. Steel fibers or glass fibers are also used to reinforce the PM and PC [18].

2.5.2 Polymer binders

Polymer binders that are commercially available are thermosetting resins, tar-modified resins, resin-modified asphalts, and vinyl monomers. Figure 2.5 shows the classification of polymer binders.

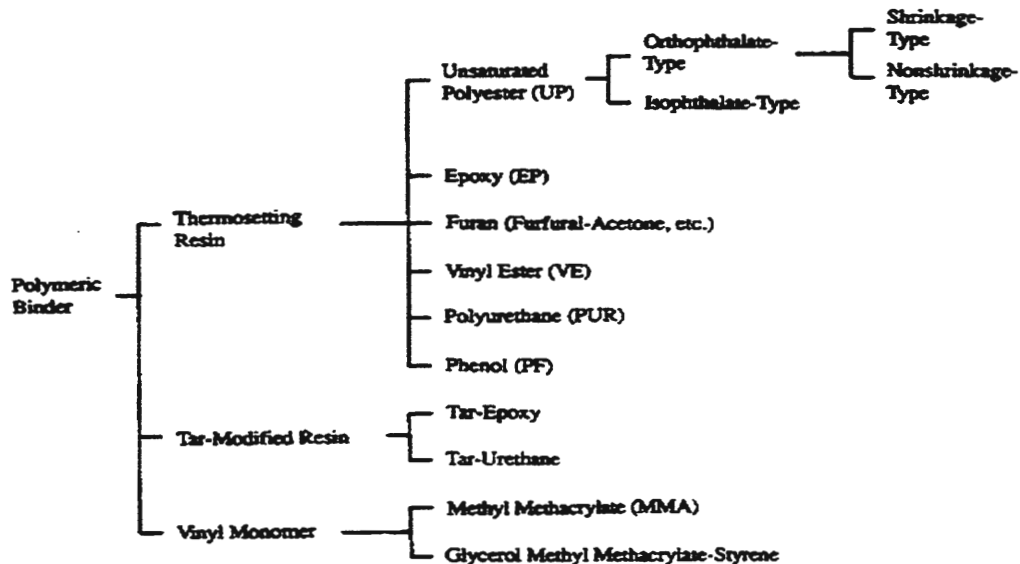


Figure 2.5 Classification of polymer binders [18]

Some thermoplastics are used as binding materials, but usually thermosets are used. Thermosetting polymers are preferred since they do not commonly show a glass transition point and therefore retain their mechanical properties up to the thermal decomposition temperature [18]. Temperature range of PC based thermoplastics can be increased by the addition of cross-linking monomers or co-monomers that have higher glass transition points. Resins that are typically used to make PC are polyester, poly (methyl methacrylate), epoxy, and furan polymer [18].

The amount of polymer used should be kept at a minimum to reduce the cost and to reduce the temperature influence on the mechanical properties. The amount of resin used

ranges between 5 percent to greater than 30 percent depending on the particle size of the filler [18]. The resin in PC ranges from 5 to 15 percent, whereas PM might require more than 30 percent. Polymer mortar has more resin material due to the greater surface area of finer materials.

2.5.3 Polymer concrete processing

The process technology for making PC is similar to that for making conventional PCC. The batching, mixing, and placing techniques are the same for both, but the curing methods are different. Properties of conventional PCC are very sensitive to the curing conditions. Moisture and temperature have to be controlled in order for PCC to cure properly. Polymer concretes are dry-cured at ambient temperatures or may be cured by heating. Curing times for PC last from a span of a few minutes to several hours depending on the temperature and the catalyst system. Curing times for PCC range from between a few days to weeks depending on curing conditions and mixture. PC achieves more than 80% of its final strength in one day whereas normal PCC only achieves 20% of its final strength in one day [21].

Two processing technologies used to make PC and PM are cast-in-place and precast application systems. The term cast-in-place refers to the manufacturing of the composite material on site. The term precast refers to manufacturing products at a manufacturing plant. For precast applications the mix is poured into the mold and then vibrated to reduce air voids. A variety of processing techniques can be used to procure precast application systems. Some of them include casting, centrifugal molding, compression molding, and extrusion molding.

Generally, cast-in-place applications use PM as the material, and precast application systems use PC, since precast is applied to produce large structural members [18].

Polymer concrete is made by mixing a liquid resin, which is the binding agent, with filler materials. Polymeric binders cannot set or harden by themselves; therefore, proper initiators, promoters, or hardeners are added to the mixture. Initiators, promoters (catalysts) or hardeners (cross-linking agents) are selected depending on the working life needed for the fresh mixture. Dried filler material is mixed together prior to the addition of the polymer to produce the desired gradation. Polymer binder is mixed with the initiator, promoter, or hardener at the specified amounts for one to three minutes and then added to the filler mixture. Filler-polymer mixture is mixed for three to five minutes. The mixture is then removed from the mixer, formed into the desired shape, and left to cure.

2.5.4 Properties and applications

When compared to PCC, PC has faster curing time, higher strengths, better chemical resistance, lower permeability, better freeze-thaw durability and better abrasion resistance [18, 10]. Since the PC cures quickly, it can easily be used in pavements and bridges, minimizing the time that the street or bridge has to be closed. PC has greater strength properties than PCC [10, 18]; therefore, it can be placed in a thinner layer while still providing adequate support. Desirable thicknesses of PM overlays are 0.5 to 1 cm, whereas PC thicknesses are generally about 5 to 10 cm [18]. A 0.5 cm coat of PM offers the same strength as a 25 to 50 cm layer of PCC [10, 19]. This also helps in reducing the dead load on structure. Overlaying PCC with PM will protect the PCC because PM acts as a barrier by providing low water and chloride permeabilities, thus providing adequate resistance against

freeze-thaw attack [10]. This will also help protect PCC steel reinforcements from corrosion [10]. PM overlays bond more effectively to PCC than PCC bonds to itself [10].

There are both organic and inorganic components in PC. The organic components are the polymer binders, while the inorganic components consist of stone, sand, and cement. It is well known that organic products have a much lower tolerance to heat than inorganic products; thus, PC cannot be excessively exposed to elevated temperatures. Temperature can have a drastic effect on the properties of the PC. As the temperature increases, the strength of the polymeric binder decreases, and thus the properties deteriorate. Figures 2.6 and 2.7 show the effect that temperature has on the strength and modulus of polymer concrete.

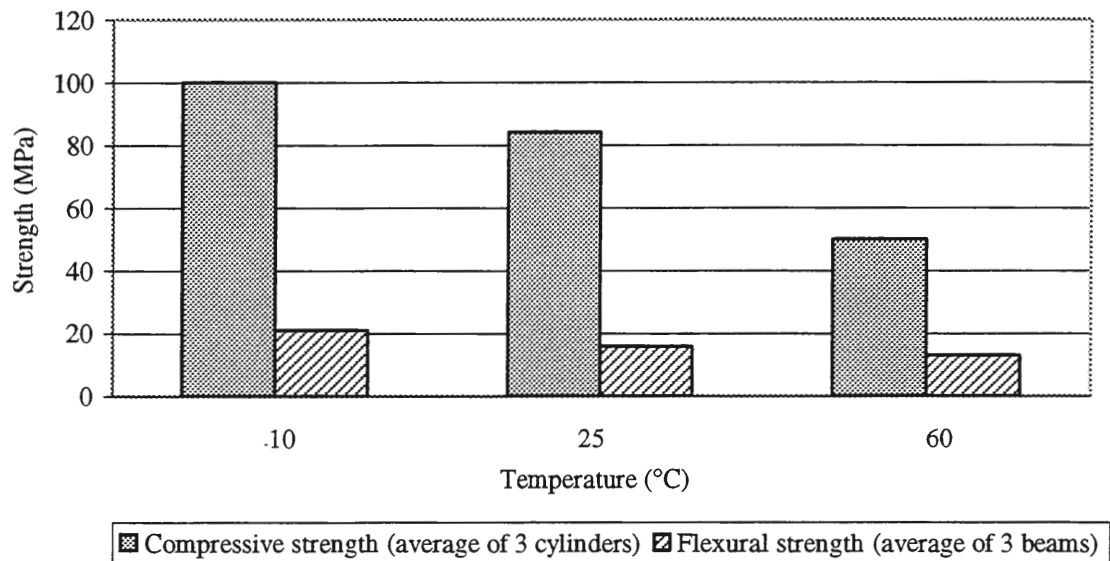


Figure 2.6 Change in strength with temperature [22]

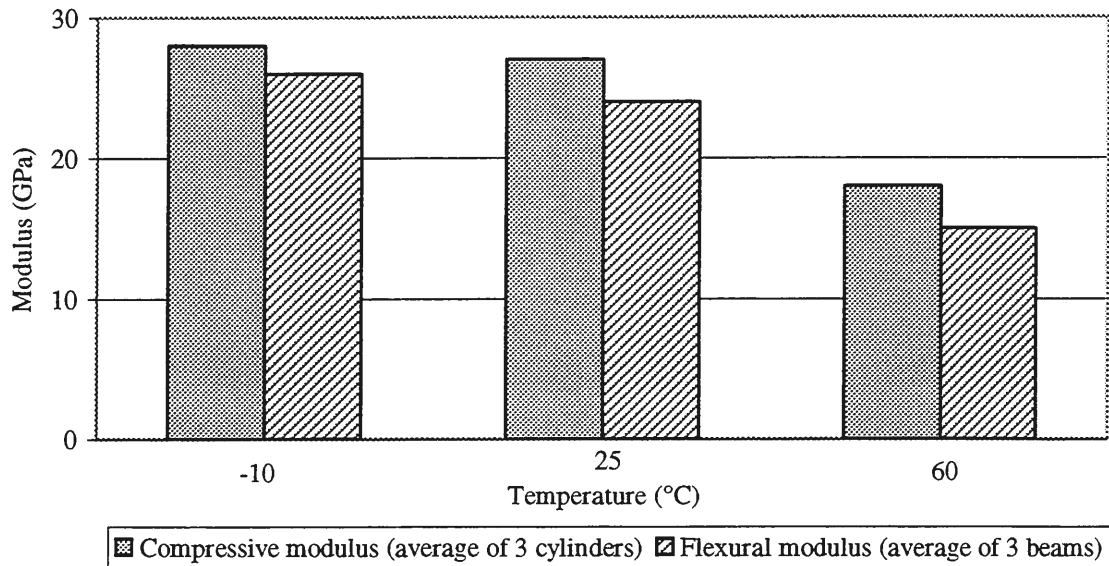


Figure 2.7 Change in modulus with temperature [22]

There are several different polymers used as binders in polymer concrete. Four of the most common binders are polyester, polymethyl methacrylate, epoxy, and furan polymer. Engineering properties for these four common polymers that are used to manufacture PC can be seen in Table 2.3. A summary of the characteristics and applications of these binders can be seen in Table 2.4.

Table 2.3 Comparison of properties of concretes made with varying binders [23]

Type of binder	Density (kg/dm ³)	Water Sorption (%)	Compressive Strength (MPa)	Tensile Strength (MPa)	Flexural Strength (MPa)	Modulus of Elasticity (GPa)	Poisson Ratio	Thermal Coefficient of Expansion (10 ⁶ °C ⁻¹)
Poly(methyl methacrylate)	2.0-2.4	0.05-0.6	70-210	9-11	30-35	35-40	0.22-0.33	10-19
Polyester	2.0-2.4	0.30-1.0	50-150	8-25	15-45	20-40	0.16-0.30	10-30
Epoxy	2.0-2.4	0.02-1.0	50-150	8-25	15-50	20-40	0.30	10-35
Furan polymer	1.6-1.7	0.2	48-64	7-8	----	----	----	38 ^b ,61 ^b
Concrete ^a	1.9-2.5	5-8	13-35	1.5-3.5	2-8	20-30	0.15-0.20	10-12

a Carbon and silica filled mortars, respectively

b Portland cement concrete

Table 2.4 Summary of characteristics and applications of polymer concrete [23]

Type of Binder Used in PC	General Characteristics	Typical Applications
Poly(methyl methacrylate)	Low tendency to absorb water, thus high freeze-thaw resistance; low rate of shrinkage during and after setting; very good chemical resistance and outdoor durability.	Used in the manufacture of stair unit, façade plates, sanitary products for curbstones
Polyester	Relatively strong, good adhesion to other materials, good chemical and freeze-thaw resistance, but have high-setting and post-setting shrinkage.	Because of lower cost, widely used in panels for public and commercial buildings, floor tiles, pipes, stairs, various precast and cast-in applications in construction works
Epoxy	Strong adhesion to most building materials; low shrinkage; superior chemical resistance; good creep and fatigue resistance; low water sorption	Epoxy polymer products are relatively costly; they are mainly used in special applications, including use in mortar for industrial flooring, skid-resistant overlays in highways, epoxy plaster for exterior walls and resurfacing of deteriorated structures
Furan-based polymer	Composite materials with high resistance to chemicals (most acidic or basic aqueous media), strong resistance to polar organic liquids such as ketones, aromatic hydrocarbons, and chlorinated	Furan polymer mortars and grouts are used for brick (e.g. carbon brick, red shale brick) floors and linings that are resistant to chemicals elevated temperatures and shocks

2.6 Composite Material from Fly Ash and Recycled Plastics

This section will discuss two applications where composite materials are produced from fly ash and recycled plastics. The first application is masonry blocks out of aggregates made from recycled plastics and fly ash. The second application is using recycled PET to produce a polyester resin for PC made with fly ash.

2.6.1 Masonry blocks

Kashi, Swan, and Malloy (2000) researched the use of postconsumer plastic along with fly ash as filler material to produce a synthetic lightweight aggregate (SLA) [6]. This SLA was then used to produce concrete masonry block. A mixture of different postconsumer

thermoplastics was used as the binding material. The plastic material that was used in the study was SPI #3-7. SPI #3-7 are plastics that are deemed unacceptable for recycling because of contamination [6]. Table 2.5 shows concentrations of different plastics used in this study. The plastic mixture consisted of clean, recycled materials, along with some virgin materials.

Table 2.5 Composition of non-recycled mixed plastic [6]

Material	Concentration by Weight (%)
PET (recycled bottle grade) #2	30
HDPE (recycled blow molding grade) #2	30
HDPE (injection molding grade) #2	5
LDPE (extrusion grade) #4	10
PP (injection molding grade) #5	10
PS (injection molding grade) #6	5
HIPS (injection molding grade) #6	10

The SLA consisted of 80% fly ash and 20% plastic material by weight. The masonry cylinders (102 mm diameter and 204 mm long) made from SLA was compared to masonry cylinders made from sand. The compressive strength of the cylinder made from the sand was 10.2 MPa and for the SLA unit was 5.5 MPa. The density of the sand unit was 1938 kg/m³ and the SLA was 1110 kg/m³. It was concluded that the SLA unit satisfied the requirements for nonloadbearing masonry and its density was well below the requirement for the lightweight masonry.

2.6.2 Recycled PET and fly ash in PC

Polymer concrete is not widely used due to the high cost of the composite material, which is typically 10 to 20 times more expensive than PCC [18]. The higher cost is due to the resin material. PET can be chemically modified to produce unsaturated polyester resins. [19, 20, 21, 22]. Using PET recovered from beverage bottles can lower the cost of the resin

[19, 20, 21, 22]. Another advantage of recycling PET to make unsaturated polyester resin, as compared to using 100% virgin materials, is that it takes about 50 % shorter processing time to produce a polyester resin with a certain molecular weight and acid number [19].

2.7 Pipes

Pipes are designed according to the material that they are constructed from; the material that the pipe is constructed from is extremely important in determining which applications they can be used. For a pipe to perform its intended function it must have enough strength and/or stiffness, and durability. Strength is the ability to resist stress; stiffness is the ability to resist deflection; and durability is the pipe's ability to withstand environmental effects with time [24].

Pipes are usually classified as either flexible or rigid, depending on how they perform after they have been installed. Whether the pipe is flexible or rigid is usually determined by whether it can deflect more than 2% without structural damage. If it can deflect more than 2%, it is a flexible pipe [24]. If it cannot, it is a rigid pipe. Some common flexible pipes are manufactured from polyvinyl chloride, polyethylene, steel, and aluminum. Two examples of rigid pipe materials are concrete and clay.

Flexible and rigid pipes distribute the load that is applied to them in different ways. As the load presses down on a flexible pipe it deflects against the backfill. The load is then transferred to and carried by the backfill [25]. Rigid pipes transfer the load through the pipe's wall into the bedding material [25].

2.7.1 Thermoplastic pipe

Thermoplastics are compounds made from resins (polymers) and additives. Additives are added to thermoplastics to enhance specific characteristics of the plastic. Some of the common additives that are added to plastic pipe materials are antioxidants, colorants, coupling agents, fibrous reinforcements, fillers and extenders, heat stabilizers, preservatives, and ultraviolet stabilizers [26]. Table 2.6 gives a listing of additives, their purpose, and benefits. Thermoplastics, such as polyvinyl chloride (PVC), chlorinated polyvinyl chloride (CPVC), polyethylene (PE), acrylonitrile-butadiene-styrene (ABS), and polypropylene (PP), are the primary plastics used to manufacture plastic pipes [26].

Table 2.6 Common additives in plastic piping material [26]

Additives	Purpose	Benefit
Antioxidants	Inhibit or retard reactions caused by oxygen or peroxides	Extends the temperature range and service life
Colorants	Pigments and dyes used to give color to plastic material	Provides any desired color
Coupling agents	Improves the bonding characteristics of plastic materials	Improves the mechanical and electrical properties of the plastic material
Fibrous reinforcements	Improves the properties of the resin	Fibers improve the strength to weight ratio
Fillers and extenders	Improves the physical and electrical properties of resin Also reduces the cost of higher priced resins	Plastic material can be more economically produced without a loss of quality
Heat stabilizers	Helps prevent the degradation of plastic materials from heat and light	Helps plastic material to be stable and retain their physical properties in excessive heat
Preservatives	Helps prevent degradation of polymers by microorganisms	Helps prevent fungi and bacteria attack on plastic material Makes the plastic material better suited for underground use
Ultraviolet stabilizers	Helps retard the degradation from sunlight	Allows plastic material to be used outdoors without any significant changes of the physical properties

Since the properties of thermoplastics vary significantly, different thermoplastics are used for different applications. Table 2.7 is a listing of the properties, temperature limit, joining methods, and applications of these common plastic pipe materials. Thermoplastic's low cost, ease of fabrication, and long life makes it popular piping material. These materials are used mainly in low pressure and low temperature applications due to thermoplastic's relatively low stiffness, low strength, and its sensitivity to temperature.

Table 2.7 Common thermoplastic properties and applications [26]

Material	Properties	Temperature limit, °C	Joining methods	Application
PVC	Outstand resistance to most corrosive fluids Offers more strength and rigidity than most other thermoplastic pipe	70	Cementing Threading Heat fusion	Drain, waste, and vent Sewage Potable water Well casings Chemical pro processing
CPVC	Has the same properties as PVC, but can be used at higher temperatures	100	Same as PVC	Used mainly in high-temperature applications
PE	Offers a relatively low mechanical strength but has good chemical resistance and is flexible at low temperatures	60	Heat fusion Insert fitting	Potable water Irrigation and sprinkler Corrosive chemical transport Gas distribution Electrical conduit
AMS	This pipe is rigid and has high-impact resistance down to -4 °C	70	Cementing Threading Mechanical seal devices	Drain, waste, and vent Potable water Sewer Treatment plants
PP	Good high-temperature properties and outstanding chemical resistance	90	Heat fusion Threading	Chemical waste Natural gas Oil field

2.7.2 Vitrified clay pipes

Vitrified clay pipes are very resistant to corrosion and abrasion but have low strength, are brittle, and are subject to impact damage [24]. They receive their name from the manufacturing process. As the pipe travels through the kiln, it reaches temperatures approaching 1100 °C where clay fuses into a hard, chemically stable compound [24]. This

hardening process is known as vitrification. Pipe sizes range from 75 mm to 1065 mm [27]. Vitrified clay pipes must meet the three-edge bearing minimum strength criteria stated in ASTM C 700 Standard Specification for Vitrified Clay Pipe, Extra Strength, Standard Strength, and Perforated [27]. These pipes are classified as “extra” strength or “standard” strength. Three-edge bearing tests for “extra” strength pipes vary with diameter and range from 29.2 to 102.2 kN/linear m. Table 2.8 shows the inside diameter 205 mm and 255 mm size, standard and extra strength, and minimum three-edge bearing strengths for vitrified clay pipes.

Table 2.8 Minimum three-edge bearing strengths for vitrified clay pipe [27]

Inside Diameter (mm)	Three-Edge Bearing Minimum Strength (kN/linear m)	
	Standard Strength	Extra Strength
205	20.4	32.1
255	23.4	35

2.7.3 Concrete pipes

Pipes manufactured with concrete are classified as either nonreinforced or reinforced. It is recommend that nonreinforced concrete pipes are used for installations where height of cover over the pipe is not excessive, severe live loads are not anticipated, and structural failure will not endanger life or property [28]. Nonreinforced is normally available in 100 to 900 mm diameters [29]. Applications were they are used are storm drains, sewers, industrial wastes, culverts, irrigation distribution systems, and groundwater recharge systems. The nonpressure nonreinforced concrete pipes are described in ASTM C 14M Standard Specification for Concrete Sewer, Storm Drain, and Culvert Pipe [29]. ASTM C 14M separates nonreinforced concrete pipes into 3 classes: Class 1, Class 2, and Class 3. These

three classes differ by requirements for minimum wall thickness and minimum three-edge bearing strengths. Minimum wall thicknesses and minimum three-edge bearing strengths for 200 mm and 250 mm internal designated diameters for the three classes are shown in Table 2.9.

Table 2.9 Nonreinforced concrete pipe requirements [29]

Internal Designated Diameter (mm)	Class 1		Class 2		Class 3	
	Minimum Thickness of Wall (mm)	Three-Edge Bearing Minimum Strength (kN/linear m)	Minimum Thickness of Wall (mm)	Three-Edge Bearing Minimum Strength (kN/linear m)	Minimum Thickness of Wall (mm)	Three-Edge Bearing Minimum Strength (kN/linear m)
200	19	22.0	22	29.0	29	35.0
250	22	23.5	25	29.0	32	35.0

Reinforced concrete pipes utilize the high compressive strength of concrete and the high tensile strength of steel. It is recommended that reinforced concrete pipes are used when the required size is larger than available in nonreinforced pipe, moderate or severe cover and/or live load conditions exist, structural failure might endanger life or property, internal hydrostatic pressure are expected up to 448 kPa, or when trenchless installation is desirable [28]. Reinforced concrete pipes retain their shape and do not collapse even though ultimate failure occurred [28]. Inside diameters for reinforced concrete pipes range from 300 to 3600mm [30]. Reinforced concrete pipes are used in the same applications nonreinforced concrete pipes.

The nonpressure reinforced concrete pipes are described in ASTM C 76M Standard Specification for Reinforced Concrete Culvert, Storm Drain, and Sewer Pipe [30]. ASTM C 76M separates reinforced concrete pipes into 5 classes, Class I, Class II, Class III, Class IV, and Class V, according to dead load (D-load) to produce a continuous crack 0.3 mm for a

length of 305 mm or the D-load to produce the ultimate load. Requirements are also given for wall thickness, concrete compressive strength, and reinforcements. D-load is the three-edge bearing load expressed in Newtons per linear meter per millimeter of inside diameter. The required strengths are calculated by multiplying the D-load in Table 2.10 by the internal diameter in millimeters. The required strengths are shown in Table 2.11 for a reinforced concrete pipe with a inside diameter of 300 mm. ASTM does not have standard specification for reinforced concrete pipe with smaller inside diameters.

Table 2.10 D-load requirements [30]

	Class I	Class II	Class III	Class IV	Class V
D-load to produce a 0.3 mm crack	40	50	65	100	140
D-load to produce the ultimate load	60	75	100	150	175

Table 2.11 Reinforce concrete pipe design strength requirements [30]

	Class I	Class II	Class III	Class IV	Class V
Minimum 3-edge bearing strength to produce a 0.3 mm crack (kN/linear m)	---	15	19.5	30	42
Minimum 3-edge bearing strength to produce ultimate load (kN/linear m)	---	22.5	30	45	52.5

--- smallest internal diameter is 1500 mm

2.7.3.1 Sulfuric acid attack

An increasingly prevalent problem is the biogenic corrosion of concrete, specifically with regards to concrete sewer pipes. In the United States there are over 1.28 million km of concrete sewer conduits that are subjected to sulfide-related corrosion [31]. This is a result of the activities of sulfate-reducing and sulfide-oxidizing bacteria. The sanitary sewage by itself is not highly corrosive, but as anaerobic bacteria decomposes sewage, it produces hydrogen sulfide gas (H_2S). As the sewage travels through the sewers turbulence from force mains, drop manholes, steep grade changes and pumping stations allow the hydrogen sulfide gas to

release into the pipe's atmosphere. An aerobic bacterium, Thiobacillus, grows on the concrete surfaces above the wastewater and converts the sulfide gas into sulfuric acid (H_2SO_4). This sulfuric acid corrodes the concrete, resulting in structural damage to the pipe. A cross-section sketch of a concrete pipe under sulfide-related corrosion is shown in Figure 2.8. Concrete pipes manufactured with cements that are high in tricalcium aluminate, C_3A , content are susceptible to deterioration when exposed to sulfate soils or sulfate waters [32]. The sulfate resistance of concrete with high C_3A contents is improved by the use of pozzolans as admixtures [32].

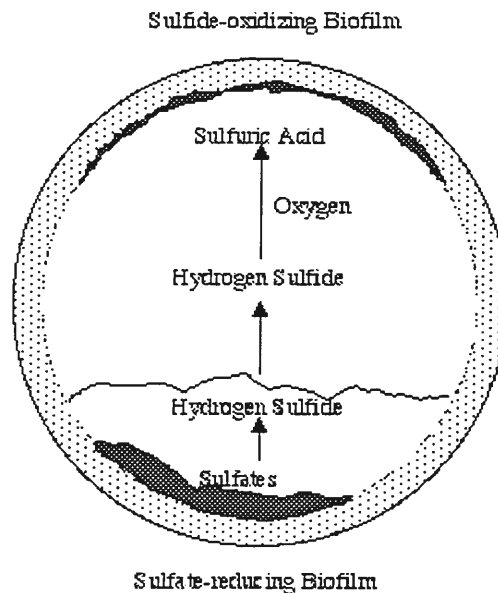


Figure 2.8 Concrete corrosion of the inner surface of the sewage conduit due to the activities of sulfur oxidizing bacteria [31]

3 EXPERIMENTAL PROCEDURE

This chapter discusses the materials that the composite is composed of, the manufacturing processes, and testing procedures. The first section will discuss the plastic material, filler material, and fiberglass fibers used to create the composite material. Next the manufacturing process and testing procedures of the cylinder specimens will be discussed. The third section will discuss the manufacturing and testing procedures for the pipe specimens. The final section in this chapter will discuss durability test that conducted.

3.1 Materials

3.1.1 Plastic material

There are three forms of PET investigated in this study: processed; clean; and dirty. The difference is due to the level at which the PET was processed. PET recycled in a plastic recycling facility is referred to as “processed”. “Clean” PET was shredded from collected bottles using a conventional wood chipper and had most of the labels and caps removed. “Dirty” PET was also shredded with a wood chipper, but contained labels and caps. Figure 3.1 shows pictures of the different forms of PET used in this study.

The PET labeled “dirty” and “clean” in Figure 3.1 was collected through the Iowa State University recycling program and consisted of clear and colored beverage bottles and food containers. Bottles and containers were stored outside in cardboard boxes where it was exposed to the weather for a period of about 24 months.

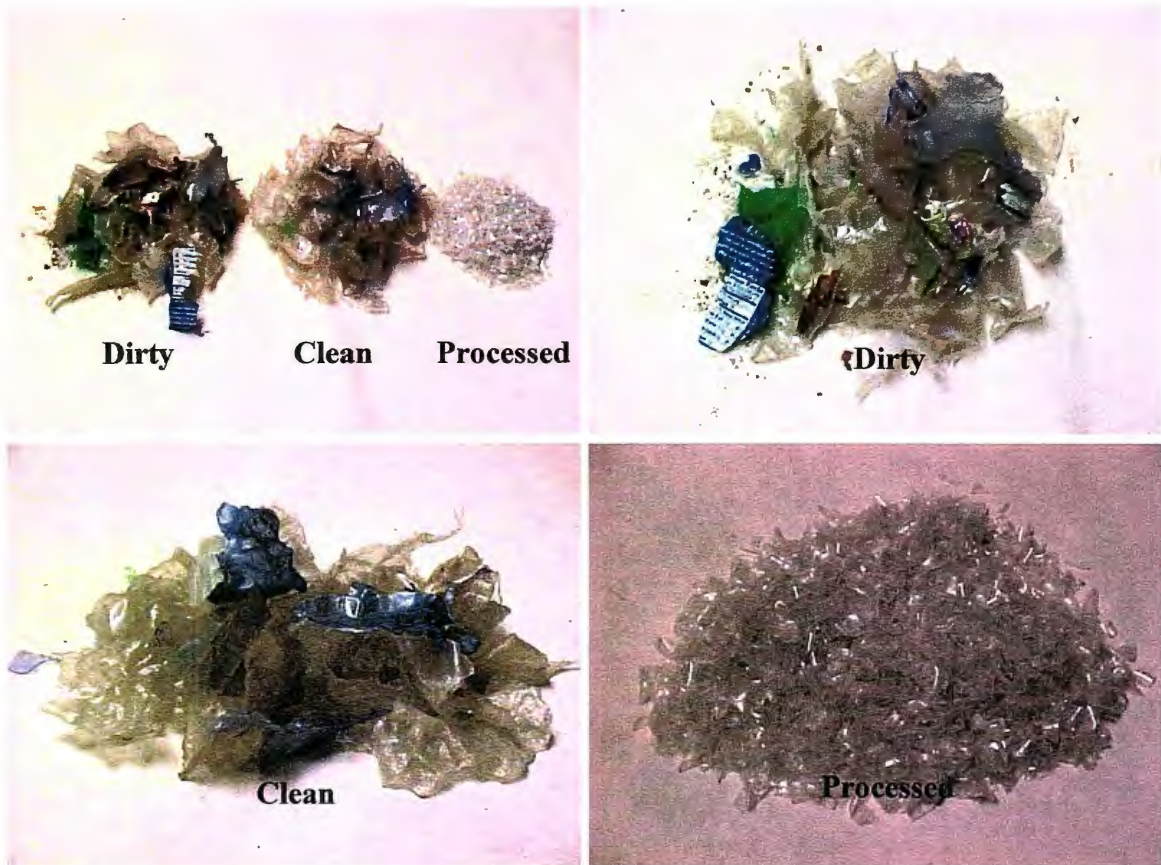


Figure 3.1 Three experimental PET processing levels (50 g shown)

In order to heat and mix the PET bottles and containers they needed to be reduced in bulk volume. To produce one pipe specimen (height 260 mm, outside diameter 305 mm, and 38 mm thickness) about 9,000 grams of PET is required. This is equivalent to 338 of the 16-ounce bottles. A Vermeer brush chipper with a 9-inch cutting blade shown in Figure 3.2 was used during the first step to reduce the volume. The brush chipper did not produce the desired volume reduction, with the bodies of the bottles remaining intact and only a portion of the bottle tops and bottoms shredded.



Figure 3.2 First stage in reducing the volume of PET from curbside recycling programs

The next step in the reduction of the PET volume was to send the bottles through a chipper-shredder. The chipper-shredder reduced the PET to the sizes shown in Figure 3.1. Although the “clean” and “dirty” sizes are significantly larger than the “processed” PET, they were manageable sizes to place into the electric melting pot.



Figure 3.3 Chipper shredder

After shredding, the “clean” PET was washed in a water bath and then left out to air-dry. The water bath did not fully remove all of the labels and HDPE cap materials. Therefore these materials had to be removed by hand. There was no attempt made to remove the adhesive material on the “clean” PET. The “dirty” PET contained the labels, HDPE cap materials, adhesives, and other impurities, such as leaves and soil, when placed into the electric melting pot.

“Processed” PET in Figure 3.1 was recycled and donated by Lavergne, Inc. This material was label free and consisted of clear pop bottles. Sizes of flakes varied between 3 to 20 mm in length. A particle size distribution of the “processed”, “clean”, and “dirty” PET can be seen in Figure 3.4. “Processed” PET had a moisture content of 0.6%.

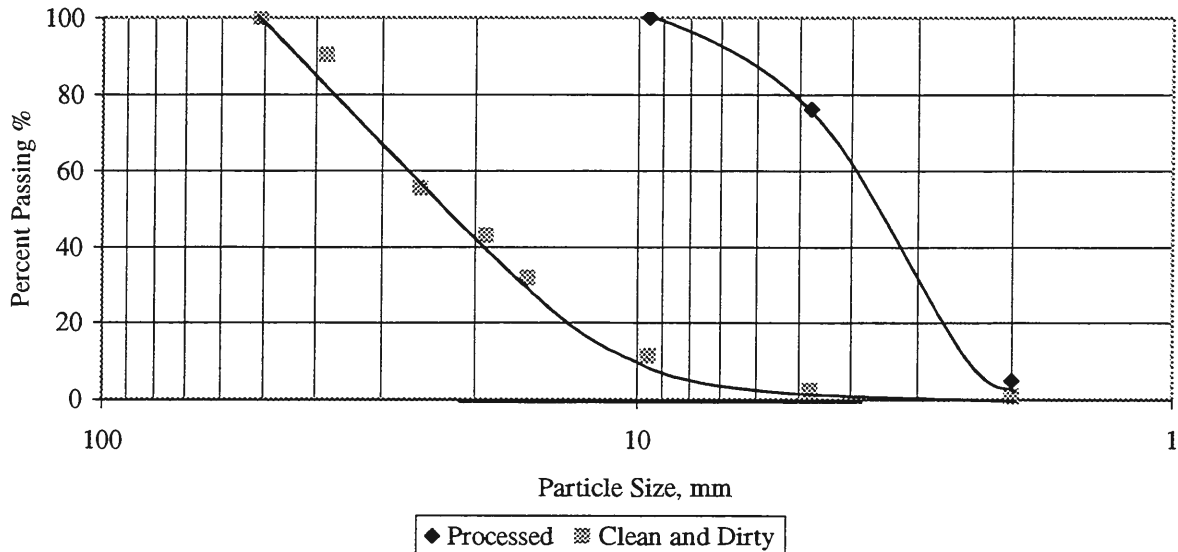


Figure 3.4 Particle distribution curves for the three forms of PET

3.1.2 Filler material

Three types of filler materials were tested for this study: coal combustion byproducts, hydrated lime, and Sioux quartzite. There were four fly ashes tested: Prairie Creek fly ash,

Ames fly ash, Iowa State University (ISU) circulating fluidized bed (CFB) fly ash, and ISU stoker fly ash. There were two bottom ashes tested: ISU CFB bottom ash and ISU stoker bottom ash. Another coal combustion byproduct was University of Northern Iowa (UNI) fluidized combustion residue. Two filler materials were not byproducts of coal combustion. They were hydrated lime and Sioux quartzite. This range of materials was selected to show the influence that different types of fillers have on the engineering properties of the composite material.

Materials Analysis and Research Laboratory (MARL) located at Iowa State University performed x-ray fluorescence (XRF) and x-ray diffraction (XRD) analysis on all filler materials. Analytical chemical composition results from XRF tests can be seen in Table 3.1. Specific gravity of the filler materials is shown in Table 3.2. Particle size distribution curves for the filler materials are shown in Figures A.1 through A.3 of Appendix A. X-ray diffractograms are shown in Figures A.5 through A.12 of Appendix A.

P. C. fly ash was supplied by the Prairie Creek Power Plant. Prairie Creek uses coal from Powder River Basin in Wyoming and pulverized boilers. All particles passed the #20 mesh sieve (0.85 mm) and 93% passed the #200 mesh sieve (0.075mm). This fly ash was the only one that classified as an ASTM class C fly ash.

The Ames fly ash was supplied by Ames Municipal Electric Systems. Ames receives its supply of coal from the Powder River Basin in Wyoming. The Ames power plant mixes its coal with about ten percent by weight of municipal solid waste. They use pulverized coal fired boilers to burn the fixture of coal and municipal solid waste. All particles passed the #20 mesh sieve and 95% passed the #200 mesh sieve. This material cannot be classified as

ASTM class C fly ash since municipal solid waste is burned with the coal. Minerals identified in the ash are quartz, anhydrite, brownmillerite, lime, periclase, and tricalcium aluminate.

ISU circulating fluidized bed (CFB) ashes and ISU stoker ashes were both supplied by Iowa State University Power Plant. The ISU power plant uses a mixture of coal from Illinois and Kentucky. The same mixture of coal is burned in their two types of boilers. The ashes receive their names from the boilers in which they are produced, circulating fluidized bed and stoker boilers, respectively. Stoker fly ash had the highest loss on ignition (42.4%) due to the combustion of coal. All CFB fly ash particles passed the #60 mesh sieve (0.25 mm) and 89% passed the #200 mesh sieve. CFB bottom ash passed the #4 mesh sieve (4.75 mm) and only 1% passed the #200. Stoker bottom ash was first crushed to reduce sizes of particles. Stoker bottom ash had all particles pass the #10 mesh sieve and 28% passed the #200. Minerals identified in the ISU CFB fly ash are quartz, anhydrite, lime, hematite, and illite. Quartz, anhydrite, lime, hematite, calcite, and portlandite are the minerals identified in the ISU CFB bottom ash. Minerals identified in the ISU stoker fly ash are quartz, mullite, hematite, and albite. Quartz, mullite, Magnetite, and hematite are the minerals identified in the ISU stoker bottom ash.

UNI fluidized bed ash was supplied by University of Northern Iowa's Power Plant. The UNI power plant uses a mixture of coal from Kentucky and West Virginia. They use a pyropower boiler to burn the coal. All particles passed the #10 mesh sieve (2 mm) and 64% passed the #200. Minerals identified in the UNI bed ash are lime, anhydrite, quartz, and hematite.

Hydrated lime was supplied by the Cedar Rapid Municipal Water Plant. Hydrated lime is pure calcium carbonate, which is a byproduct of water treatment facilities. Lime was sieved through the #10. The only mineral identified in the lime was calcite.

Sioux quartzite is the fine material that is produced from rock quarrying. Sioux quartzite will be referred to as Sump. All the particles passed the #100 mesh sieve (0.15 mm) and 74% passed the #200. Minerals identified in the Sump were quartz, kaolinite, and Talc-2M. The Sump was not analyzed by XRF.

Table 3.1 Chemical analyses of the filler materials by XRF

Constituent	ISU CFB Fly Ash (%)	ISU CFB Bottom Ash (%)	ISU Stoker Fly Ash (%)	ISU Stoker Bottom Ash (%)	Ames Fly Ash (%)	PC Fly Ash (%)	UNI FB (%)	LIME (%)
Silicon Dioxide (SiO ₂)	27.80	7.50	25.80	50.70	35.20	37.02	14.91	0.25
Aluminum Oxide (Al ₂ O ₃)	12.70	3.00	12.20	23.90	16.70	19.96	8.21	0.12
Ferric Oxide (Fe ₂ O ₃)	9.00	1.48	10.70	8.60	6.40	5.86	4.06	0.30
Sum	49.50	11.98	48.70	83.20	58.30	62.85	27.18	0.67
Sulfur Trioxide (SO ₃)	12.50	30.70	0.51	0.44	2.94	2.00	29.23	0.07
Calcium Oxide (CaO)	24.30	52.60	1.30	3.01	26.80	22.87	37.97	54.78
Magnesium Oxide (MgO)	0.58	0.33	0.65	0.91	5.72	4.28	0.64	1.27
Phosphorous Pentoxide (P ₂ O ₅)	0.30	0.07	1.14	0.14	2.28	1.65	0.39	-----
Potassium Oxide (K ₂ O)	1.36	0.29	2.64	2.53	0.38	0.53	0.69	-----
Sodium Oxide (Na ₂ O)	0.12	0.06	0.50	0.29	1.20	1.38	0.07	-----
Titanium Oxide (TiO ₂)	0.63	0.19	0.86	1.24	1.61	1.56	0.47	-----
Strontium Oxide (SrO)	0.04	0.03	0.04	0.05	0.33	0.40	0.04	0.07
Barium Oxide (BaO)	0.02	0.00	0.01	0.01	0.78	0.78	-----	-----
Mn ₃ O ₄	-----	-----	-----	0.02	-----	-----	-----	-----
MnO ₂	-----	-----	-----	-----	-----	-----	-----	0.15
V ₂ O ₃	-----	-----	-----	-----	-----	-----	0.23	-----
LOI (Loss On Ignition)	10.40	3.60	42.40	7.99	0.30	1.80	-----	-----
Moisture + LOI	-----	-----	-----	-----	-----	-----	2.9	43
Total	99.75	99.85	98.75	99.81	100.64	100.10	99.81	100.01

Table 3.2 Specific gravity of filler materials

Filler Material	Specific Gravity
ISU stoker bottom ash	2.42
ISU stoker fly ash	2.43
ISU CFB bottom ash	3.04
ISU CFB fly ash	3.06
Ames fly ash	2.96
P. C. fly ash	2.68
UNI fluidized bed ash	2.79
Lime	2.62
Sump	2.66

3.1.3 Fiberglass fibers

Fiberglass fibers were added to the composite material to improve its engineering properties. The fibers were donated by Vetrotex America. Two different lengths of fiberglass fibers, both with a width of 2 mm, were tested: 13 mm and 6 mm. They were both chopped strand 919-4 CT fiberglass fibers. Product numbers for the two fibers are CA4J919053 and CA4J919022 for the 13 mm and 6 mm fibers, respectively. They were a white-yellowish color. A picture of the two fiberglass fibers is shown in Figure 3.5.



Figure 3.5 6 mm and 13 mm fiberglass fibers

3.2 Cylinder Specimen Process

3.2.1 Manufacturing process

Cylinder specimens of diverse materials were made in order to gain a better understanding of the variables being studied. The variables included the effects that different filler material, percentage of PET to filler material, form of PET, percentage of fiberglass fibers, length of the fiberglass fibers, and particle size had on the compressive and splitting tensile strengths of the composites. Cylinder specimens had a diameter of 50.8 mm and length of 101.6 mm. A total of 51 batches were made, two batches for each design mix. Two cylinder specimens from every composite design mix were tested in compression and splitting tension.

The viscosity of the composites did not allow for the cylinders to be poured separately. Therefore, four cylinder specimens were made from the same batch at the same time. Cylinder specimens were made by pouring the liquid composite material into a heated outer cylinder mold. Four conduit cylinders were inserted into the liquid composite. Pressing the conduit cylinders into the composite caused the composite to fill the insides of the conduits.

Outer mold was constructed from a 152 mm diameter and 152 mm long snap lock pipe used in air ventilation systems. Snap lock pipe was used because the joint on the side of the cylinder made it possible for the mold to open so that the cooled composite material could be removed. The joint was then closed and the cylinder was reused. Inner molds were constructed by cutting 50.8 mm diameter conduit pipes into 152 mm sections. These lengths allowed for the tops and the bottoms of the composite cylinders to be cut off in order to

smooth and level the surfaces. Eighteen of these inner molds were used to make the composite cylinders. Each batch consisted of one snap-lock pipe and four conduit pipes.

The first step in making the cylinder specimens was to weigh the desired amount of filler, PET, and fiberglass. Second step in the process was to turn on the electric melting pot to a setting of 5.5 which produced a temperature of 270 °C. Next, the PET material was introduced to the electric melting pot and then oven dried filler material was placed on top of it. The cover was placed back onto the electric melting pot to prevent heat from escaping and left alone to melt the PET. Next, one outer cylinder mold and four inner cylinder molds were placed into the oven and the oven was turned on. Two hours was sufficient time for the molds to heat to 270 °C. A metal rod with a 12.7 mm diameter was used to stir the specimens. Stirring frequency increased as more material melted. Once all of the plastic was melted and the composite was uniform, the fiberglass was stirred into the mixture until it reached uniform consistency.

Outer mold cylinder and the inner mold cylinders were taken out of the oven and set on a metal table. The metal table formed the bottom of the mold. The four inner molds were then spayed with silicon so the cylinders could be removed from the mold easier. After the lid was taken off, the electric melting pot was tipped on its side. Two large spoons were used to move the melted composite material into the outer mold cylinder. The melted composite material filled the outer cylinder mold to a level about 25 mm from the top. Four inner molds were then placed on top of the melted composite material and then pressed into the material. The melted composite material was not allowed to flow over the top edges of the

four inner molds. This prevented the inner cylinder molds from becoming sealed. The melted composite material was left alone to cool at room temperature as shown in Figure 3.6.

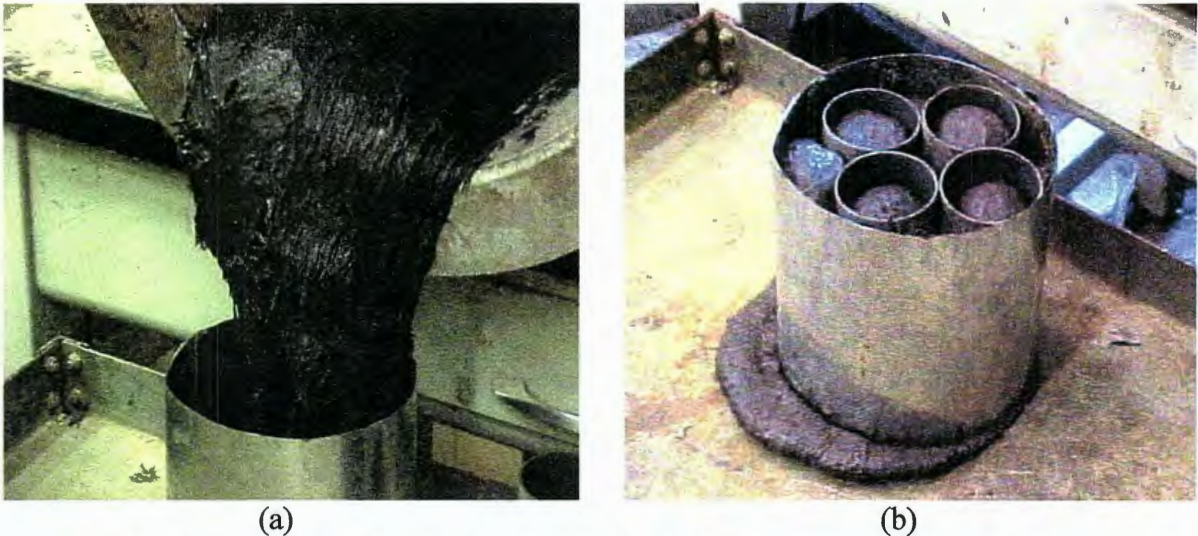


Figure 3.6 (a) Composite flowing into mold, (b) cylinder specimens cooled

The next day the outer mold was taken off and the excess composite material was removed from the outer edges of the four inner molds. Excess material was removed by using a screwdriver and hammer and chiseling the material off of the inner cylinder molds. Composite cylinders were then removed from the inner molds by pressing on the tops of the composite cylinders. Composite cylinders slid easily out of the inner molds. Each cylinder was marked with an identification number and letter. Cylinders were then cut to a length of 102 mm using a power miter saw with a masonry blade.

Two batches for every design mix were made for a total of 52 batches. There were four batches made without fiberglass for the design mix with 50/50 PET to filler ratio. Four batches were necessary to produce the eight specimens needed for testing. The composite material, without fiberglass, cracks and/or breaks during the removal of the mold.

3.2.2 Compressive testing process

ASTM C 39/C 39M-99 Standard Test Method for Compressive Strength of Cylindrical Concrete Specimens [33] was used as a guide to test the compressive strength for the composite cylinder specimens. A Soiltest machine was used to produce the compressive force. The smallest division on the testing machine was 0.2 kN. Loading rate was calculated by measuring the elapsed time for increment 2 kN. The load of 2 kN was then divided by the cross-sectional area to determine the compressive strength. Compressive strength was then divided by the elapsed time in seconds to determine the loading rate.

Test specimens were constructed from different composite design mixes. Two cylinder specimens from every composite design mix were tested in compression. Test specimens had a diameter of 50.8 mm and a length of 101.6 mm. Load rate was continuous and without shock and within the range of 0.15 to .35 MPa/s. The diameter of the cylinder specimens was determined by averaging two diameters in the middle of the specimen at right angles from each other. Lengths of the cylinder specimens were determined by averaging two lengths.

Cylinder specimens were positioned by centering them vertically on one of their ends in the middle of the bearing block. The ram was then lowered so that it came into contact with the top end of the cylinder specimen. The testing machine was then set to controlled test, which started the loading. Loading continued until the load indicator decreased significantly. This decrease indicated that the cylinder specimen failed. The maximum load was then recorded to the nearest 0.2 kN division. The testing machine was then unloaded

and the sample removed. This process continued until all of the cylinder specimens were tested.

All specimens marked with the letter “A” were tested for vertical deformation to determine the modulus of elasticity. A dial gage was placed so it came in contact with the ram, with loads recorded every 0.254 mm. This continued until the cylinder failed. A picture of compression test setup can be seen in Figure 3.7.



Figure 3.7 Compression test for cylinder specimens with vertical deformation measurements

3.2.3 Splitting tensile test

In order to determine the splitting tensile strength, the compressive force that was applied along the length of the cylinder specimen substituted Equation 1. ASTM C 496-96 Standard Test Method for Splitting Tensile Strength of Cylindrical Concrete Specimens [34] was used as a guide to test the tensile strength for the composite cylinder specimens. A Soiltest machine was used to produce the compressive force.

Bearing strips were constructed from 6.4 mm thick oak plywood. Widths of the plywood bearing strips were 25 mm and the lengths were 114.3 mm. Supplementary bearing bar was constructed from a 12.7 mm thick aluminum bar. Aluminum bar had a width of 38 mm and the length of the bar was 114.3 mm. Test specimens were constructed from different composite design mixes and had diameters of 50.8 mm and lengths of 101.6 mm. One hundred fifty-two millimeter diameter steel spacer blocks were used as the lower bearing platform.

Loading rate was constant and within the range of 689 to 1380 kPa/min. A centerline was drawn on one end of the cylinder specimens. The testing machine was positioned in front of a wall so that lining the cylinder specimens from the backside was impossible due to the lack of space behind the testing machine. The centerline was determined by sweeping a ruler back and forth to determine the maximum diameter. This diameter was then chosen as the centerline and marked using a straight edge and a pencil. Diameter of the cylinder specimens was determined by averaging three diameters along the centerline. Three diameter measurements were taken, 25 mm from each end and one in the middle of the cylinder specimens. Lengths of the cylinder specimens were determined by averaging two lengths.

Cylinder specimens were positioned by centering one plywood strip on the lower bearing platform lengthwise and placing the cylinder specimen lengthwise so that the centerline was vertically over the center of the width of the plywood strip. Then the top plywood strip was placed over the cylinder specimen lengthwise and centered over the centerline. The upper bearing bar was then centered over the top plywood strip. The ram

was lowered so that it came in contact with the upper bearing bar. The cylinder specimen, plywood strips, and upper bearing bar were then aligned and centered.

The testing machine was then set to controlled test, which started the loading. Loading continued until the load indicator decreased significantly. This decrease indicated that the cylinder specimen failed. Maximum load was then recorded to the nearest 0.2 kN division. The testing machine was unloaded and the sample removed. Plywood strips were then disposed. This process continued until all of the cylinder specimens were tested. Figure 3.8 shows the splitting tensile strength setup and a specimen that failed.

Smallest division on the testing machine was 0.2 kN. Loading rate was calculated by measuring the elapsed time for an increment of 2 kN. The load of 2 kN was substituted for the load in Equation 3.1 to determine the splitting tensile strength. Splitting tensile strength was then divided by the elapsed time in minutes to determine the loading rate. Splitting tensile strength was determined using Equation 3.1.

$$T = \frac{2P}{\pi ld} \quad \text{Equation 3.1}$$

Where:

T = splitting tensile strength, (kPa)

P = maximum applied load indicated by the testing machine, (kN)

l = length, (m)

d = diameter, (m)

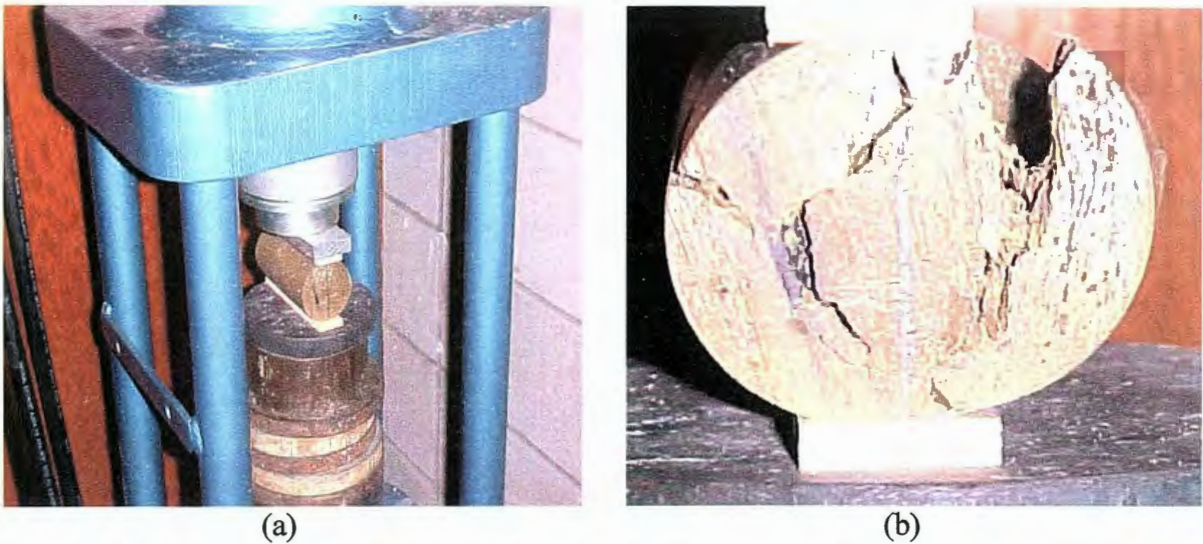


Figure 3.8 (a) Splitting tension test setup, (b) specimen failing

3.3 Pipe Specimens

3.3.1 Manufacturing process

Pipe specimens were created by melting PET and then mixing filler material and fiberglass in an electric melting pot. Equipment used to produce the pipe specimens included: electric melting pot with lid, metal stirring rod, oven, hydraulic ram/piston, inner collapsible cylinder mold, outer cylinder mold with base plate, 2 bolts, moveable cart, silicon spray, heat resistant gloves, metallic spoons, concrete spacers, wooden spacers, metal pans, 3 hose clamps, screwdriver, and sledgehammer. Eighteen thousand grams of material was used to produce one pipe specimen.

Approximately 12 hours before the pipe was to be constructed, the filler material and molds were preheated. The desired amount of filler was weighed out then placed into the oven at approximately 270 °C. Preheating the filler at least twelve hours was found to shorten the cooking time and decrease the moisture content. The base plate, outer cylinder mold, and inner cylinder mold were sprayed with silicon spray to ensure the pipe separated

easily from the mold. The mold was also placed into the oven at (270 °C) as shown in Figure 3.9. The outer cylinder mold was fastened with two bolts to the bottom plate prior to placing it into the oven. Dimensional diagrams of the mold and the piston are shown in Figures C.27 through C.29 in Appendix C.

The second part of the process involved creating the composite mixture. PET was weighed to the desired amount then placed into the electric melting pot. The electric melting pot (Figure 3.10) was turned on and set to a temperature of approximately 270 °C. Not all of the PET would fit into the electric melting pot for most of the mixes, so PET was added occasionally as it melted. The melted PET was mixed by hand using a metal rod.

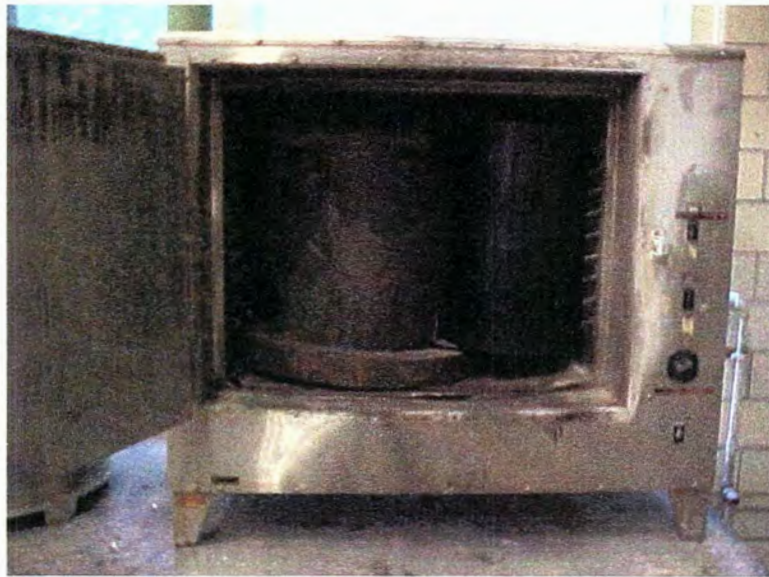


Figure 3.9 Preheating molds in oven



Figure 3.10 Electric melting pot used to melt PET

Filler material was added as space became available due to the melting of the PET. After placing filler material into the electric melting pot, the composite was stirred a few minutes and left to melt. The mixture was stirred every 15 to 30 minutes to increase melting and composite uniformity as shown in Figure 3.11.



Figure 3.11 Melted composite material

As the mixture melted, lumps of unmelted PET and filler material formed, which increased the cooking time. Once the composite had a uniform consistency, the desired

amount of fiberglass was added to the mixture. One handful of fibers was added and then stirred until the mixture had a uniform consistency before adding more fibers as shown in Figure 3.12. The addition of fibers increased viscosity and also added more air voids to the composite material.

The third part of the process was the production of the pipe specimen. While the composite was cooking, the piston was attached to the hydraulic ram and centered using a pocket level. Once the composite was ready, the inner collapsible cylinder mold was taken out of the oven and placed onto the piston. Placing the inner cylinder mold onto the piston was a two-person process. One person held the inner cylinder mold onto the piston while the other person tightened the hose clamp. The slit of the inner cylinder mold was placed at the back of the piston. The inner cylinder mold was fastened to the piston using a hose clamp.



Figure 3.12 Melted composite material with fiberglass

After the inner cylinder mold and the piston were ready, the outer cylinder mold was removed from the oven. Moving the outer cylinder mold was a two-person task due to the weight of the mold. The outer cylinder mold was placed onto three spacer blocks on a moveable cart. Spacer blocks provided access to the bottom of the mold base plate thus

ensuring better handling of the mold. The cart was then wheeled over to the electric melting pot. Two people lifted and tilted the electric melting pot above and in direction of the mold, while a third person assisted the flow of the composite into the mold utilizing two metallic spoons. The one third to one half filled mold was then wheeled to the hydraulic ram. Two people then lifted the mold onto the platform under the piston. The piston was then lowered so the bottom of the piston was 50 to 100 mm from the melted composite material. Three pine wood spacer blocks with dimensions of 38 mm wide by 64 mm long with a thickness of 19 mm were used to center the piston over the mold as shown in Figure 3.13.



Figure 3.13 Centering the pipe with the wooden spacers

After the piston was centered, the piston was lowered into the composite material. As the piston came into contact with the composite material, the piston pressed the composite between the inner and outer cylinder molds. The pipe thickness was then equal to the distance between the molds, approximately 38 mm. Once the piston came in contact with the base plate, the hose clamp was loosened to detach the inner cylinder mold from the piston. The piston was withdrawn and removed from the hydraulic ram, leaving the inner cylinder mold in place.

The fourth and final part of the process was the cooling of the composite material. The mold was then placed on spacer blocks that were on the floor. The inner cylinder mold diameter was reduced by tightening the hose clamp periodically. This was done to reduce the pressure from cooling, resulting from thermal dynamic shrinkage of the composite material. The pipe was allowed to cool at room temperature for 30 minutes. After the two bolts were removed from the mold, the mold was set on its side and the base plate was removed using a sledgehammer. Outer cylinder mold with the pipe and the inner cylinder mold still attached were setup vertically on the floor. The outer cylinder mold was then lifted straight up and removed. The inner cylinder mold was removed by decreasing the diameter of the inner cylinder mold with the hose clamp and lifting up the inner cylinder mold. Often the inner cylinder mold would get stuck about half way, therefore, another hose clamp was placed towards the middle of the inner cylinder mold to reduce the diameter at the bottom of the cylinder. The inner cylinder mold was then lifted up and removed from the pipe. The pipe was then allowed to cool on the concrete floor at room temperature.

Pipes were allowed to cool for 24 hours which was a sufficient amount of time for the pipes to cool completely. A wet masonry chop saw was used to cut the top end. The top portion of the pipes were cut to level the ends and to yield a length of approximately 260 mm. Figure 3.14 shows the cooling process and a pipe specimen.

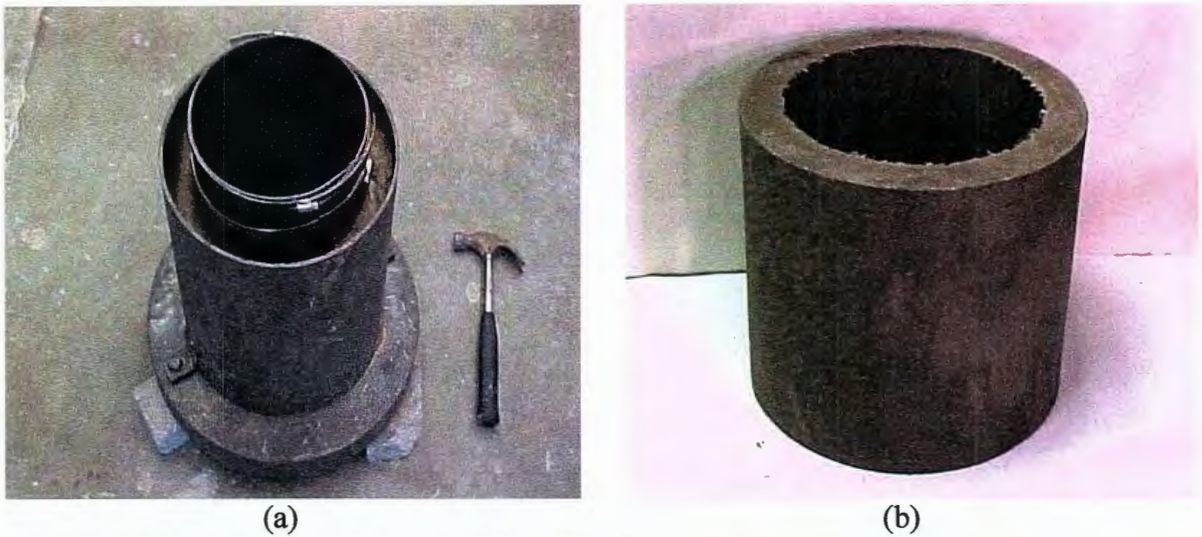


Figure 3.14 (a) Pipe specimens cooling, (b) pipe specimen

3.3.2 Testing process

ASTM C 497-98 Standard Test Method for Concrete Pipe, Manhole Sections, or Tile [35] was used as a guide to test the tensile strength for the composite pipe specimens. MTS machine was used to produce the compressive force. Three-edge-bearing method of loading was used to test the ultimate 3-edge bearing strength of the pipe specimens. D-load to produce the 0.3 mm crack was not determined since the pipe was less than 305 mm [35].

The pipe specimen were supported on the bottom by two parallel longitudinal bearing strips and the load was applied through an upper longitudinal bearing strip. The bearing strips were constructed from pinewood that was sound, free of knots, and straight and true from end to end. Each lower bearing wooden strip had a cross-section of 50.8 mm, a height

of 36 mm, and a length of 330 mm. Inside corners were rounded to a radius of 13 mm. The lower wooden bearing strips were fastened to a rigid wooden base with Elmer's wood glue. Lower wooden bearing strips were spaced apart the minimum distance of 25.4 mm. The rigid wooden base was constructed from oak. The rigid wooden base was 171 mm wide, 61 mm high, and 330 mm long. The upper wooden bearing strip was glued to a steel I-beam with liquid nail caulk. The steel I-beam had a width of 50.8 mm, a height of 77 mm, and a length of 330 mm. A dimensional diagram of the upper and lower bearing strips is shown in Figure C.30 of Appendix C.

Vertical displacement during loading was determined using a direct current displacement transducer (DCDT). A special carriage device from wood was machined to hold the DCDT to enable measurements of vertical displacement. The wooden base was rounded on the bottom to fit the inner radius of the pipe specimens. A threaded steel rod was screwed into the top of the wooden base to hold the DCDT. The DCDT was secured to the threaded steel rod using two zip ties. The top of the DCDT rested in a small hole in the upper wooden base. The top of the upper base was also rounded to fit the inner diameter of the pipe specimens. A picture of this device can be seen in Figure 3.15.

The rigid wooden base was centered under the loading ram. A pipe specimen was then placed on its side on the lower wooden bearing strips so that it was centered longitudinally and rested firmly. Next the upper bearing device was placed on top of the pipe specimen with the wooden strip touching the pipe specimen. The ram was lowered so that it touched the steel I-beam. The lower bearing, upper bearing, and pipe were then centered. The DCDT was then placed into the center of the pipe specimen and centered.

After zeroing the MTS machine the pipe specimens were then loaded. Loading rate was variable, but did not exceed 30 kN/linear meter throughout the duration of the test. Load and displacement were both recorded two times per second. Test was terminated after the maximum load decreased 200 pounds. Some pipe specimens were loaded, unloaded, and loaded again until failure occurred. Figure 3.15 shows the MTS machine and the 3-edge bearing test setup.



(a)



(b)



(c)



(d)

Figure 3.15 Pipe testing (a) Stack of the pipe specimens, (b) vertical displacement setup, (c) 3-edge bearing test, (d) MTS machine

3.4 Durability tests

Two durability tests were conducted to determine if the composite design mixes could withstand field conditions to which sewer pipes are subjected. The two durability tests conducted were water absorption and acid resistance. Specimens for the water absorption and acid resistance tests were made by cutting discs off of the cylinder specimens.

3.4.1 Water absorption procedure

Water absorption tests were conducted to indicate the amount of water the various design mixes absorbed. ASTM standard testing procedure D 570-98 Standard Test Method for Water Absorption of Plastics [36] was used as a guide to test the water absorption of the composite specimens. The discs were cut off of the cylinders using a power miter saw with a masonry blade. Discs were cut to a thickness of 6 mm instead of 3.175 mm as the ASTM test specifies; the power saw that was used caused the pieces of suggested size to break near the bottom edge. The discs had a diameter of 50.8 mm and a thickness of 6.35 mm.

One disc for each design mix was tested for water absorption. Discs were placed in the same container of tap water. The disc's weight, thickness, and two diameters at a right angle from each other were measured prior to submerging them into the water. Discs were placed into the water so a section of one part of the circumference touched the side of the container and another section of the same edge touched the bottom of the water container. The specimen discs were then left alone for a period of one week at room temperature. After one week, discs were removed from the water one at a time. Surfaces of the specimen discs were then dried with a cotton cloth rag. Their weights were recorded and then the discs were immediately placed back into the water container. The scale used to weigh the discs

measured to the nearest hundredth of a gram. The water absorption test was conducted after one week and every two weeks thereafter for a period of seven weeks.

3.4.2 Acid resistance procedure

Sulfuric acid, produced by Thiobacillus bacteria, is responsible for destroying Portland cement concrete sewer pipes. For this reason, it was used to determine the acid resistance of the composite material. The composite design mixes were tested with a 10% by volume sulfuric acid and water solution. ASTM standard testing procedure D 543-95 Standard Practices for Evaluating the Resistance of Plastics to Chemical Reagents [37] was used as a guide for this procedure. Specimens were cut from the cylinders in 6 mm thicknesses using a power miter saw with a masonry blade. One disc for each design mix was tested. Discs' weights, thicknesses at the center, and two diameters at right angles to each other were measured prior to introducing them into the acid. Dimensions were measured to at least 0.025 mm and the weights were measured to the nearest 0.01 grams.

Sulfuric acid was placed into Mason canning jars and the discs were then submerged into the acid. Each disc was placed in a separate jar. After placing the discs into jars, the lids were screwed on and the jars were left alone at room temperature for a period of one week. After one week, the lids of the jars were removed and specimens were taken out of the jar using tongs. Specimens were rinsed under running tap water to remove the sulfuric acid. Then, the surfaces of the specimen were wiped dry using a cotton cloth rag. The weight, thickness, and diameters of the specimen were then recorded. The specimen was placed back into the jar and the lid screwed down. Observations were recorded on the appearance of the specimen. These procedures were followed again at two week intervals for a period of seven weeks.

4 RESULTS

This chapter provides and discusses results for the tests conducted on cylinder specimens, pipe specimens, and disc specimens. Results for cylinder compression and splitting tensile tests along with statistical analysis of the results will be discussed first, followed by ultimate 3-edge bearing results for the pipe specimens, and then the results from the durability tests. The final section will discuss viscosity observations for the melted composite material.

4.1 Cylinder Specimens

Results for the cylinder specimens tested in compressive and splitting tensile had a wide range of variation between and within same design mix batches. This variation is believed to be a result of the manufacturing process, which affects the fiber orientation, uniformity, and air void development in the composite material. Compressive and splitting tensile average strengths are shown in Figures 4.1 through 4.14. Most figures show least squares linear regression line along with the equation and R^2 . The 95% confidence interval is also plotted for reference. A listing of cylinder specimen design mixes is provided in Table B.1 of Appendix B.

4.1.1 Statistical analysis of results

A statistical analysis was performed on the strength data for the cylinder specimens that were tested in compression and splitting tension in order to establish factors to most greatly affect engineering properties. Variables that were tested include: type of filler; filler to PET ratio; form of PET; percentage of fiberglass; length of fiberglass; and maximum particle size. There are 24 combinations, or treatments, which are a set of variables that are

being studied. The treatments are given the same name as their design mix number. Table B.4 in Appendix B shows the different treatments that were analyzed.

An analysis of variance (ANOVA) tests were performed first, and if significance was found, a least significant difference (LSD) test was performed. ANOVA tests tell whether or not there is a significant difference between treatments to offset the variance within a treatment. LSD is basically a t-test that compares the average compression and splitting tensile strengths for each treatment. It indicated if there is a significant difference between a pair of treatments. Significance was set at a 5% significance level. This significance level implies that there is a 5% chance/probability that the average differences are significant, when in fact they are not. The mean difference and significance for the variables that were tested can be seen in Tables B.4 through B.11 of Appendix B. If the significance is greater than 5% (0.05) then it is marked as “not significant”.

4.1.2 Compressive strength

Compressive strength results for the cylinder specimens are shown in Figures 4.1 through 4.7. The average compressive strengths for 96 specimens is 38.8 MPa, which is slightly greater than the ordinary PCC strength of 15 to 35 MPa. Although design mix variables were held constant, variability still existed within the manufacturing process, fiber orientation, material uniformity, and cooking time. Density of the composite ranged from 1.21 to 1.81 kg/dm³ with an average of 1.63 kg/dm³, which is lower than ordinary PPC densities of 1.9 to 2.5 kg/dm³. Cylinder specimens' dimensions, mass, load, compressive strengths, and densities are shown in Table C.2 of Appendix C.

Table 4.1 shows the elastic modulus for several design mixes. Values for elastic modulus varied from 920 MPa to 5700 MPa. The average elastic modulus was 3300 MPa (24 specimens), which is 7 to 10 times lower than ordinary Portland cement concrete. Stress vs. strain plots for the “A” specimens are shown in Figures B.1 through B.24 of Appendix B.

Table 4.1 Cylinder design mixes with average elastic modulus values

Specimens	Filler	PET to Filler Ratio	Form of PET	Fiber (%)	Length of fibers (mm)	Largest Particle Size (mm)	Average Elastic Modulus (MPa)
1-A and 2-A	P.C. fly ash	50/50	Processed	3	13		3247
3-A and 4-A	UNI FB	50/50	Processed	3	13	2	4108
5-A and 6-A	Ames	50/50	Processed	0			3196
7-A and 8-A	Ames	50/50	Processed	3	13		3394
9-A and 10-A	Ames	45/55	Processed	3	13		3286
11-A and 12-A	Ames	40/60	Processed	3	13		4043
13-A and 14-A	Ames	35/65	Processed	3	13		5656
15-A and 16-A	Ames	50/50	Processed	1	13		3216
17-A and 18-A	Ames	50/50	Processed	2	13		4250
19-A and 20-A	Ames	50/50	Processed	4	13		4605
21-A and 22-A	ISU CFB fly ash	50/50	Processed	3	13		5070
23-A and 24-A	ISU stoker bottom ash	50/50	Processed	3	13	2	4102
25-A and 26-A	Ames	50/50	Processed	3	6		2968
27-A and 28-A	Ames	50/50	Processed	4	6		2337
29-A and 30-A	Ames	50/50	Processed	5	6		2730
31-A and 32-A	Ames	50/50	Processed	6	6		3504
33-A and 34-A	Ames	50/50	Dirty	3	13		1956
35-A and 36-A	Ames	100/0	Clean	3	13		4129
37-A and 38-A	Plastic	50/50	Processed	3	13		1612
39-A and 40-A	Lime	50/50	Processed	3	13	2	1264
41-A and 42-A	ISU CFB bottom ash	50/50	Processed	3	13	4.750	1790
43-A and 44-A	ISU CFB bottom ash	50/50	Processed	3	13	0.425	1334
45-A and 46-A	ISU CFB bottom ash	50/50	Processed	3	13	0.150	2556
47-A and 48-A	Sump	50/50	Processed	3	13	0.150	4364

Figures 4.1 and 4.2 compare the different filler materials and indicate that most fillers add strength to the composite material. Filler material was varied while keeping all other design mix variables constant. ISU stoker bottom ash and pure plastic had similar strengths, whereas lime was half as strong. There is more variation in strength between fillers for the cylinder specimen than for the pipe specimens. UNI fluidized ash and ISU CFB fly ash are

the strongest filler materials with average compressive strengths of 112 MPa and 116 MPa, respectively. Table 4.2 shows significant statistical difference between the compressive strengths of filler materials.

Table 4.2 Statistical significance between compressive strengths for different fillers

Treatments	Compressive Strength (MPa)	Treatments	Compressive Strength (MPa)
P.C. fly ash - UNI FB	Y	Ames fly ash - Lime	Y
P.C. fly ash - Ames fly ash	N	Ames fly ash - ISU CFB bottom ash	N
P.C. fly ash - ISU CFB fly ash	Y	Ames fly ash - Sump	Y
P.C. fly ash - ISU stoker bottom ash	N	ISU CFB fly ash - IUS stoker bottom ash	Y
P.C. fly ash - No filler	N	ISU CFB fly ash - Plastic	Y
P.C. fly ash - Lime	Y	ISU CFB fly ash - Lime	Y
P.C. fly ash - CFB bottom ash	N	ISU CFB fly ash - ISU CFB bottom ash	Y
P.C. fly ash - Sump	Y	ISU CFB fly ash - Sump	N
UNI FB - Ames fly ash	Y	ISU stoker bottom ash - Plastic	Y
UNI FB - ISU CFB fly ash	N	ISU stoker bottom ash - Lime	Y
UNI FB - ISU stoker bottom ash	N	ISU stoker bottom ash - ISU CFB bottom ash	Y
UNI FB - No filler	Y	ISU stoker bottom ash - Sump	N
UNI FB - Lime	Y	Plastic - Lime	N
UNI FB - ISU CFB bottom ash	Y	Plastic - ISU CFB bottom ash	N
UNI FB - Sump	N	Plastic - Sump	Y
Ames fly ash - ISU CFB fly ash	Y	Lime - ISU CFB bottom ash	Y
Ames fly ash - ISU stoker bottom ash	N	Lime - Sump	Y
Ames fly ash - Plastic	N	ISU CFB bottom ash - Sump	Y

Y - significant difference

N - no significant difference

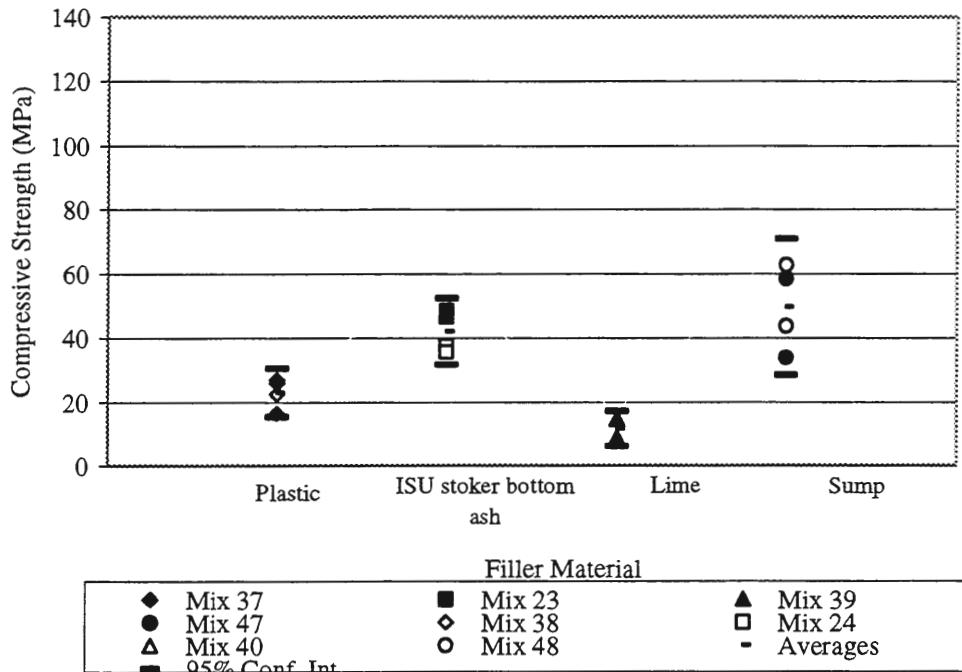


Figure 4.1 Cylinder specimens' compressive strength vs. filler material plot for different filler materials with, 13 mm long fiberglass fibers, 3% fiberglass by weight with 50/50 PET to filler ratio by weight

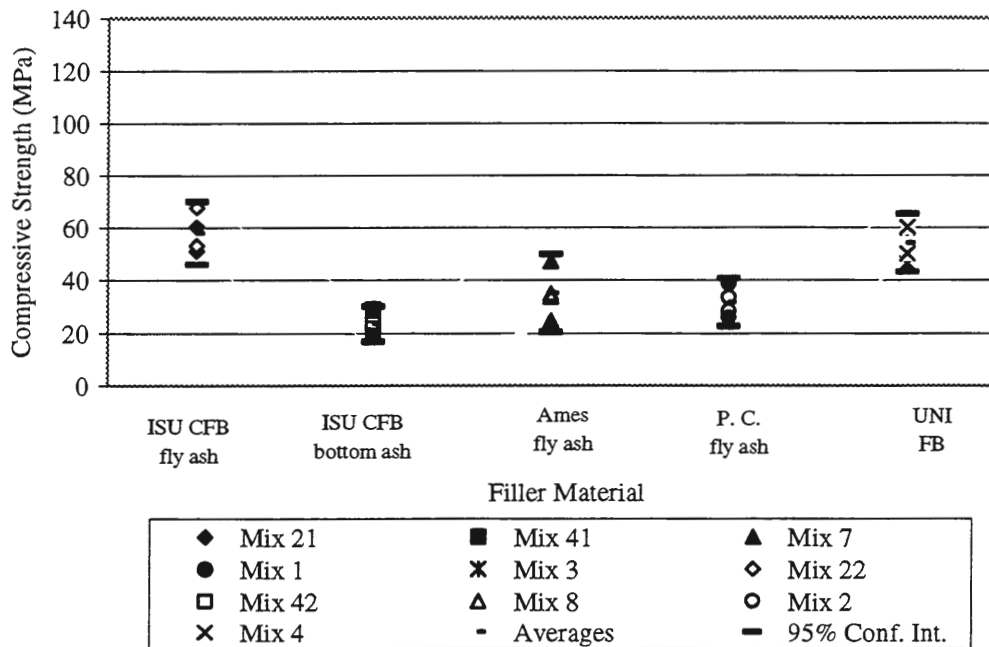


Figure 4.2 Cylinder specimens' compressive strength vs. filler material plot for different filler materials with, 13 mm long fiberglass fibers, 3% fiberglass by weight with 50/50 PET to filler ratio by weight

An analysis of PET to filler ratio was conducted utilizing Ames fly ash, keeping all other design mix variables constant. Results are presented in Figure 4.3 and indicate that increasing the PET to filler ratio increases the compressive strength. Optimum PET to filler ratio for the Ames fly ash was 35/65, which was the highest filler ratio attempted. There is a significant statistical difference between all PET to filler ratios except for 45/55-40/60, 50/50-40/60, 50/50-45/55, and 100/0-50/50.

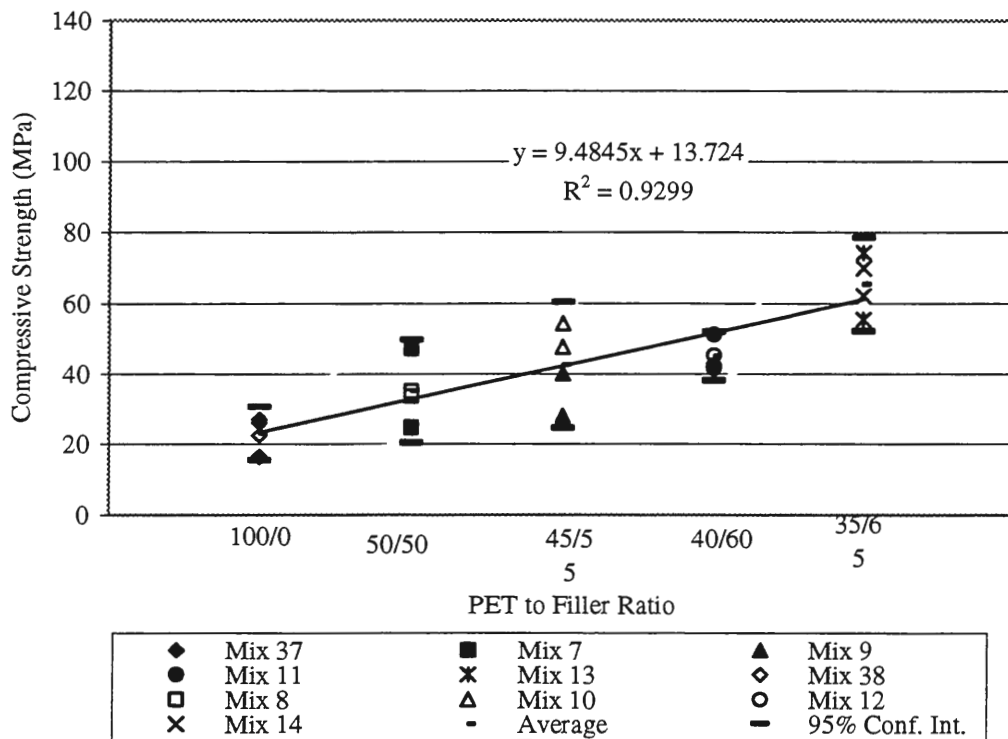


Figure 4.3 Cylinder specimens' compressive strength vs. PET to filler ratio for Ames fly ash, 13 mm long fiberglass fibers, 3% fiberglass by weight with different PET to filler ratio by weight

Tests were conducted to determine whether the 6 mm long fiberglass content would affect the compressive strength of the composite. These tests were conducted using Ames fly ash as the filler material. Fiber contents tested were 0, 3, 4, 5, and 6% by weight, keeping all other design mix variables constant. Figure 4.4 indicates no significant difference for fiber

contents from 3 to 6%. It also indicates the addition of fibers lowers the variability in the compressive strength. Six millimeter fibers produced a lower viscosity than the 13 mm fibers; therefore, 5 and 6% fiber content were manufactured. It was determined from a statistical analysis that there is not a significant difference between 6 mm long fiber contents and compressive strengths.

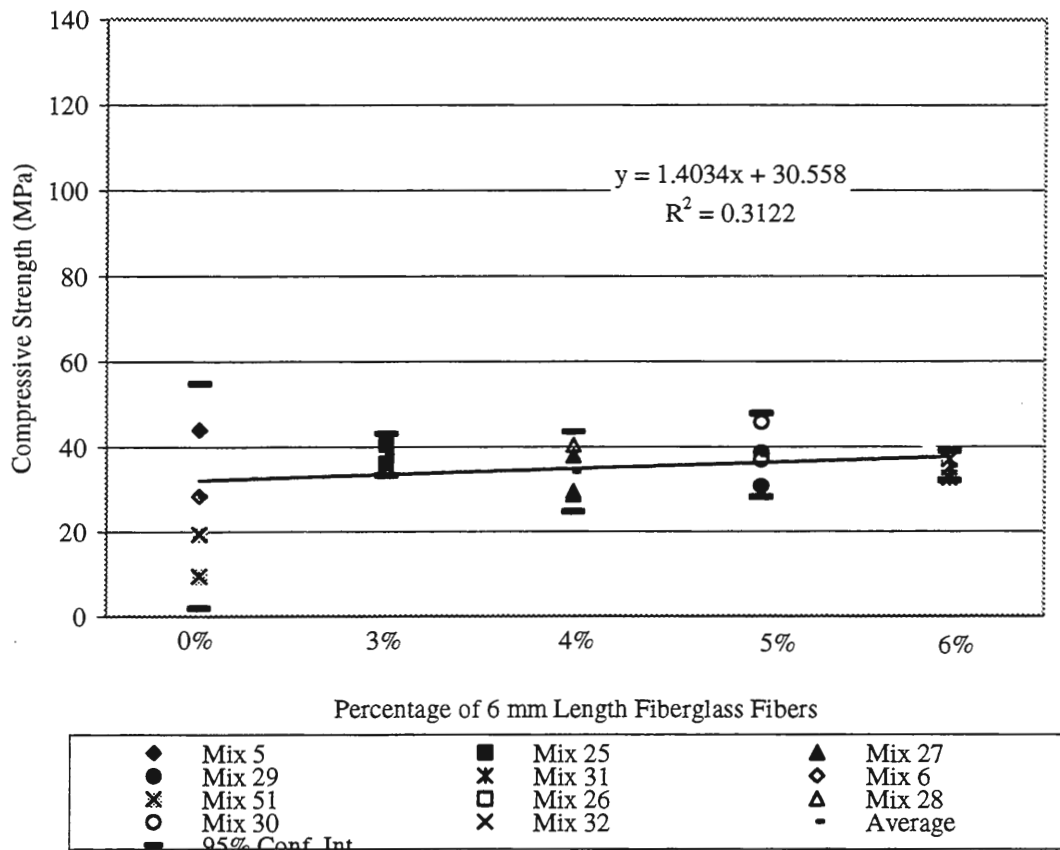


Figure 4.4 Cylinder specimens' compressive strength vs. percentage of 6 mm fiberglass fibers, Ames fly ash, variable fiberglass by weight with 50/50 PET to filler ratio by weight

An analysis of 13 mm long fiberglass content was conducted utilizing Ames fly ash as the filler material. Percentage of fibers varied from 0 to 4% by weight, keeping all other design mix variables constant. Figure 4.5 indicates a slight increase in the compressive

strength for fiber contents from 0 to 4%. There is a wider range in variation compared to the 6 mm long fibers in Figure 4.4. Statistical significant difference between fiber contents was determined from a statistical analysis for 0%-2%, 0%-4%, 3%-2%, 3%-4%, and 1%-4%.

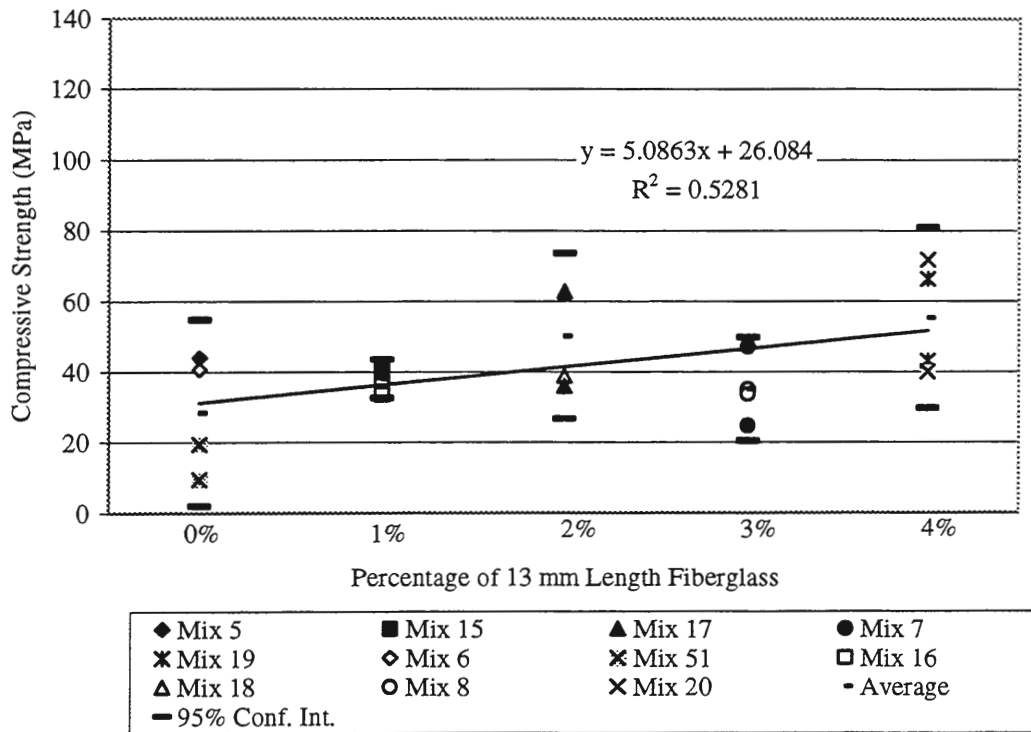


Figure 4.5 Cylinder specimens' compressive strength vs. percentage of 13 mm fiberglass fibers, Ames fly ash, variable fiberglass by weight with 50/50 PET to filler ratio by weight

Tests were conducted to determine whether the form of PET would affect the compressive strength of the composite. Figure 4.6 shows compressive strengths for the three forms of PET utilizing Ames fly ash, and keeping all other design mix variables constant. This figure indicates “clean” PET is stronger than the other two. This figure also shows impurities in the “dirty” PET affect the compressive strength. The statistical analysis determined there is a significant difference between compressive strengths for “processed”- “clean” and “dirty”- “clean” forms of PET.

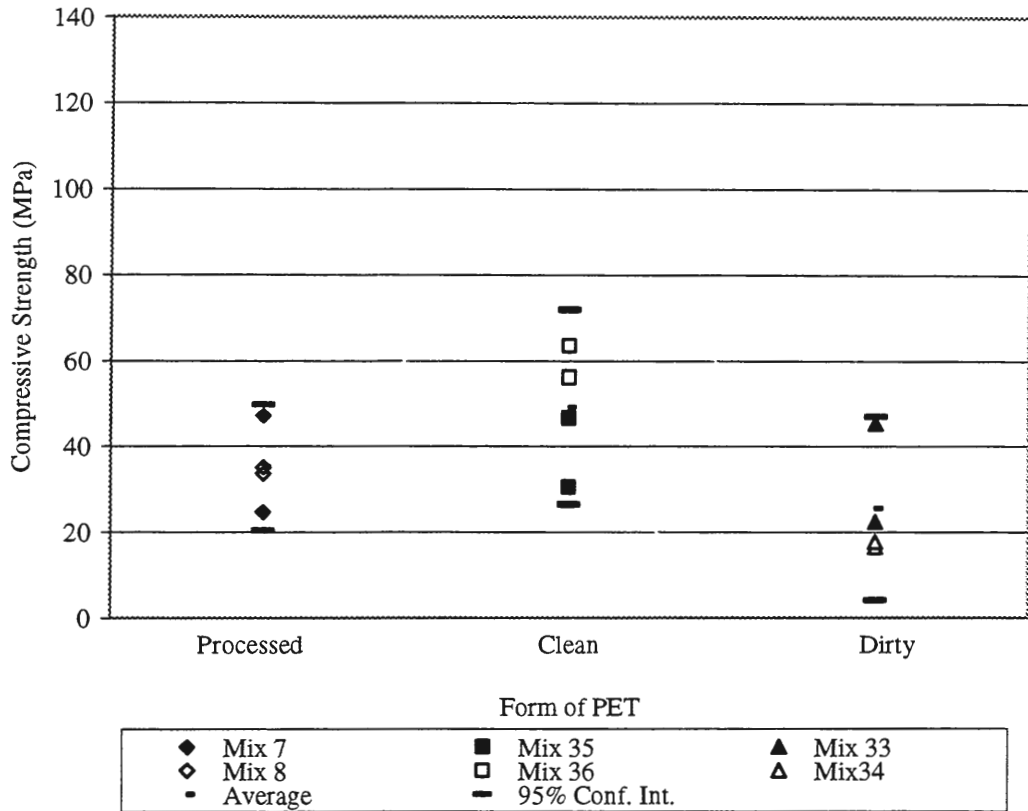


Figure 4.6 Cylinder specimens' compressive strength vs. form of PET for Ames fly ash, 13 mm long fiberglass fibers, 3% fiberglass by weight with 50/50 PET to filler ratio by weight

An analysis of the effect of maximum particle size was conducted utilizing ISU CFB bottom ash, keeping all other design mix variables constant. Figure 4.7 indicates particle size has a slight effect on the compressive strength. The three particle size limits were 4.75 mm, 0.425 mm, and 0.150 mm. Average values indicate compressive strengths increase as particle sizes decrease. It was determined from a statistical analysis that there is not a significant difference between maximum particle size and compressive strengths.

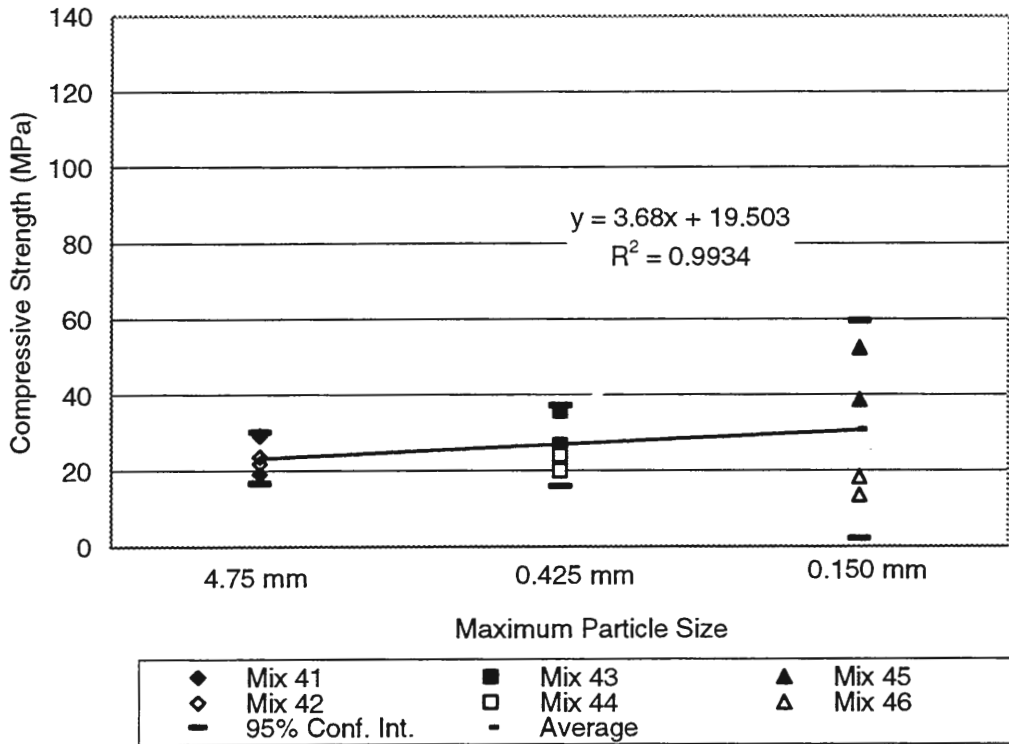


Figure 4.7 Cylinder specimens' compressive strength vs. maximum particle size plot for ISU CFB bottom ash, 13 mm long fiberglass fibers, 3% fiberglass by weight with 50/50 PET to filler ratio by weight

4.1.3 Splitting tensile strength

Splitting tensile strength results for cylinder specimens are shown in Figures 4.8 through 4.14. The average splitting tensile strengths for 96 specimens is 4.31 MPa, which is greater than the ordinary PCC strength of 1.5 to 3.5 MPa. Although design mix variables were held constant, variability still existed within the manufacturing process, fiber orientation, material uniformity, and cooking time. A listing of cylinder specimen design mixes can be seen in Table B.1 of Appendix B. Cylinder specimens' dimensions, tensile load, and splitting tensile strengths data are shown in Table B.3 of Appendix B.

Figures 4.8 and 4.9 compare the different filler materials and indicate most fillers add strength to the composite material. The filler material varied while keeping all other design

mix variables constant. Ames fly ash, P. C. fly ash, lime, and pure plastic all had similar splitting tensile strengths. ISU CFB fly ash and bottom ash had the highest average splitting tensile strengths, 8.6 MPa and 7.95 MPa, respectively. Table 4.3 shows significant statistical difference between the splitting tensile strengths of filler materials.

Table 4.3 Statistical significance between compressive strengths for different fillers

Treatments	Splitting Tensile Strength (MPa)	Treatments	Splitting Tensile Strength (MPa)
P.C. fly ash - UNI FB	Y	Ames fly ash – Lime	N
P.C. fly ash - Ames fly ash	N	Ames fly ash - ISU CFB bottom ash	Y
P.C. fly ash - ISU CFB fly ash	Y	Ames fly ash – Sump	Y
P.C. fly ash - ISU stoker bottom ash	Y	ISU CFB fly ash - IUS stoker bottom ash	Y
P.C. fly ash - No filler	N	ISU CFB fly ash – Plastic	Y
P.C. fly ash - Lime	N	ISU CFB fly ash – Lime	Y
P.C. fly ash - CFB bottom ash	Y	ISU CFB fly ash - ISU CFB bottom ash	N
P.C. fly ash - Sump	Y	ISU CFB fly ash – Sump	N
UNI FB - Ames fly ash	Y	ISU stoker bottom ash - Plastic	N
UNI FB - ISU CFB fly ash	Y	ISU stoker bottom ash - Lime	Y
UNI FB - ISU stoker bottom ash	N	ISU stoker bottom ash – ISU CFB bottom ash	Y
UNI FB - No filler	Y	ISU stoker bottom ash - Sump	Y
UNI FB - Lime	Y	Plastic – Lime	N
UNI FB - ISU CFB bottom ash	Y	Plastic - ISU CFB bottom ash	Y
UNI FB - Sump	N	Plastic – Sump	Y
Ames fly ash - ISU CFB fly ash	Y	Lime - ISU CFB bottom ash	Y
Ames fly ash - ISU stoker bottom ash	N	Lime – Sump	Y
Ames fly ash - Plastic	N	ISU CFB bottom ash – Sump	N

Y - significant difference

N - no significant difference

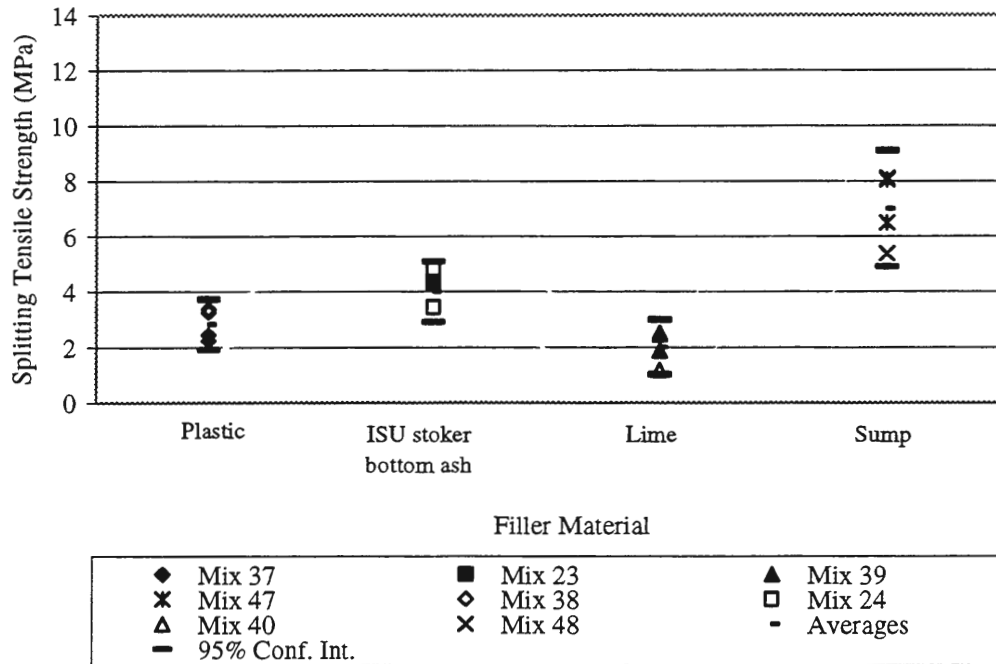


Figure 4.8 Cylinder specimens' splitting tensile strength vs. filler material plot for different filler materials with, 13 mm long fiberglass fibers, 3% fiberglass by weight with 50/50 PET to filler ratio by weight

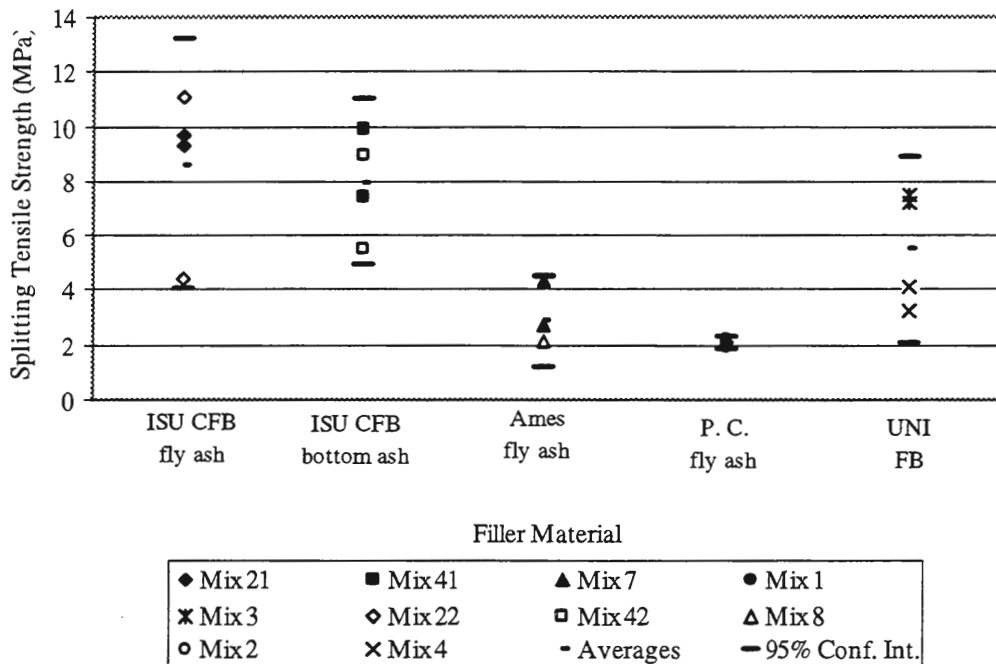


Figure 4.9 Cylinder specimens' splitting tensile strength vs. filler material plot for different filler materials with, 13 mm long fiberglass fibers, 3% fiberglass by weight with 50/50 PET to filler ratio by weight

An analysis of PET to filler ratio was conducted for the splitting tensile strength utilizing Ames fly ash, keeping all other design mix variables constant. Results are presented in Figure 4.10 and indicate increasing the PET to filler ratio increases the splitting tensile strength. Optimum PET to filler ratio for the Ames fly ash was 35/65, which was the highest filler ratio attempted. It was determined from a statistical analysis that there is a difference between the 35/65 PET to filler ratio and the other ratios. The other ratios did not show a significant difference.

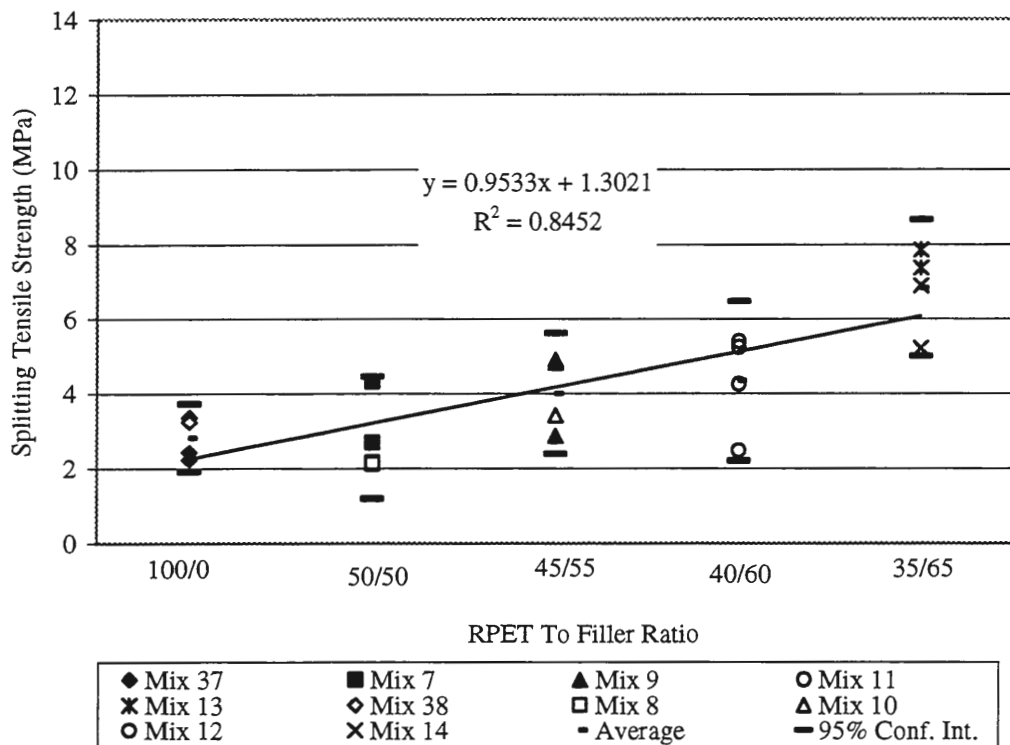


Figure 4.10 Cylinder specimens' splitting tensile strength vs. PET to filler ratio for Ames fly ash, 13 mm long fiberglass fibers, 3% fiberglass by weight with different PET to filler ratio by weight

An analysis of 6 mm long fiberglass content for the splitting tensile strength was conducted utilizing Ames fly ash as the filler material. Fiber contents tested were 0, 3, 4, 5, and 6% by weight, keeping all other design mix variables constant. Figure 4.11 indicates an

increase in the splitting tensile strength for fiber contents from 0 to 6%. The statistical analysis determined that there is a significant difference between the 0% and 6% fiber contents. This was the only significant statistical difference between 6 mm long fiberglass contents and splitting tensile strengths.

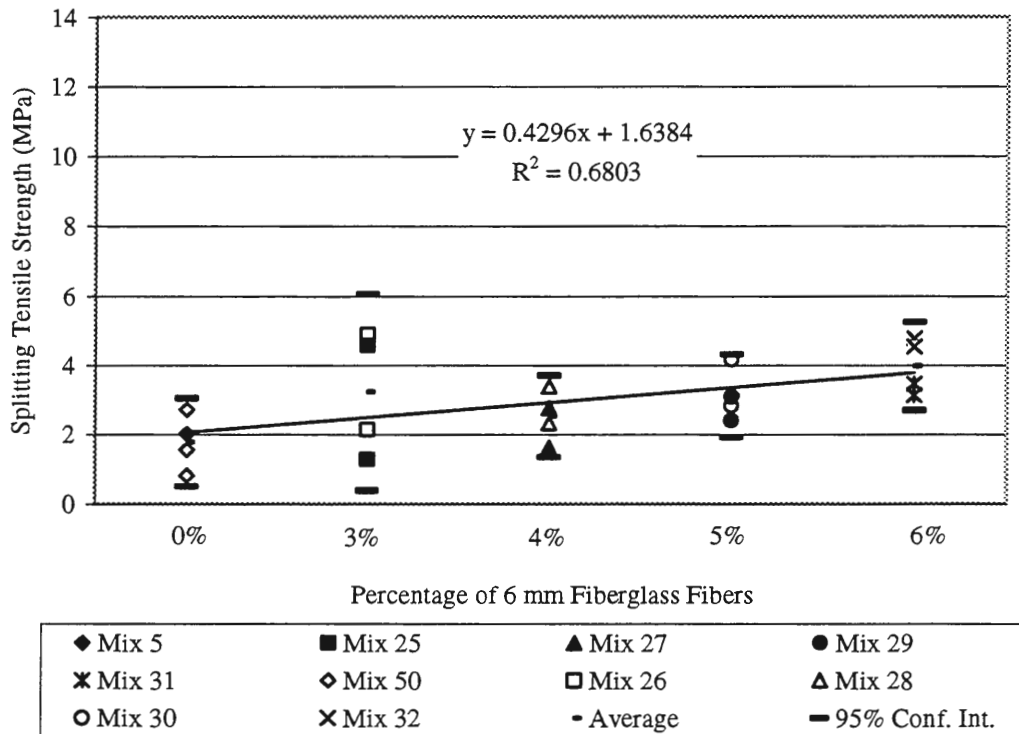


Figure 4.11 Cylinder specimens' splitting tensile strength vs. percentage of 6 mm fiberglass fibers, Ames fly ash, variable fiberglass by weight with 50/50 PET to filler ratio by weight

An analysis of 13 mm long fiberglass content for the splitting tensile strength was conducted utilizing Ames fly ash as the filler material. Percentage of fibers varied from 0 to 4% by weight, keeping all other design mix variables constant. Figure 4.12 indicates an increase in the splitting tensile strength for fiber contents from 0 to 4%. It was determined from a statistical analysis that there is not a significant difference between 13 mm long fiber contents and splitting tensile strengths.

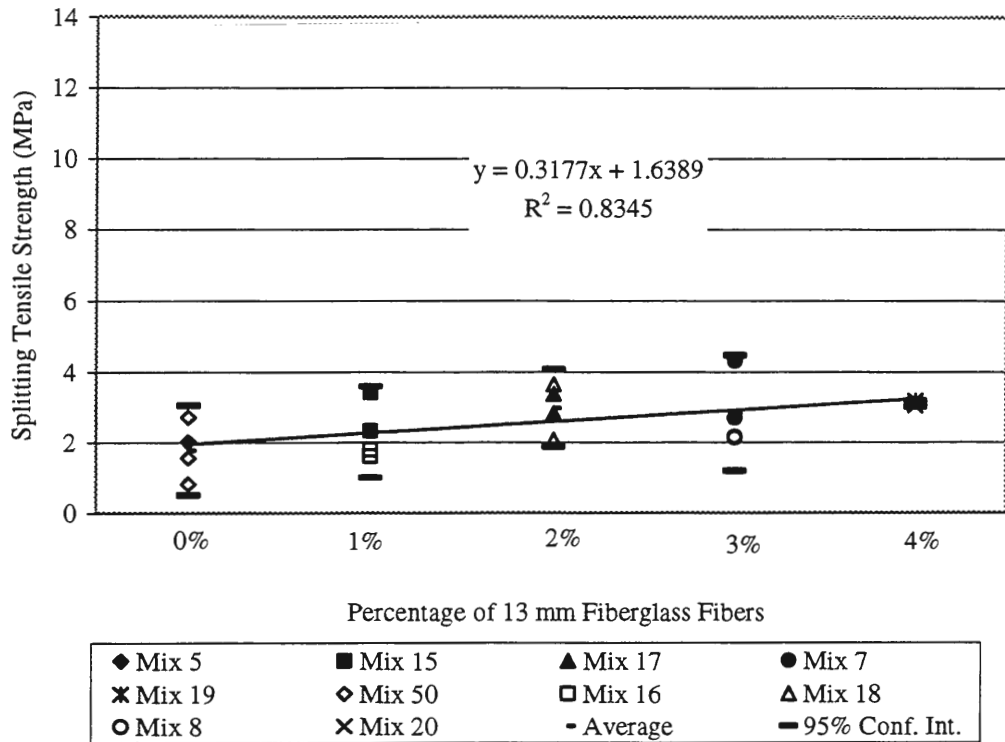


Figure 4.12 Cylinder specimens' splitting tensile strength vs. percentage of 13 mm fiberglass fibers, Ames fly ash, variable fiberglass by weight with 50/50 PET to filler ratio by weight

Tests were conducted to determine whether the form of PET would affect the splitting tensile strength of the composite. Figure 4.13 shows splitting tensile strengths for the three forms of PET utilizing Ames fly ash and keeping all other design mix variables constant. This figure indicates "clean" PET is stronger than the other two. Splitting tensile strengths for the "dirty" PET are larger than "processed" values. This figure shows impurities in the "dirty" PET did not affect the splitting tensile strength as they did for the compressive strength. It was determined from a statistical analysis that there is not a significant difference between the form of PET and splitting tensile strengths.

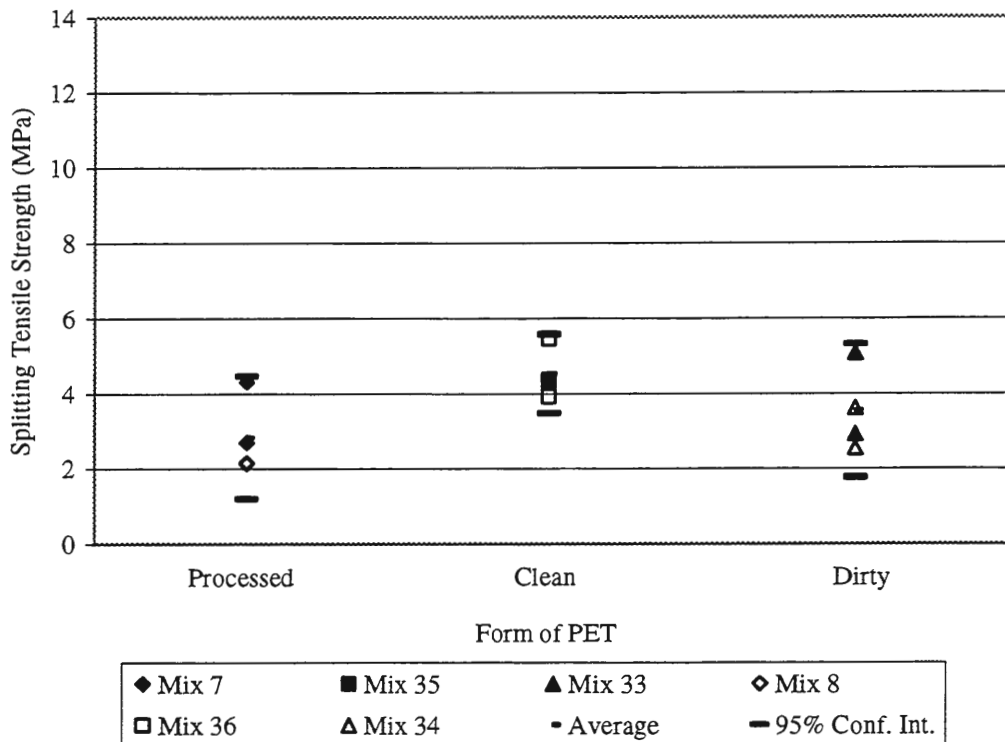


Figure 4.13 Cylinder specimens' splitting tensile strength vs. form of PET for Ames fly ash, 13 mm long fiberglass fibers, 3% fiberglass by weight with 50/50 PET to filler ratio by weight

An analysis of the effect of maximum particle size was conducted utilizing ISU CFB bottom ash, keeping all other design mix variables constant. Figure 4.14 indicates particle size has a slight effect on the splitting tensile strength. The three particle size limits were 4.75 mm, 0.425 mm, and 0.150 mm. Average values indicate splitting tensile strength decreases as particle sizes decrease. It was determined from a statistical analysis that there is not a significant difference between particle sizes and splitting tensile strengths.

Specimens without fibers develop cracks during the cooling process and would break as they were removed from their molds as shown in Figure 4.15. This specimen shows air voids of different size occurring throughout the sample, typical for all of the composite specimens. It also shows the accumulation of air voids towards the top of the cylinder.

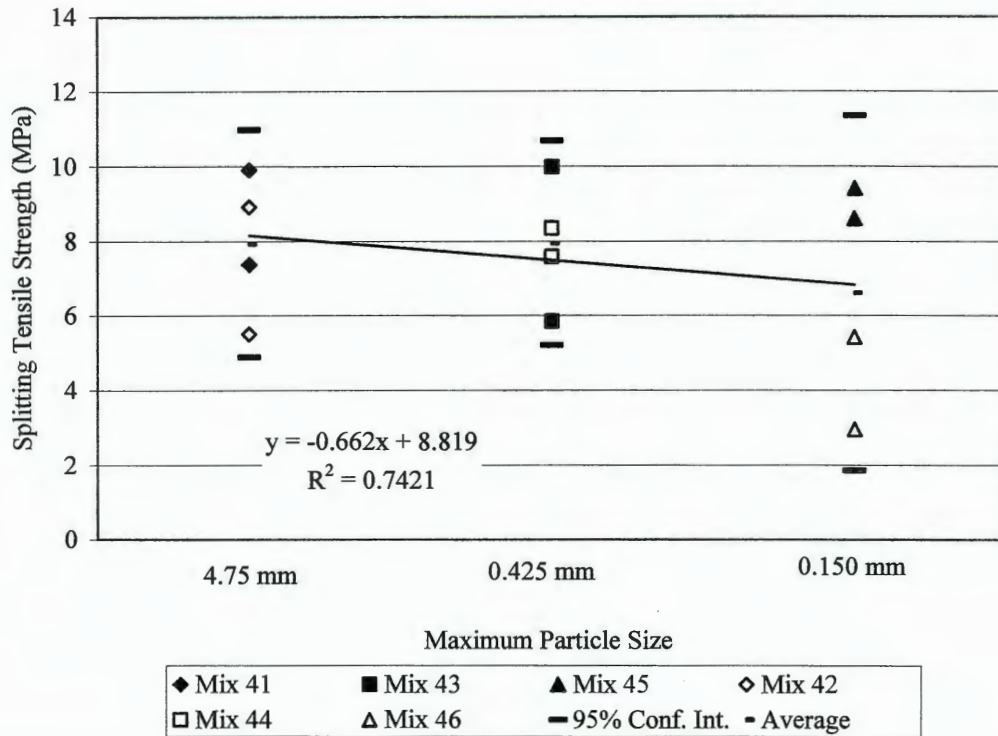


Figure 4.14 Cylinder specimens' splitting tensile strength vs. maximum particle size plot for ISU CFB bottom ash, 13 mm long fiberglass fibers, 3% fiberglass by weight with 50/50 PET to filler ratio by weight

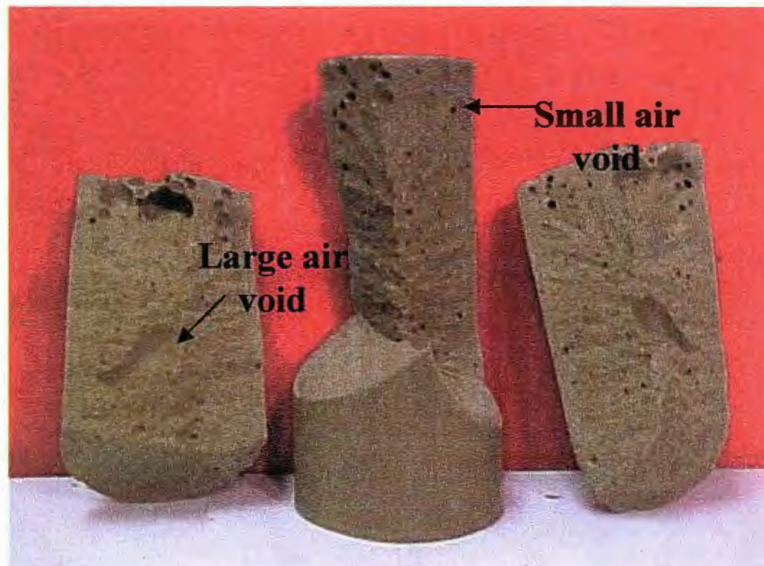


Figure 4.15 Composite material with no fiberglass

Figure 4.16 shows two cylinder specimens with the same design mix (UNI fluidized bed ash, 50/50 PET to filler ratio, 13 mm long fibers, and 3% fiber content). The specimen on the left had less than half the splitting tensile strength as the one on the right. The specimen on the right with the greater strength also had the greatest amount of fibers exposed. It is believed the variation in fiber orientation caused this strength difference.

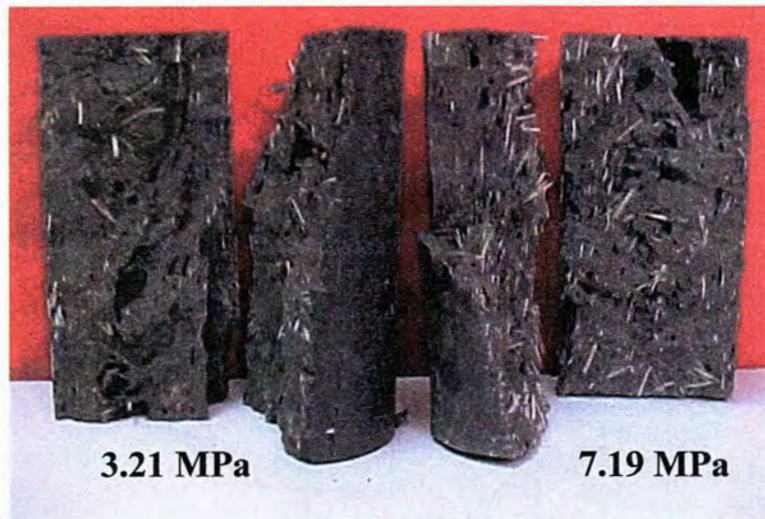


Figure 4.16 Cylinder specimens made from UNI FB with 3% fiberglass by weight tested in splitting tension

4.2 Pipe Specimens

4.2.1 Ultimate 3-edge bearing strength

Ultimate 3-edge bearing strength results of the 26 pipe specimens are shown in Figures 4.17 through 4.26. Although design mix variables were held constant, variability within the manufacturing process, such as wall thickness, fiber orientation, cooking time, and material uniformity, still existed. A list of pipe specimen design mixes can be seen in Table C.1 of Appendix C. Pipe specimens' heights; top, bottom, and average thicknesses; and average area is shown in Table C.2 of Appendix C. Graphs showing the crushing strengths vs. stains for the pipe specimens are shown in Figures C.1 through C.26 of Appendix C.

Pipe specimens with a 230 mm inside diameter and a 38 mm wall thickness were produced from composite materials. Loads to produce ultimate D-loads, ranged from 21.65 to 94.65 N/m/mm. Average ultimate D-load for the 26 pipe specimens was 53.18 N/m/mm. Although no ASTM ultimate D-load specification exists for pipes with a 230 mm inside diameters, there are requirements for diameters ranging from 200 to 250 mm. Twenty-three of the 26 pipe specimens exhibited greater ultimate D-load strengths than are required by ASTM for the 200 and 250 mm diameter vitrified extra strength clay pipes and all classes of nonreinforced concrete pipes.

Figures 4.17 and 4.18 compare different filler materials and indicate fillers add strength to the RPET. Type of filler material used also affected the ultimate 3-edge bearing strength. All pipe specimens for these two figures had a PET to filler ratio of 50/50, 3% fiberglass content by weight, and fibers with a length of 13 mm.

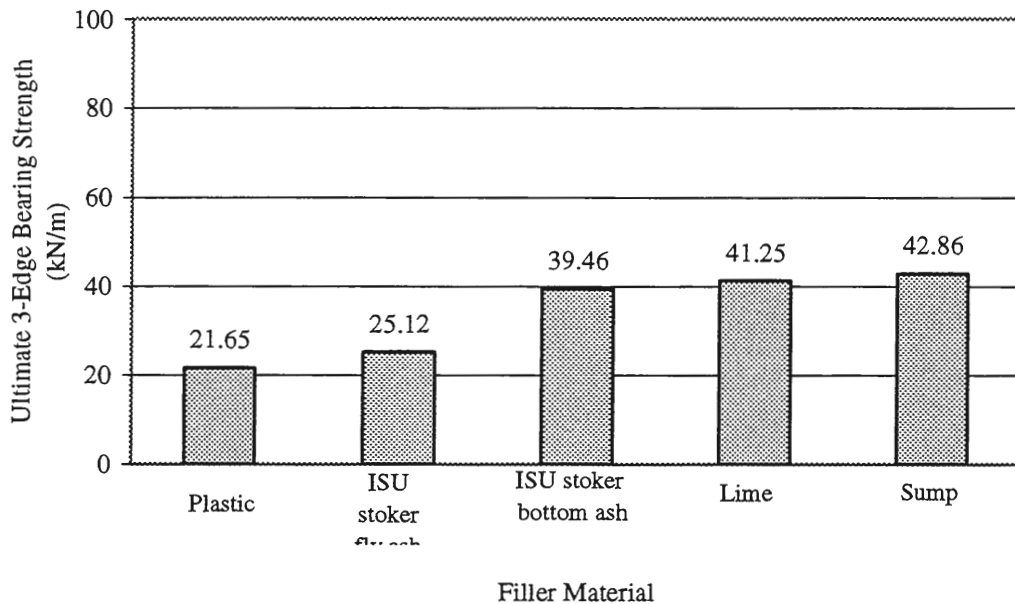


Figure 4.17 Pipe specimens ultimate 3-edge bearing strength vs. filler material for different filler materials, 13 mm long fiberglass fiber, and 3% fiberglass by weight with 50/50 PET ratio by weight

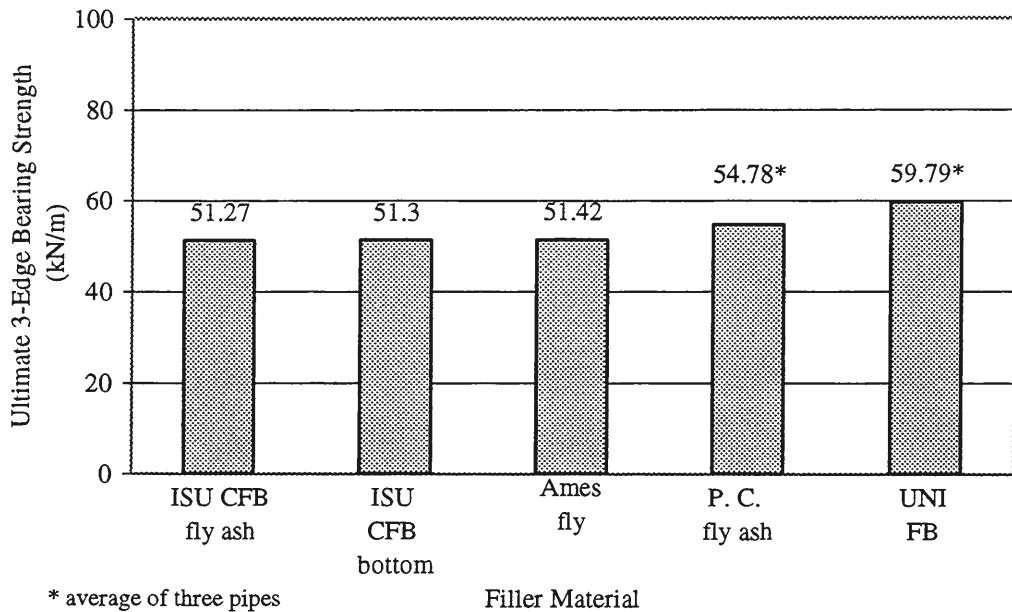


Figure 4.18 Pipe specimens ultimate 3-edge bearing strength vs. filler material for different filler materials, 13 mm long fiberglass fiber, and 3% fiberglass by weight with 50/50 PET ratio by weight

An analysis of PET to filler ratio was conducted utilizing UNI fluidized bed ash, keeping all other design mix variables constant. Results are presented in Figure 4.19, and indicate increasing PET to filler ratio increases the ultimate 3-edge bearing strength. Optimum PET to filler ratio for UNI fluidized bed ash was 40/60. A higher PET to filler ratio at 33/67 resulted in a lower ultimate 3-edge bearing strength. Even higher filler contents were attempted, but the PET was not able to completely coat the filler material.

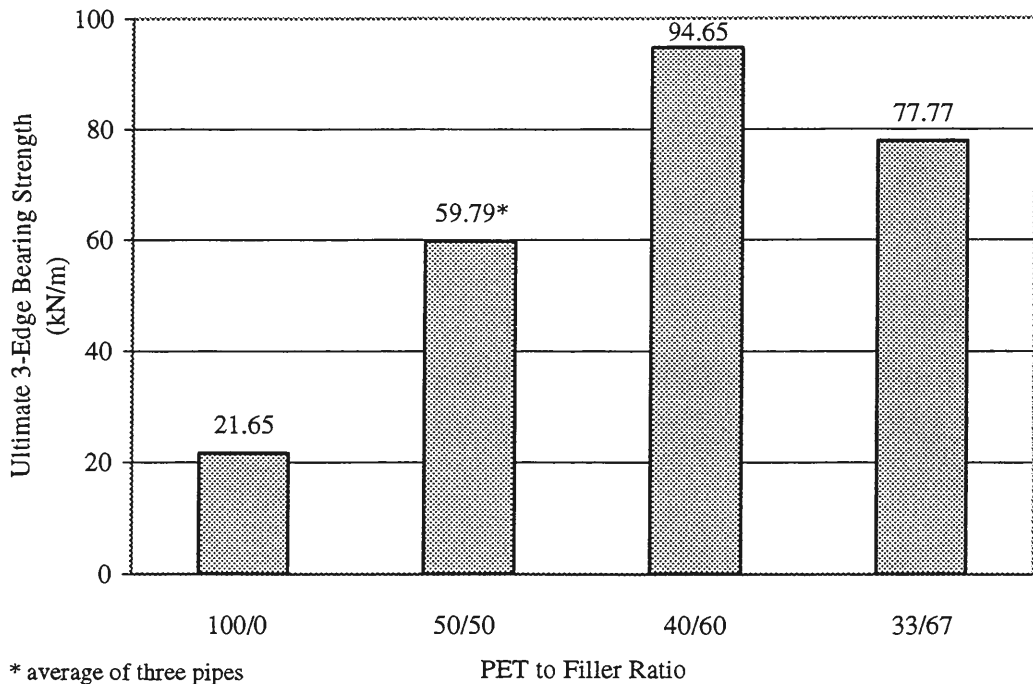


Figure 4.19 Pipe specimens ultimate 3-edge bearing strength vs. PET to filler ratio for UNI fluidized bed ash, 13 mm long fiberglass fiber, 3% fiberglass by weight with changing PET to filler ratio by weight

An analysis of the influence of fiberglass content was conducted utilizing lime as filler material. Percentage of fibers varied from 3 to 4% by weight (plastic and filler), keeping all other design mix variables constant. Figure 4.21 indicates the optimum fiberglass content is 3.5%. However, variation in wall thickness due to manufacturing is believed to have contributed to changes in the ultimate 3-edge bearing strengths. Wall thickness varied for both specimens with 4% fiber content. Figure 4.20 shows the variation in wall thickness for one of the pipes with 4% fiber content. Strengths for the two specimens with 4% fiber were 50.5 and 55.1 kN/m. The manufacturing process limits the maximum fiberglass content to 4% for the 13 mm fibers. Fiberglass content greater than 4% could not be produced due to high viscosity and inability to homogenize the mixture. In the future, alternative manufacturing methods could be developed to overcome this problem.



Figure 4.20 Pipe specimen #18 with 4% fiberglass content

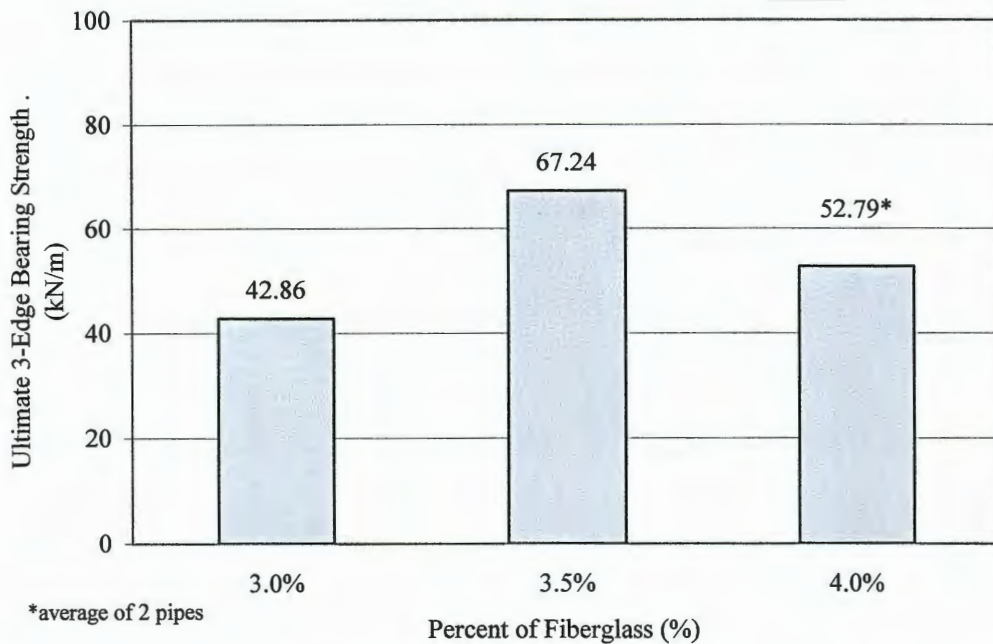


Figure 4.21 Pipe specimens ultimate 3-edge bearing strength vs. percent of fiberglass for Lime, 13 mm long fiberglass fiber, changing fiberglass percent by weight with 50/50 PET to filler ratio by weight

Ultimate 3-edge strength tests were also conducted to determine whether the PET material would influence the strength. Figure 4.22 shows the ultimate 3-edge bearing

strengths for the three forms of PET (“processed”; “clean”; and “dirty”) utilizing Ames fly ash and keeping all other design mix variables constant. All three specimens had very similar wall thicknesses. Results indicate that all forms of PET are similar in ultimate 3-edge bearing strength, with “dirty” being the strongest. The impurities in the “dirty” PET, therefore, do not adversely affect the strength of the composite. If this is true, then impurities would not need to be removed from beverage bottles, which would lower PET processing cost.

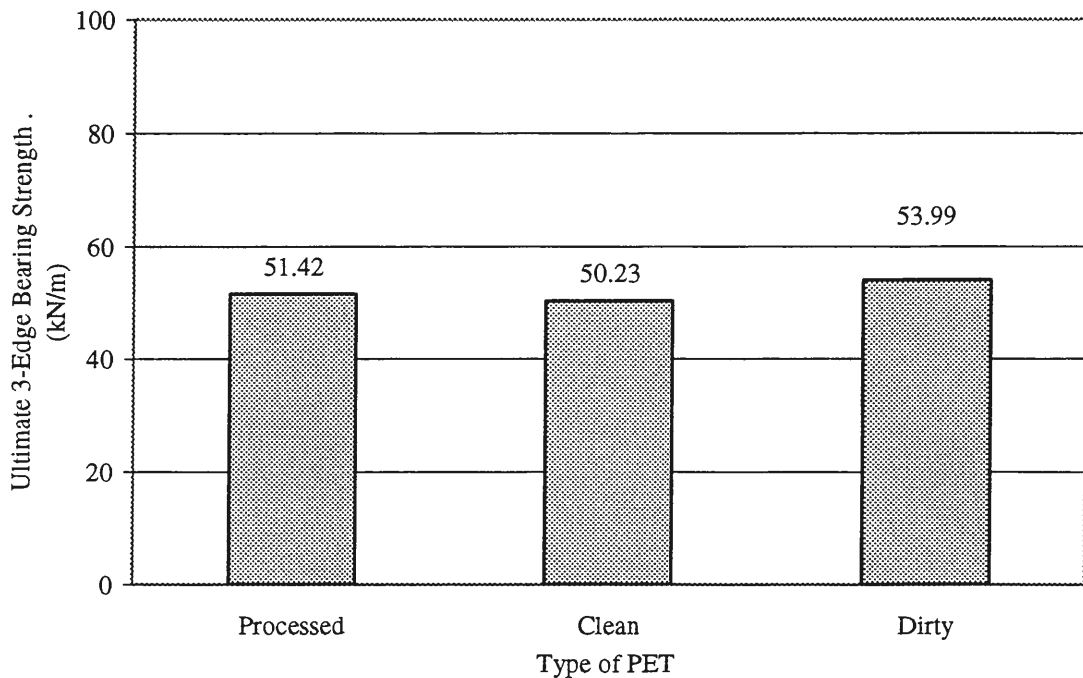


Figure 4.22 Pipe specimens ultimate 3-edge bearing strength vs. form of PET for Ames fly ash, 13 mm long fiberglass fiber, and 3% fiberglass by weight with 50/50 PET to filler ratio by weight

An analysis of the maximum particle size was conducted utilizing ISU CFB bottom ash, keeping all other design mix variables constant. Figure 4.24 indicates that particle size affects the ultimate 3-edge bearing strength. The four particle size limits were 4.75 mm, 2 mm, 0.425 mm and 0.150 mm. Prior to testing, the wall thicknesses for both the 4.75 and 2

mm specimens expanded slightly at the ends. This is believed to be a result of water absorption from humidity in the air. Ash material from the 2 mm specimen was dusting prior to being tested as shown in Figure 23. The ultimate 3-edge bearing strength for this specimen is nearly half as much as the other specimens. It is believed PET did not uniformly coat all particles in the 2 mm specimen.

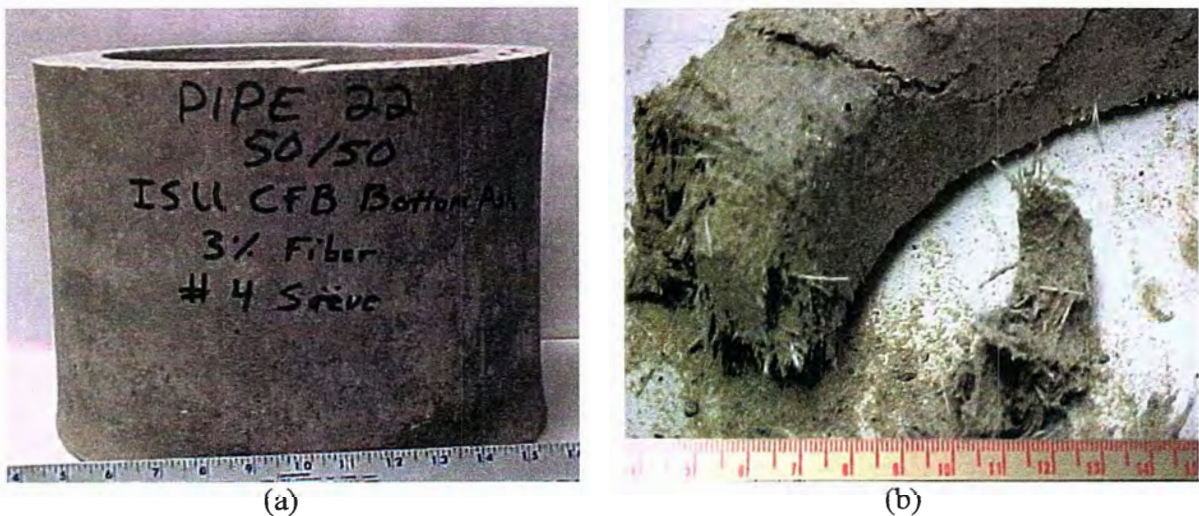


Figure 4.23 (a) Ends of pipes expanding due to the moisture in the air, (b) dusting

To verify the recyclability of this composite, two pipes were made from end pieces that were cut from pipe specimens. The end pieces were crushed to the size of particles as shown in Figure 4.25. The crushed recycled composite consisted of several different design mixes. This material (composite and fibers) was then manufactured into a pipe specimen. An additional 3% fibers were added to one recycled pipe. As indicated in Figure 4.26, the addition of fibers weakens the ultimate 3-edge bearing strength. It is believed fibers in the specimen with additional fibers were not evenly coated with the composite material due to manufacturing processes.

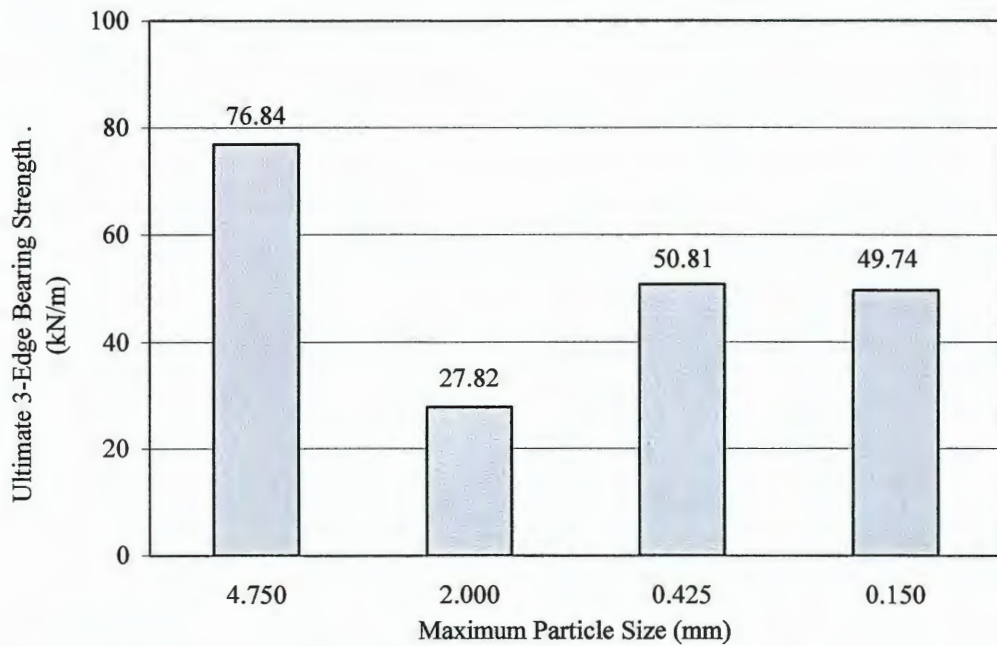


Figure 4.24 Pipe specimens ultimate 3-edge bearing strength vs. maximum particle size for ISU CFB bottom ash, 13 mm long fiberglass fiber, and 3% fiberglass by weight with 50/50 PET to filler ratio by weight



(a)



(b)

Figure 4.25 (a) Crushed pipe composite material, (b) pipe made from recycled composite pipe material

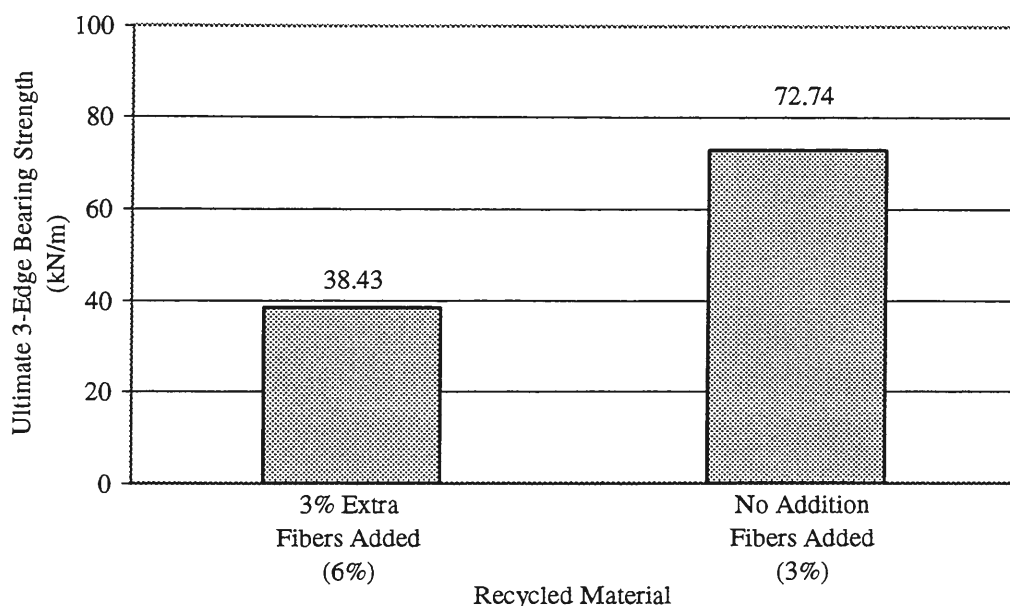


Figure 4.26 Pipe specimens ultimate 3-edge bearing strength vs. recycled material, 13 mm long fiberglass fiber, 3% to 6% fiberglass by weight with recycled composite material

4.2.2 Microstructural observations

A scanning electron microscope (SEM) was used to give an indication of the interaction between the PET binder and filler and the fiberglass fibers. Sump with a 50/50 PET to filler ratio and 3% fiberglass content by weight was the composite design mixture scanned. Figure 4.27 is images from the SEM at different magnifications. The fiberglass fibers shown in Figure 4.27 are different than the fibers used during this study. The fibers shown have lengths of 12 mm and widths of 0.75 mm. Figure 4.27 (a) is an image showing good bonding between the composite and fiberglass fibers magnified 600 times and (b) is the same image magnified 3,500 times. 4.27 (c) and (d) shows the fibers failed by shearing, which would also indicate good bonding between the fiber and the composite.

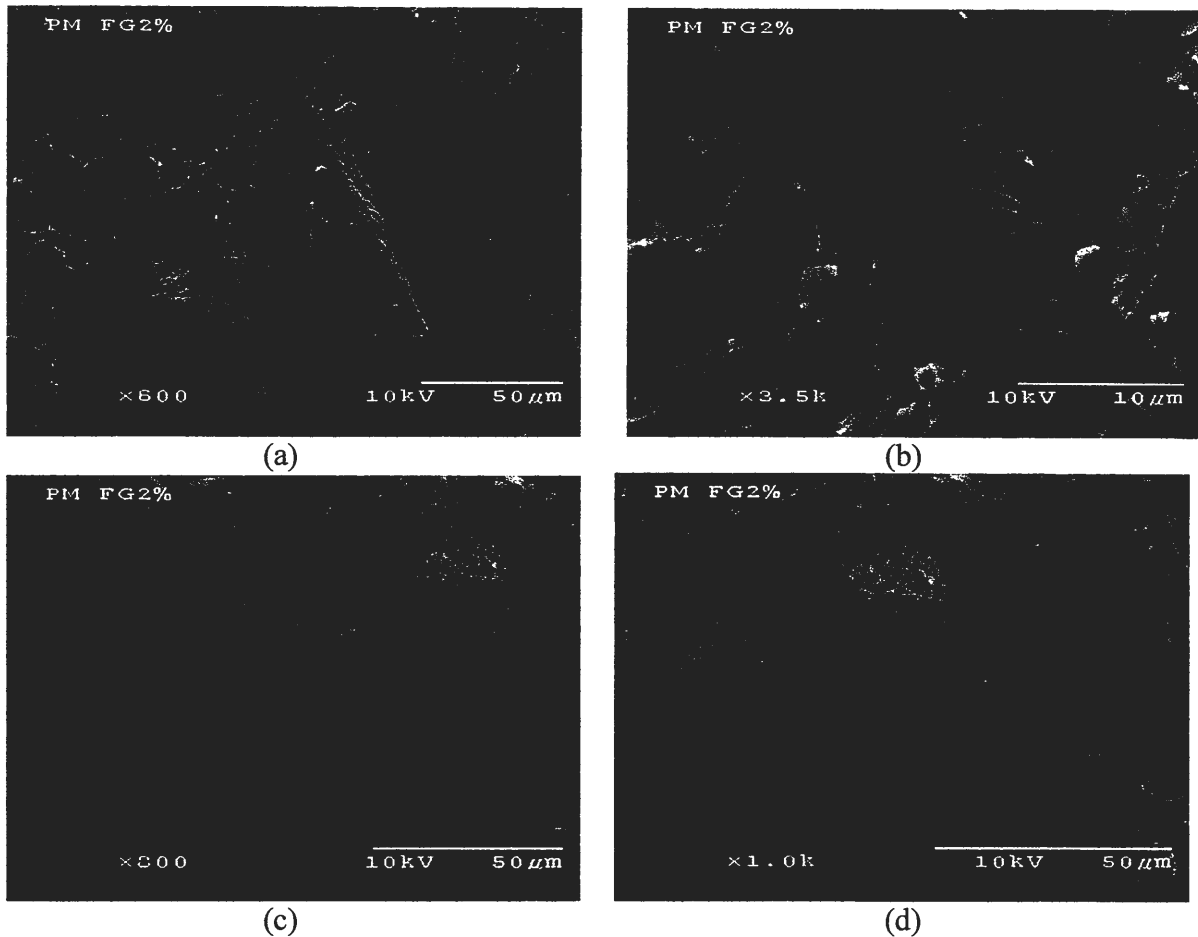


Figure 4.27 Bonding between the fiberglass fibers and the composite, (a) depicts good bonding magnified 600 times, (b) depicts good bonding magnified 3,500 times, (c) sheared fiberglass magnified 800 times, (d) sheared fiberglass magnified 1,000 times

The failure planes for the pipe specimens are shown in Figure 4.28. It is believed pipe specimens failed because the fiberglass pulled out of the composite material along the failure planes. These fibers were not evenly coated with composite material. Figure 4.29 (a) and (b) shows the failure plane of a pipe specimen. It is believed that the uncoated fibers did not contribute sufficient strength to the composite material, possibly creating points of weakness. Cracks could propagate along the composite and fiber interface. The thin fibers in Figure 4.29 (b) were evenly coated producing good bonding between the fiber and the

composite. As a result of the good bonding, the fibers failed by shearing throughout the length of the fiber.

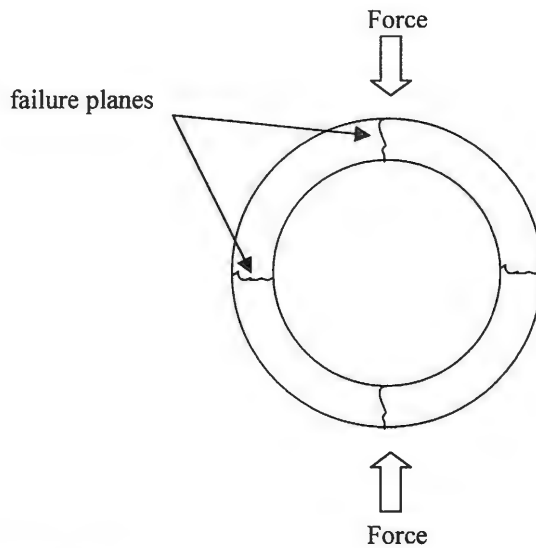
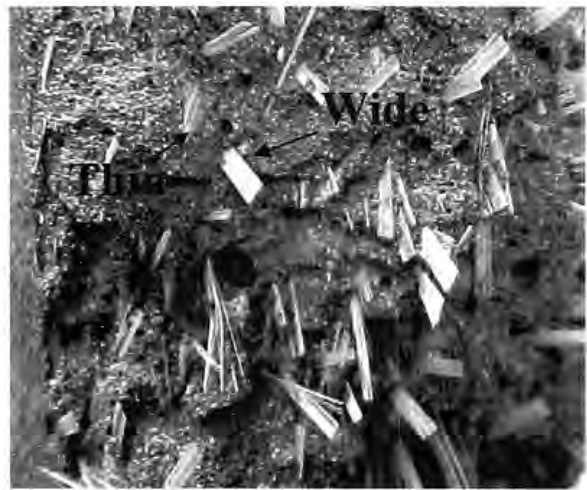


Figure 4.28 Diagram of pipe failure



(a)



(b)

Figure 4.29 Pipe failure plane, (a) longitudinal angle of the failure plane, (b) close up of fiberglass

Figure 4.30 shows different samples of ISU CFB bottom ash, (a) is the filler material before processing, (b) shows the effect of moisture from the air, (c) shows crystals on the

pipe specimen after being submerged in water for one month, (d) shows thickness of specimen after being submerged for one month.

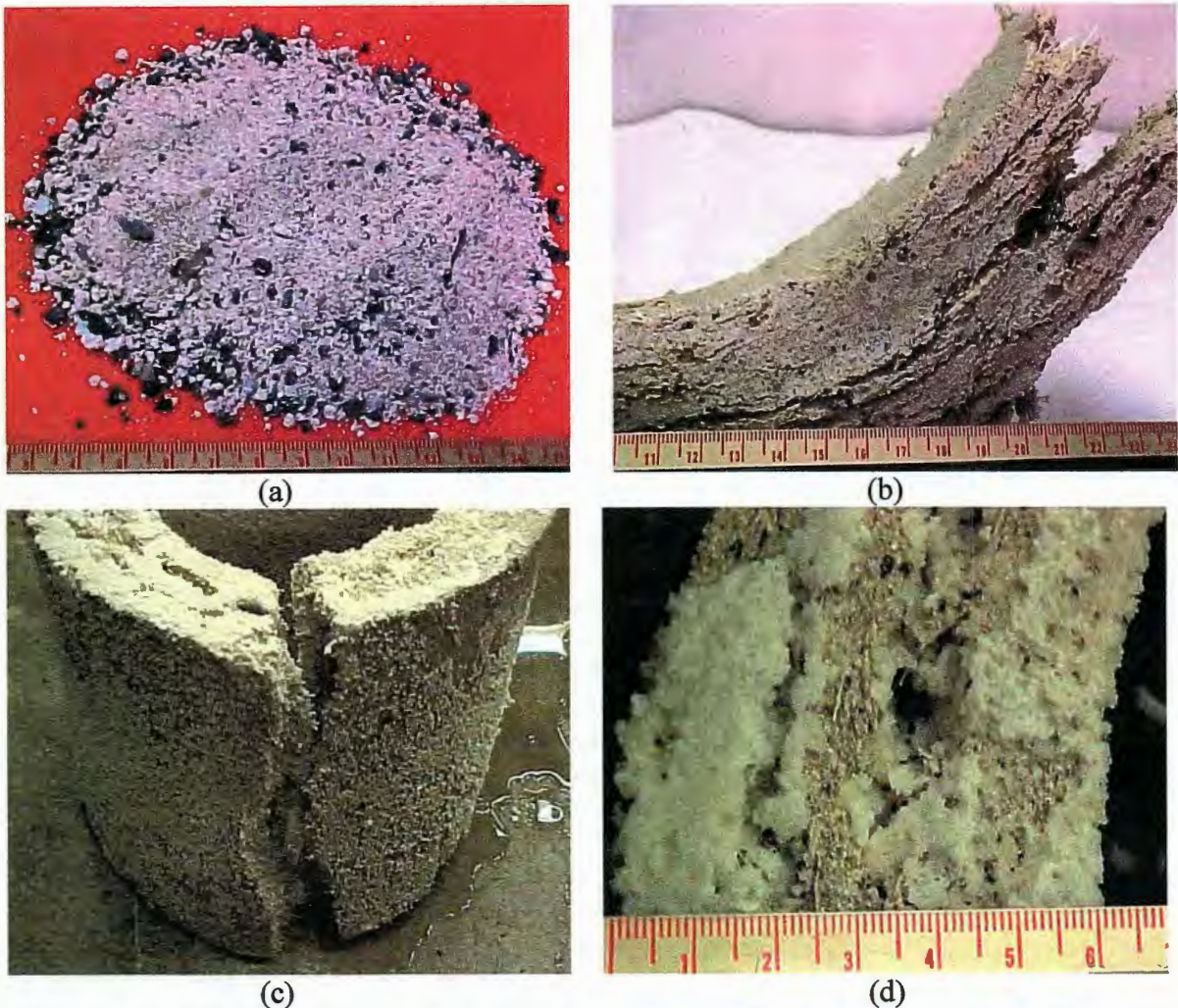


Figure 4.30 ISU CFB bottom ash water absorption, (a) filler material, (b) end piece exposed to air, (c) pipe specimen submerged in water for 1 month, (d) thickness of pipe submerged in water for 1 month

4.3 Durability Tests

4.3.1 Water absorption tests

Water absorption tests were conducted for 7 weeks. The results are presented in Table 4.4. The Δ symbol is the percent difference in water absorption between composites with filler and pure plastic. Positive numbers indicated that the composites with filler

absorbed more water than the pure plastic. All specimens with sulfur trioxide contents higher than 12% had high water absorption. Specimens with ISU CFB bottom ash, which has a sulfur trioxide content of 30.7%, exhibited water absorption of approximately 12%. The Sump material absorbed the least water. Figure 4.31 shows the Sump (47) and one of the ISU CFB bottom ash specimens (46). Water absorption weekly data results are shown in Table D.1 of Appendix D.

Table 4.4 Water absorption results

Specimen	Filler Type	PET to Filler Ratio	Form of PET	Length of Fibers (mm)	Fibers (%)	Largest particle size	Water Absorbed (%)	Δ (%)
1	P. C. fly ash	50/50	Processed	13	3	---	4.62	0.17
4	UNI FB	50/50	Processed	13	3	2	8.58	4.13
8	Ames	50/50	Processed	13	3	---	4.48	0.03
10	Ames	45/55	Processed	13	3	---	4.04	-0.42
11	Ames	40/60	Processed	13	3	---	3.99	-0.46
13	Ames	35/65	Processed	13	3	---	5.76	1.30
16	Ames	50/50	Processed	13	1	---	3.79	-0.66
17	Ames	50/50	Processed	13	2	---	4.40	-0.05
19	Ames	50/50	Processed	13	3	---	5.05	0.60
22	ISU CFB fly ash	50/50	Processed	13	3	---	10.65	6.20
24	ISU stoker bottom ash	50/50	Processed	13	3	2	5.26	0.81
26	Ames	50/50	Processed	6	3	---	3.74	-0.71
28	Ames	50/50	Processed	6	4	---	3.56	-0.89
29	Ames	50/50	Processed	6	5	---	3.90	-0.55
31	Ames	50/50	Processed	6	6	---	4.09	-0.36
33	Ames	50/50	Dirty	13	3	---	4.68	0.22
36	Ames	50/50	Clean	13	3	---	4.07	-0.38
38	Plastic	100/0	Processed	13	3	---	4.45	0.00
39	Lime	50/50	Processed	13	3	2	7.17	2.72
42	ISU CFB bottom ash	50/50	Processed	13	3	4.750	11.76	7.31
44	ISU CFB bottom ash	50/50	Processed	13	3	0.425	12.19	7.73
46	ISU CFB bottom ash	50/50	Processed	13	3	0.150	12.36	7.91
47	Sump	50/50	Processed	13	3	0.150	1.80	-2.66

Δ - percent of absorbed water above (+) or below (-) plastic specimen



Figure 4.31 Water absorption test specimens

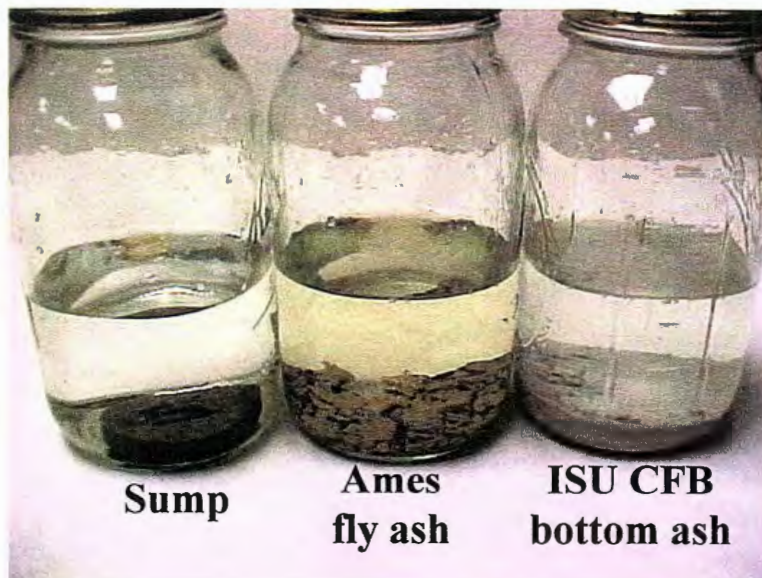
4.3.2 Acid tests

Summary of the results for the acid resistance tests are shown in Table 4.5.

Specimens in Table 4.5 have the same design mixes that are in Table 4.4. The positive numbers indicate specimens absorbed sulfuric acid solution. This test indicated the only specimens which could withstand a solution of 10% sulfuric acid are the Sump (47) and pure plastic (38). Figure 4.32 shows the Sump (47), Ames fly ash (26), and ISU CFB bottom ash (42) specimens. The pieces shown in the Ames fly ash specimen in Figure 4.32 were similar to all other specimens that failed except for the ISU CFB bottom ash. ISU CFB bottom ash specimens turned into a powdery substance during the first week of testing. The test specimens' weights and dimensions prior to being introduced into the sulfuric acid can be seen in Table D.2 in Appendix D. Periodical test results are shown in Tables D.3 through D.6 of Appendix D.

Table 4.5 Summary of acid test results

Specimen	Weight (g)	Thickness (mm)	Diameter 1 (mm)	Diameter 2 (mm)	Comments
1					Specimen was destroyed during the fifth week of testing
4					Specimen was destroyed during the third week of testing
5	0.73	0.03	0.94	0.64	sides starting to crack
8					Specimen was destroyed during the fifth week of testing
10					Specimen was destroyed during the third week of testing
11					Specimen was destroyed during the fifth week of testing
13					Specimen was destroyed during the fifth week of testing
16					Specimen was destroyed during the fifth week of testing
17	0.04	0.76	1.91	2.36	pieces fell off while drying
19					Specimen was destroyed during the fifth week of testing
22					Specimen was destroyed during the fifth week of testing
24	0.84	0.03	0.46	0.89	slight crack
26					Specimen was destroyed during the first week of testing
28					Specimen was destroyed during the fifth week of testing
29					Specimen was destroyed during the fifth week of testing
31					Specimen was destroyed during the fifth week of testing
33					Specimen was destroyed during the fifth week of testing
36	2.15	0.43	1.85	2.64	starting to crack
38	0.20	0.05	0.36	0.48	
39					Specimen was destroyed during the fifth week of testing
42					Specimen was destroyed during the first week of testing
44					Specimen was destroyed during the first week of testing
46					Specimen was destroyed during the first week of testing
47	0.23	-0.18	0.15	0.36	looks the best

**Figure 4.32 Sulfuric acid test**

4.4 Viscosity Observation

It was visually observed that the viscosity of the mixture changed as a function of the filler material, filler to PET ratio, percentage of fiberglass, length of fiberglass, form of PET, and cooking time. Viscosity is an important parameter in determining possible means of manufacturing a composite material and can also be used as a quality control program. The viscosity was greater for bottom ash fillers than for fly ash fillers. Further, increasing the filler to PET ratio increased the viscosity of the mixture. As the fiberglass percentage increased, the viscosity also increased. The 6 mm length fiberglass mixtures had a lower viscosity than the 13 mm fiberglass mixtures. The PET that was recycled by hand seemed to have a lower viscosity than the “processed” PET. The “clean” recycled PET had a lower viscosity than the “dirty” PET with impurities. As the cooking time increased, the viscosity also increased. Cooking time for the pipe mixtures ranges from 4:00 to 8:30 hours depending on design mixture.

5 CONCLUSIONS

Composite material was produced utilizing waste from PET beverage bottles, coal combustion, and other byproducts. The major conclusions of this research are as followed:

- Results indicate engineering properties of the composite material are greatly affected by the processing technique;
- Average elastic modulus is 7 to 10 times lower than ordinary PCC;
- Average compressive strength is slightly greater than ordinary PCC;
- Average tensile strength is greater than ordinary PCC;
- The average density of the composite is 50% less than ordinary PPC;
- Increasing the filler content will increase compressive and splitting tensile strengths;
- Fiberglass fibers increase strength and resist the propagation of shrinkage cracks;
- Maximum particle size has a slight influence on engineering properties;
- Acid tests indicated that only the Sump filler can withstand the 10% sulfuric acid solution;
- Fillers with high levels of sulfur trioxide experience increased water absorption, resulting in a volume increase; and
- Twenty-three of the 26 pipe specimens exhibited greater ultimate 3-edge bearing strengths than are required by ASTM for the 200 and 250 mm diameter vitrified extra strength clay pipes and all classes of nonreinforced concrete pipes.

6 RECOMMENDATIONS

- Further research should focus on developing better processing techniques to produce composite specimens. One possible processing technique that should be explored is using an extruder with a circular die to produce cylinder specimens.
- Vital to the manufacturing process, is the melt flow index, which should be tested in concert with develop in new manufacture technologies.
- Thermal gravimetric analysis should be conducted to determine the minimum and maximum temperatures for processing.
- The effect of a wide range of reinforcement fibers with different aspect ratios should be investigated. In order to better understand the bonding between the composite material and fiber reinforcements, more SEM tests should be conducted.
- Further investigation should be conducted on the influence of filler chemistry on durability. Other durability tests that should be conducted include: ultraviolet; abrasion; and freeze-thaw.
- The leachate characteristics should be investigated to determine if heavy metals, such as barium, are precipitating out of the composite material.
- Future research should also focus on other possible applications for this composite material.

APPENDIX A: MATERIAL DATA

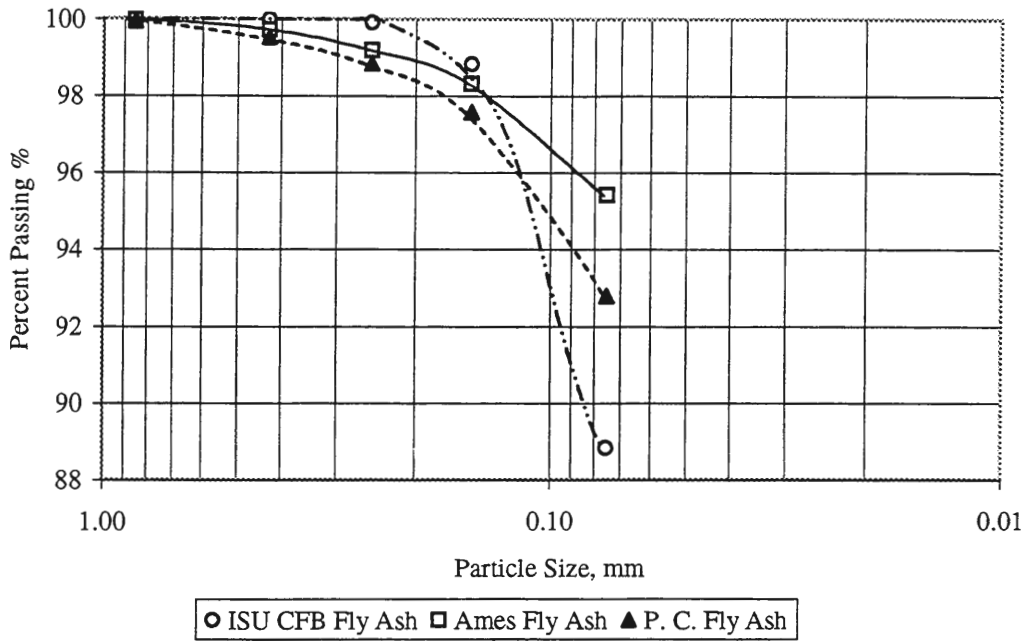


Figure A.1 Fly ash particle distribution curves

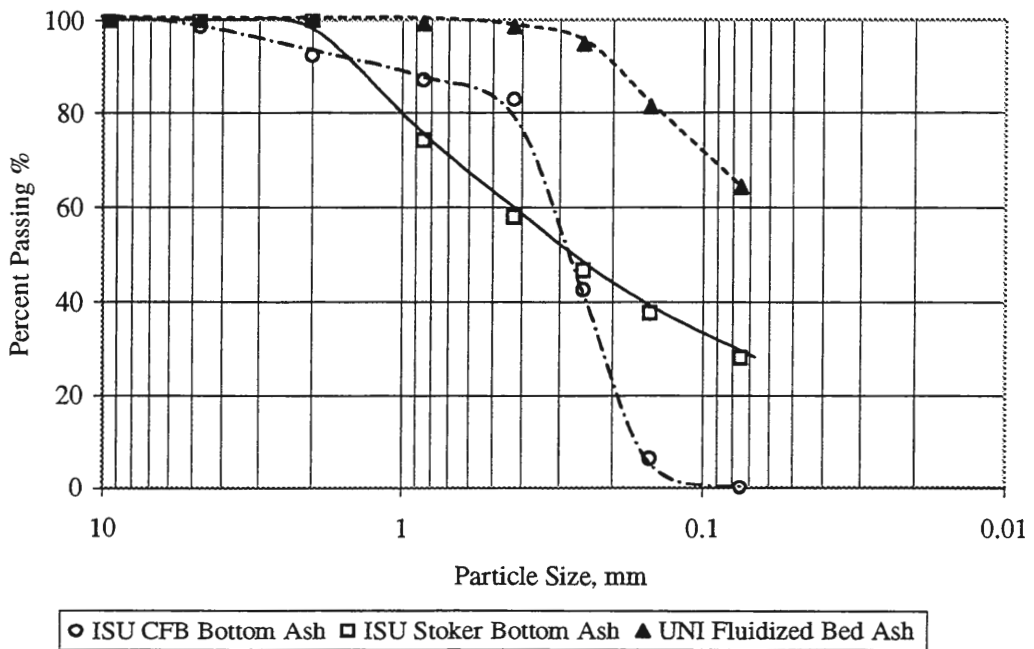


Figure A.2 Bottom ash particle and UNI fluidized bed ash distribution curves

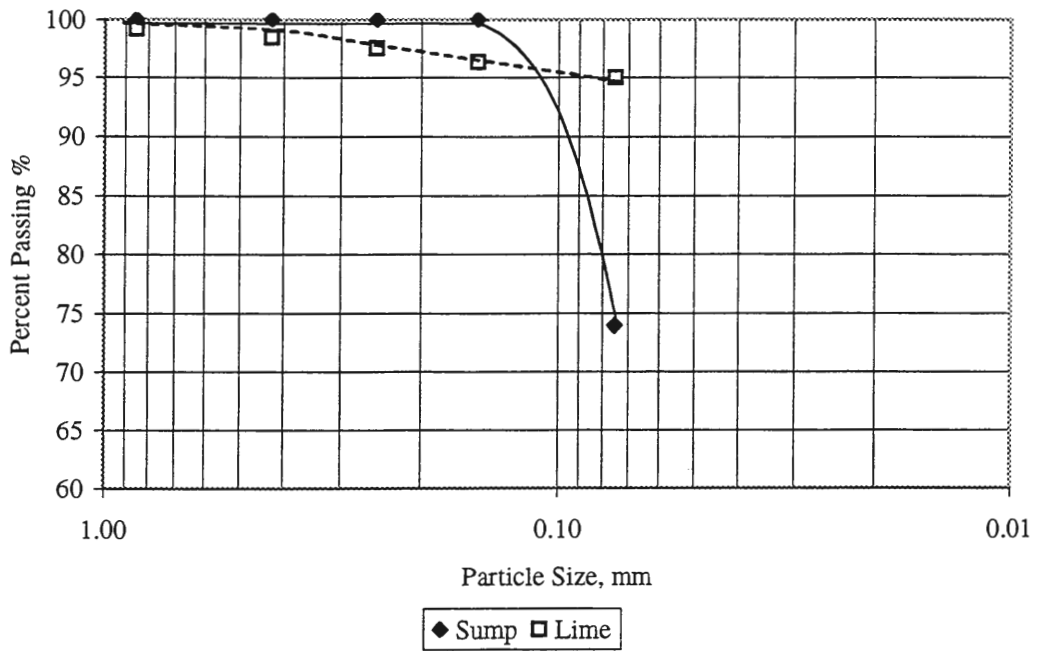


Figure A.3 Non-coal combustion byproducts particle distribution curves

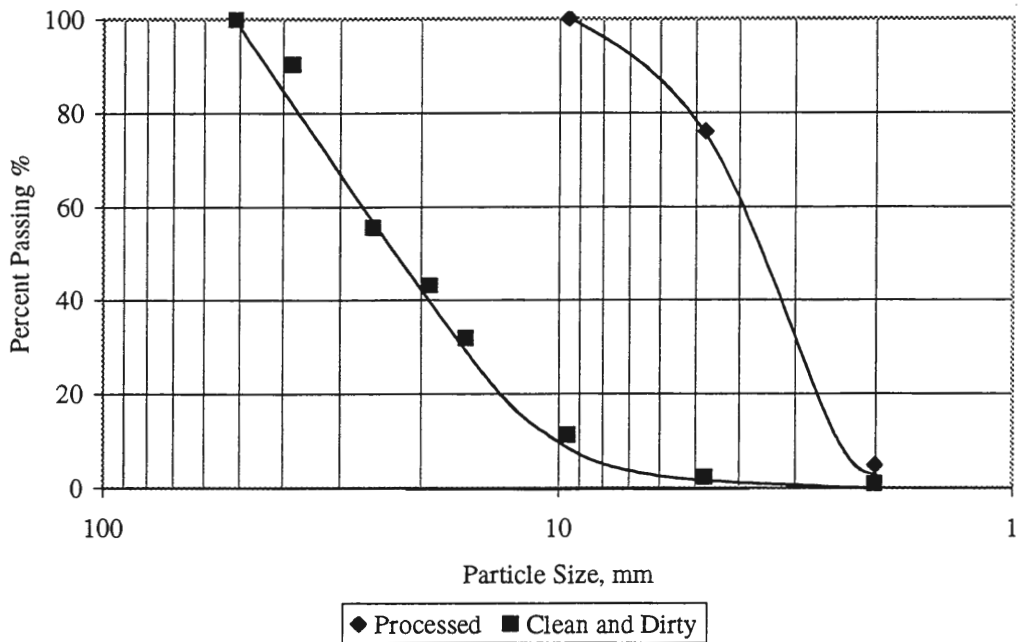


Figure A.4 Particle distribution curves for the three forms of PET

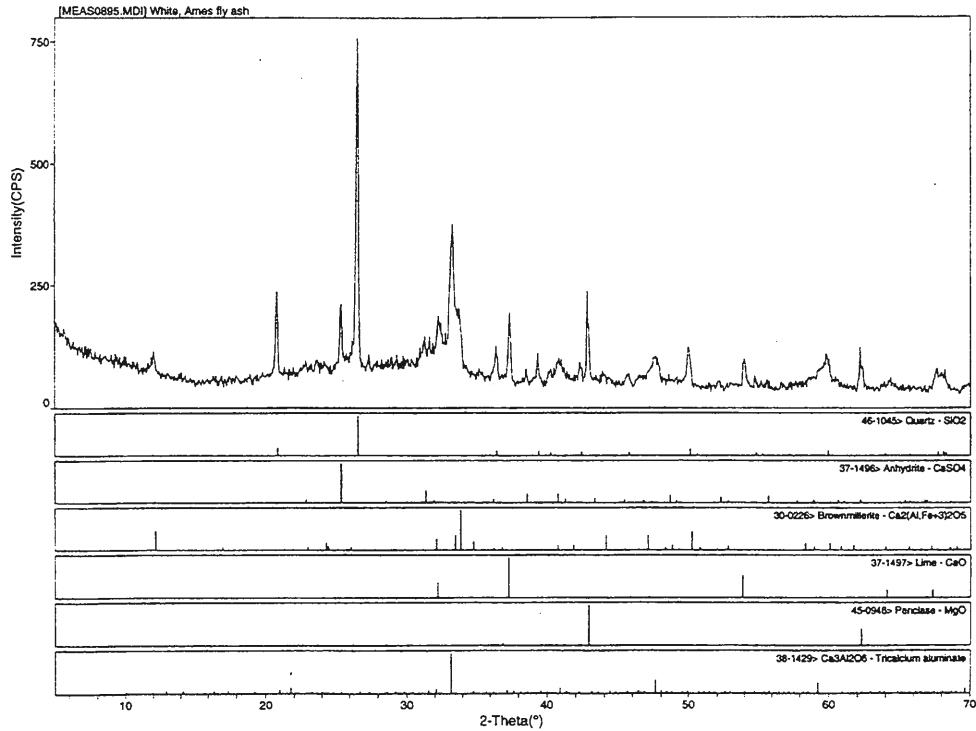


Figure A.5 X-ray diffractogram and mineral identification for Ames fly ash

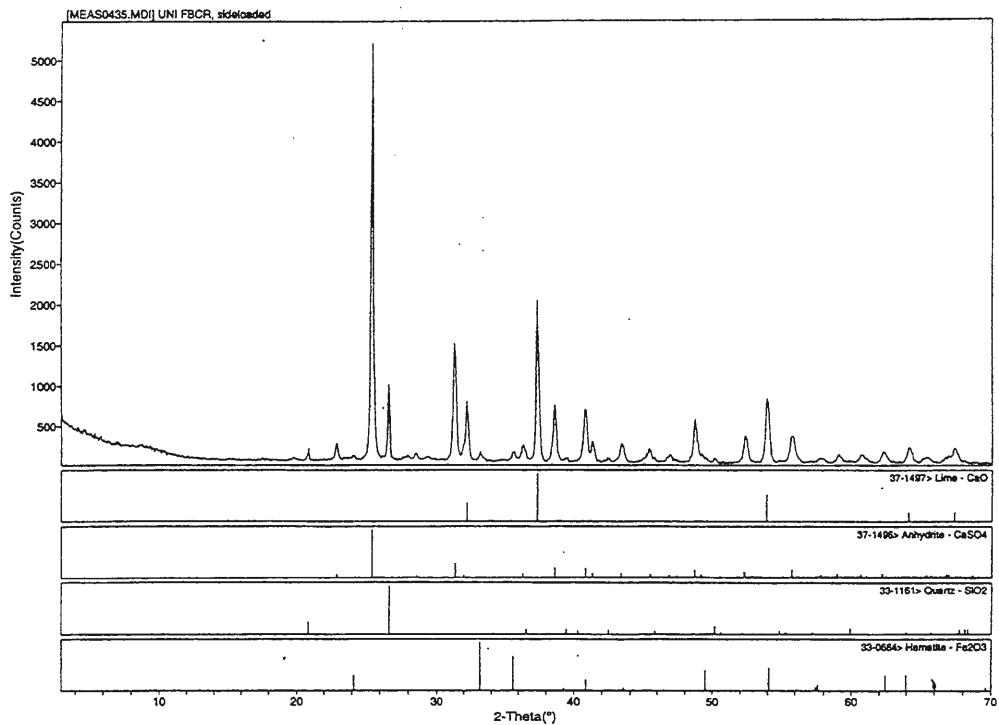


Figure A.6 X-ray diffractogram and mineral identification for UNI fluidized bed ash

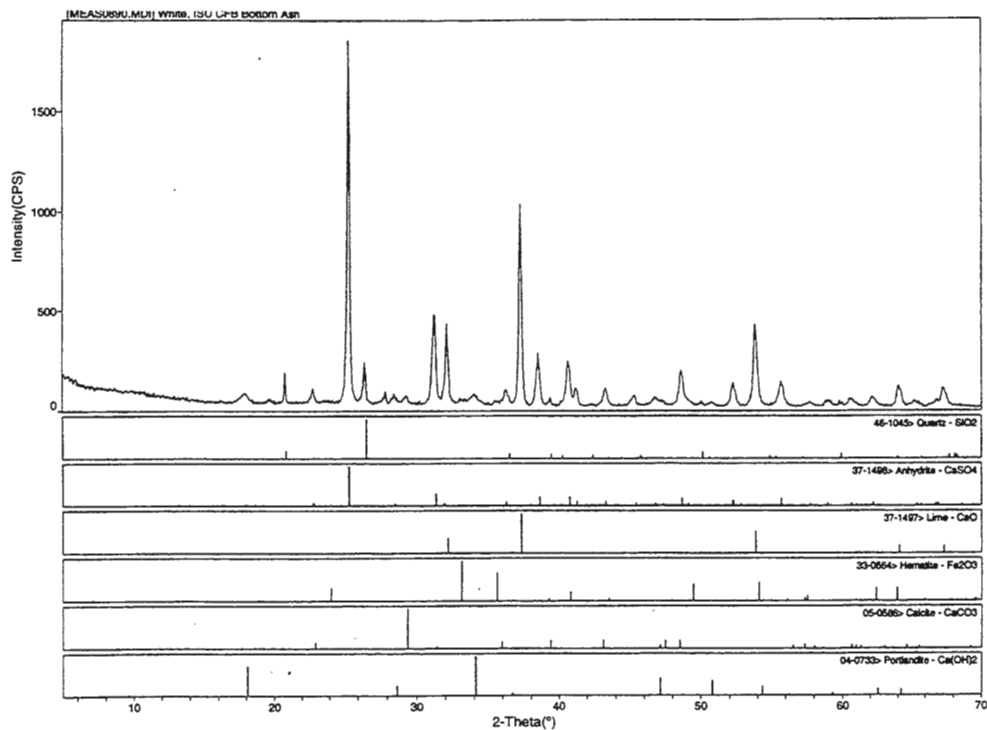


Figure A.7 X-ray diffractogram and mineral identification for ISU CFB bottom ash

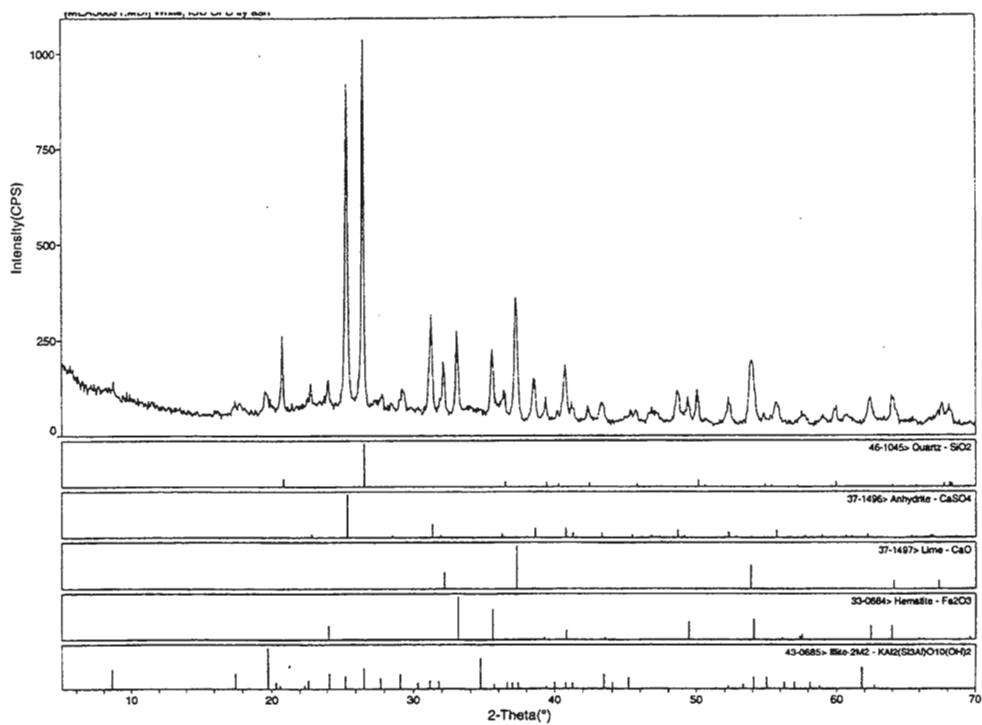


Figure A.8 X-ray diffractogram and mineral identification for ISU CFB fly ash

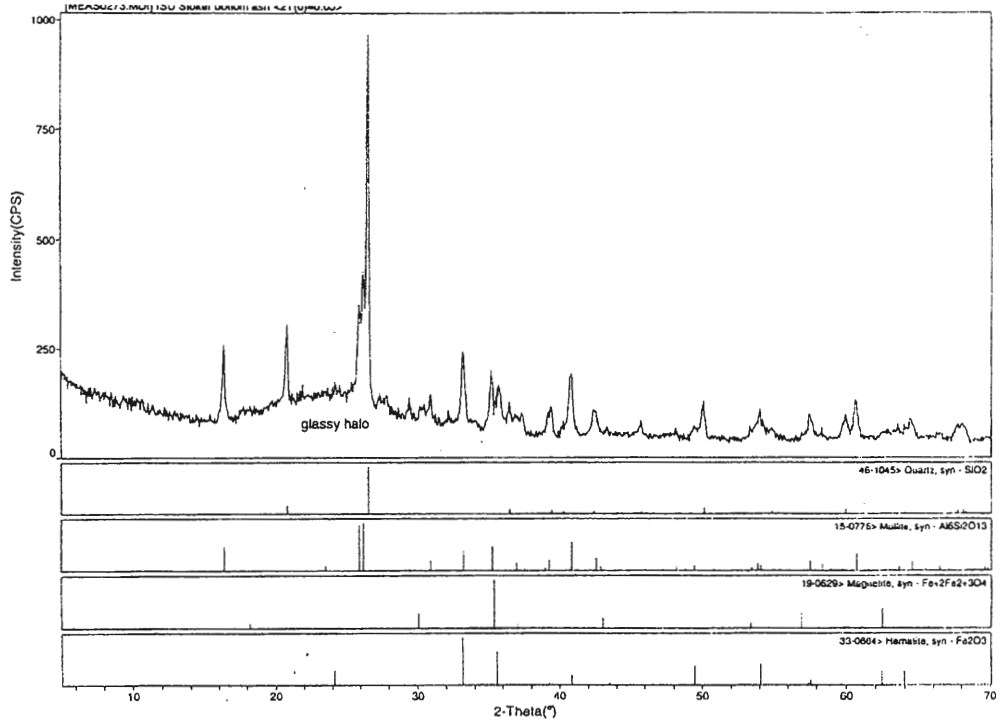


Figure A.9 X-ray diffractogram and mineral identification for stoker bottom ash

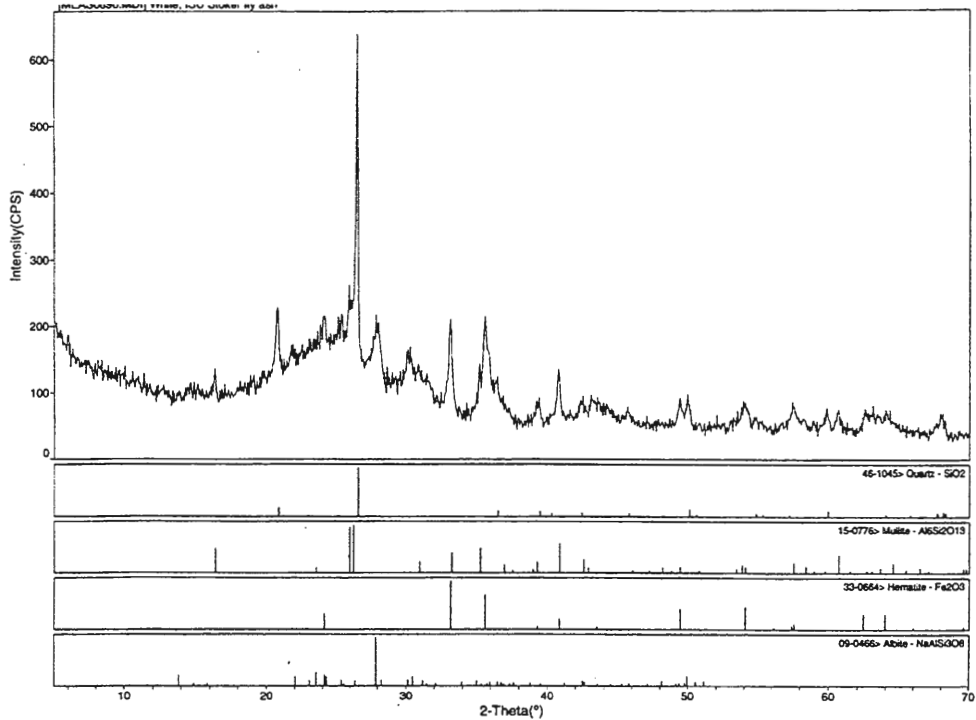


Figure A.10 X-ray diffractogram and mineral identification for stoker fly ash

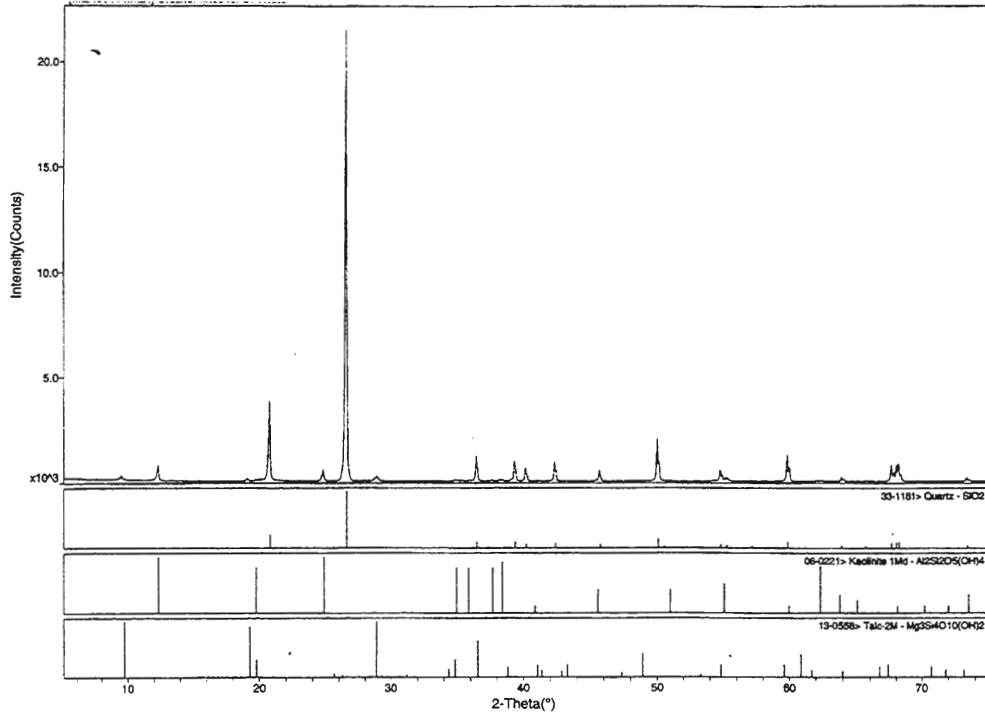


Figure A.11 X-ray diffractogram and mineral identification for Sump

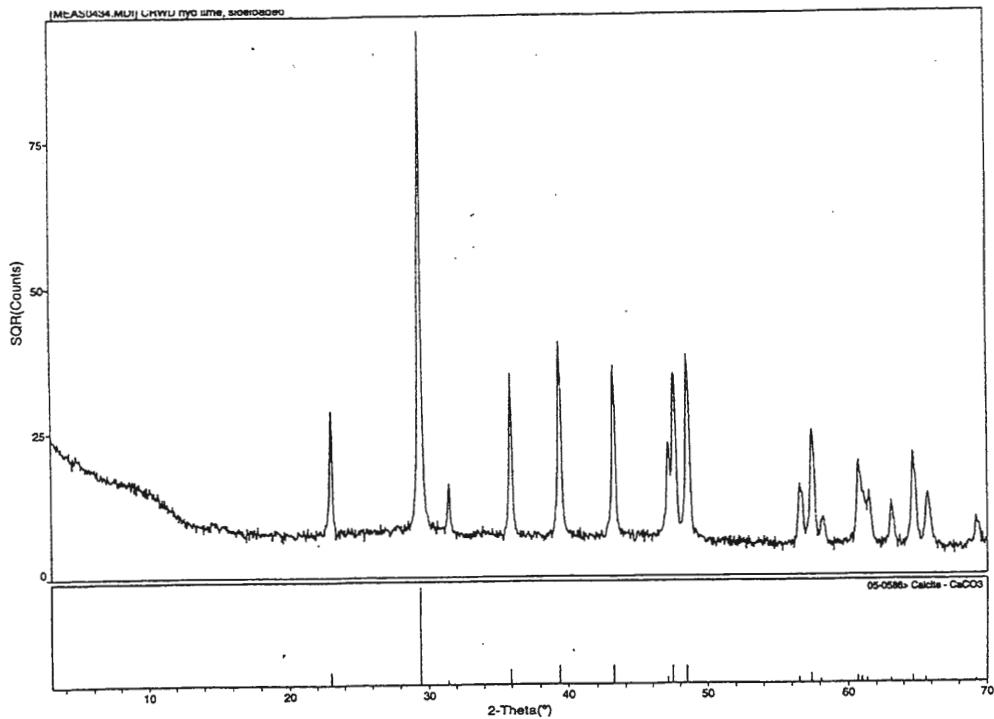


Figure A.12 X-ray diffractogram and mineral identification for Lime

APPENDIX B: CYLINDER SPECIMEN DATA

Table B.1 Cylinder specimen design mixes

Cylinder Number	Filler	PET	Plastic to Filler Ratio	Percent Fiberglass (%)	Length of Fiberglass (mm)	Largest Particle Size (mm)	Cooking Time (hours)
1	P.C.	Processed	50/50	3	13		4.50
2	P.C.	Processed	50/50	3	13		4.25
3	UNI Fluidized Bed Ash	Processed	50/50	3	13	2	
4	UNI Fluidized Bed Ash	Processed	50/50	3	13	2	
5	Ames	Processed	50/50	0			2.25
6	Ames	Processed	50/50	0			2.50
7	Ames	Processed	50/50	3	13		3.25
8	Ames	Processed	50/50	3	13		3.50
9	Ames	Processed	45/55	3	13		2.50
10	Ames	Processed	45/55	3	13		2.25
11	Ames	Processed	40/60	3	13		2.50
12	Ames	Processed	40/60	3	13		3.75
13	Ames	Processed	35/65	3	13		2.00
14	Ames	Processed	35/65	3	13		2.25
15	Ames	Processed	50/50	1	13		2.50
16	Ames	Processed	50/50	1	13		2.25
17	Ames	Processed	50/50	2	13		2.50
18	Ames	Processed	50/50	2	13		2.75
19	Ames	Processed	50/50	4	13		
20	Ames	Processed	50/50	4	13		2.75
21	ISU CFB Fly Ash	Processed	50/50	3	13		3.25
22	ISU CFB Fly Ash	Processed	50/50	3	13		3.25
23	ISU Stoker Bottom Ash	Processed	50/50	3	13	2	2.75
24	ISU Stoker Bottom Ash	Processed	50/50	3	13	2	3.75
25	Ames	Processed	50/50	3	6		3.50
26	Ames	Processed	50/50	3	6		3.25
27	Ames	Processed	50/50	4	6		3.00
28	Ames	Processed	50/50	4	6		2.75
29	Ames	Processed	50/50	5	6		2.25
30	Ames	Processed	50/50	5	6		2.75
31	Ames	Processed	50/50	6	6		3.25
32	Ames	Processed	50/50	6	6		3.50
33	Ames	Dirty	50/50	3	13		
34	Ames	Dirty	50/50	3	13		2.75
35	Ames	Clean	50/50	3	13		2.75
36	Ames	Clean	50/50	3	13		3.50
37	Plastic	Processed	50/50	3	13		4.00
38	Plastic	Processed	50/50	3	13		4.50
39	Lime	Processed	50/50	3	13	2	3.00
40	Lime	Processed	50/50	3	13	2	3.50
41	ISU CFB Bottom Ash	Processed	50/50	3	13	2	3.00
42	ISU CFB Bottom Ash	Processed	50/50	3	13	2	2.00
43	ISU CFB Bottom Ash	Processed	50/50	3	13	0.425	3.00
44	ISU CFB Bottom Ash	Processed	50/50	3	13	0.425	2.75
45	ISU CFB Bottom Ash	Processed	50/50	3	13	0.150	2.50
46	ISU CFB Bottom Ash	Processed	50/50	3	13	0.150	2.25

Table B.1 (continued)

Cylinder Number	Filler	PET	Plastic to Filler Ratio	Percent Fiberglass (%)	Length of Fiberglass (mm)	Largest Particle Size (mm)	Cooking Time (hours)
47	Sump	Processed	50/50	3	13	0.150	2.75
48	Sump	Processed	50/50	3	13	0.150	
50	Ames	Processed	50/50	0			3.00
51	Ames	Processed	50/50	0			3.25

Table B.2 Cylinder compressive strength data

Sample	Height (mm)	Diameter 1 (mm)	Diameter 2 (mm)	Average Diameter (mm)	Mass (g)	Load (kN)	Compressive Strength (MPa)	Density (kg/dm ³)
1-A	101.85	51.69	51.21	51.45	332.14	80.6	38.8	1.57
1-B	101.63	51.64	51.36	51.50	333.71	54.0	25.9	1.58
2-A	102.21	51.49	51.38	51.44	336.21	58.8	28.3	1.58
2-B	102.46	51.08	51.56	51.32	339.99	69.2	33.5	1.60
					Average	65.6	31.6	1.58
3-A	102.49	51.13	51.26	51.19	343.79	123.0	59.8	1.63
3-B	101.42	51.21	51.31	51.26	338.03	95.8	46.4	1.62
4-A	101.57	51.16	51.21	51.18	345.46	103.0	50.1	1.65
4-B	101.65	51.51	51.44	51.47	340.75	125.2	60.2	1.61
					Average	111.8	54.1	1.63
7-A	100.69	51.18	51.36	51.27	342.49	50.8	24.6	1.65
7-B	102.13	51.31	50.90	51.10	347.08	96.6	47.1	1.66
8-A	102.49	50.80	51.08	50.94	347.7	71.2	34.9	1.66
8-B	102.62	51.18	51.00	51.09	344.72	68.8	33.6	1.64
					Average	71.8	35.0	1.65
9-A	102.57	51.18	51.41	51.30	360.03	57.8	28.0	1.70
9-B	102.97	51.38	51.18	51.28	356.46	82.8	40.1	1.68
10-A	102.64	51.18	51.28	51.23	357.64	98.0	47.5	1.69
10-B	103.00	51.10	51.36	51.23	360.8	112.0	54.3	1.70
					Average	87.7	42.5	1.69
11-A	102.26	51.41	51.51	51.46	368.3	106.4	51.2	1.73
11-B	102.21	51.46	51.33	51.40	373.9	87.8	42.3	1.76
12-A	102.62	51.05	51.10	51.08	372.87	92.6	45.2	1.77
12-B	102.34	51.05	51.05	51.05	372.35	84.8	41.4	1.78
					Average	92.9	45.0	1.76

Table B.2 (continued)

Sample	Height (mm)	Diameter 1 (mm)	Diameter 2 (mm)	Average Diameter (mm)	Mass (g)	Load (kN)	Compressive	
							Strength (MPa)	Density (kg/dm ³)
13-A	102.57	51.36	51.31	51.33	390.38	153.4	74.1	1.84
13-B	102.44	51.31	51.18	51.24	384.81	114.4	55.5	1.82
14-A	102.03	51.03	51.64	51.33	387.01	144.6	69.9	1.83
14-B	102.16	51.31	51.64	51.47	390.08	129.2	62.1	1.83
					Average	135.4	65.4	1.83
15-A	102.54	51.56	50.34	50.95	346.6	81.0	39.7	1.66
15-B	102.82	51.49	50.17	50.83	348.58	84.0	41.4	1.67
16-A	100.79	50.90	51.03	50.97	338.53	76.0	37.3	1.65
16-B	102.08	50.60	51.05	50.83	346.15	68.0	33.5	1.67
					Average	77.3	38.0	1.66
17-A	102.39	50.93	51.05	50.99	345.47	128.2	62.8	1.65
17-B	102.51	51.31	50.72	51.02	348.67	73.4	35.9	1.66
18-A	102.24	51.26	50.85	51.05	351.97	128.8	62.9	1.68
18-B	101.83	50.90	50.88	50.89	345.95	79.0	38.8	1.67
					Average	102.3	50.1	1.67
19-A	102.46	51.05	51.03	51.04	348.21	135.6	66.3	1.66
19-B	102.69	51.28	50.93	51.10	349.38	88.2	43.0	1.66
20-A	102.62	51.00	51.10	51.05	348.21	146.8	71.7	1.66
20-B	102.62	51.56	51.16	51.36	347.44	82.8	40.0	1.63
					Average	113.4	55.2	1.65
21-A	102.72	51.05	51.56	51.31	347.13	124.6	60.3	1.63
21-B	102.46	51.23	51.21	51.22	345.66	105.0	51.0	1.64
22-A	102.24	51.31	46.25	48.78	331.18	126.4	67.6	1.73
22-B	102.01	51.28	51.44	51.36	338.95	110.0	53.1	1.60
					Average	116.5	58.0	1.65
23-A	102.51	51.41	50.75	51.08	329.84	95.6	46.7	1.57
23-B	102.59	51.31	51.00	51.16	327.15	99.8	48.6	1.55
24-A	102.46	51.13	51.36	51.24	335.25	77.4	37.5	1.59
24-B	103.25	51.05	51.44	51.24	336.22	73.4	35.6	1.58
					Average	86.6	42.1	1.57
25-A	102.49	50.55	51.31	50.93	350.04	73.4	36.0	1.68
25-B	102.49	51.10	50.62	50.86	349.39	83.4	41.0	1.68
26-A	102.67	50.75	50.72	50.74	347.04	81.6	40.4	1.67
26-B	103.43	50.77	51.16	50.97	351.42	71.2	34.9	1.67
					Average	77.4	38.1	1.67

Table B.2 (continued)

Sample	Height (mm)	Diameter 1 (mm)	Diameter 2 (mm)	Average Diameter (mm)	Mass (g)	Load (kN)	Compressive Strength (MPa)	Density (kg/dm ³)
27-A	103.43	50.47	51.36	50.91	351.06	76.8	37.7	1.67
27-B	103.20	50.83	50.80	50.81	350.33	59.6	29.4	1.67
28-A	102.57	51.61	50.50	51.05	346.4	58.8	28.7	1.65
28-B	103.33	50.75	51.05	50.90	347.88	82.2	40.4	1.65
					Average	69.3	34.1	1.66
29-A	102.36	51.51	50.98	51.24	351.53	63.2	30.6	1.67
29-B	102.92	51.36	50.93	51.14	350.67	79.2	38.6	1.66
30-A	102.34	50.72	51.41	51.07	346.17	93.4	45.6	1.65
30-B	102.57	51.74	50.80	51.27	346.95	76.0	36.8	1.64
					Average	78.0	37.9	1.65
31-A	102.74	51.31	50.90	51.10	351.07	71.8	35.0	1.67
31-B	102.74	51.16	51.03	51.09	352.02	66.8	32.6	1.67
32-A	102.77	51.18	51.05	51.12	348.34	76.6	37.3	1.65
32-B	102.29	51.08	51.08	51.08	343.8	75.6	36.9	1.64
					Average	72.7	35.5	1.66
33-A	103.02	51.31	50.70	51.00	347.9	45.6	22.3	1.65
33-B	103.30	51.36	50.80	51.08	344.2	92.8	45.3	1.63
34-A	102.67	51.18	51.36	51.27	344.45	34.2	16.6	1.63
34-B	102.06	51.10	51.26	51.18	345.92	36.4	17.7	1.65
					Average	52.3	25.5	1.64
35-A	103.20	51.10	50.93	51.02	352.57	95.2	46.6	1.67
35-B	103.76	51.05	51.03	51.04	354.01	62.2	30.4	1.67
36-A	102.62	50.57	51.05	50.81	336.46	128.8	63.5	1.62
36-B	102.44	50.80	51.18	50.99	342.49	114.6	56.1	1.64
					Average	100.2	49.2	1.65
37-A	102.51	50.22	50.93	50.57	249.45	54.2	27.0	1.21
37-B	102.59	50.09	50.60	50.34	246.71	32.6	16.4	1.21
38-A	102.34	51.05	50.19	50.62	248.54	45.2	22.5	1.21
38-B	102.54	50.50	50.85	50.67	250.45	52.4	26.0	1.21
					Average	46.2	23.0	1.21
39-A	103.20	51.77	51.92	51.84	302.76	31.2	14.8	1.39
39-B	103.48	51.69	51.99	51.84	277.26	19.0	9.0	1.27
40-A	102.62	51.87	51.84	51.85	285.69	17.4	8.2	1.32
40-B	102.69	51.82	51.99	51.90	293.34	30.6	14.5	1.35
					Average	24.5	11.6	1.33

Table B.2 (continued)

Sample	Height (mm)	Diameter 1 (mm)	Diameter 2 (mm)	Average Diameter (mm)	Mass (g)	Load (kN)	Compressive Strength (MPa)	Density (kg/dm ³)
41-A	102.62	52.04	51.49	51.77	347.44	61.2	29.1	1.61
41-B	103.12	51.92	51.49	51.70	351.31	40.0	19.1	1.62
42-A	102.79	51.69	51.44	51.56	345.98	49.0	23.5	1.61
42-B	102.87	51.94	51.44	51.69	340.02	45.8	21.8	1.58
					Average	49.0	23.4	1.60
43-A	104.34	51.56	51.56	51.56	354.1	55.4	26.5	1.63
43-B	103.58	51.36	51.31	51.33	354.16	73.8	35.7	1.65
44-A	102.57	51.28	51.46	51.37	346.63	41.4	20.0	1.63
44-B	103.17	51.23	51.36	51.30	349.91	49.4	23.9	1.64
					Average	55.0	26.5	1.64
45-A	102.97	51.26	51.31	51.28	351.1	108.0	52.3	1.65
45-B	103.33	51.56	51.08	51.32	351.11	80.0	38.7	1.64
46-A	103.07	51.82	51.33	51.57	355.28	38.2	18.3	1.65
46-B	103.38	51.44	51.26	51.35	359.4	28.2	13.6	1.68
					Average	63.7	30.7	1.66
47-A	102.67	51.31	51.23	51.27	345.91	120.6	58.4	1.63
47-B	101.83	51.26	51.41	51.33	339.98	70.0	33.8	1.61
48-A	102.54	51.33	51.21	51.27	349.06	90.2	43.7	1.65
48-B	102.16	51.23	51.21	51.22	345.84	129.0	62.6	1.64
					Average	102.5	49.6	1.63
51-A	101.65	51.13	50.42	50.77	349.49	19.2	9.5	1.70
51-B	101.68	49.66	51.94	50.80	349.28	39.4	19.4	1.69
5-A	102.24	51.71	50.52	51.12	339.8	90.0	43.9	1.62
6-A	101.80	51.77	50.17	50.97	336.49	82.8	40.6	1.62
					Average	57.9	28.3	1.66

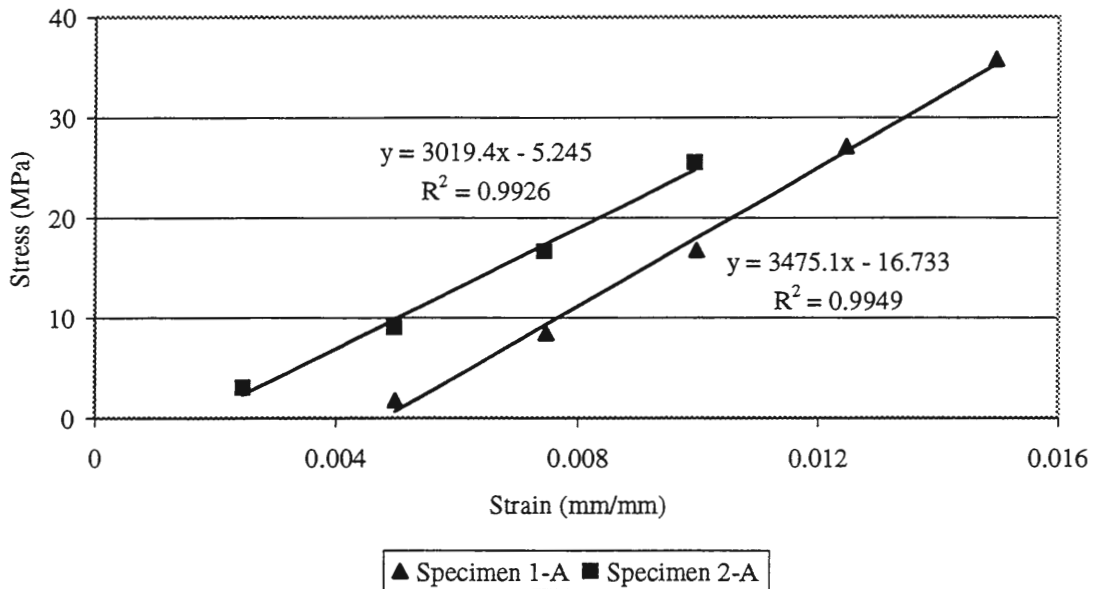


Figure B.1 Stress vs. strain plot for P.C. fly ash, 13 mm long fiberglass fibers, 3% fiberglass by weight with 50/50 PET to filler ratio by weight

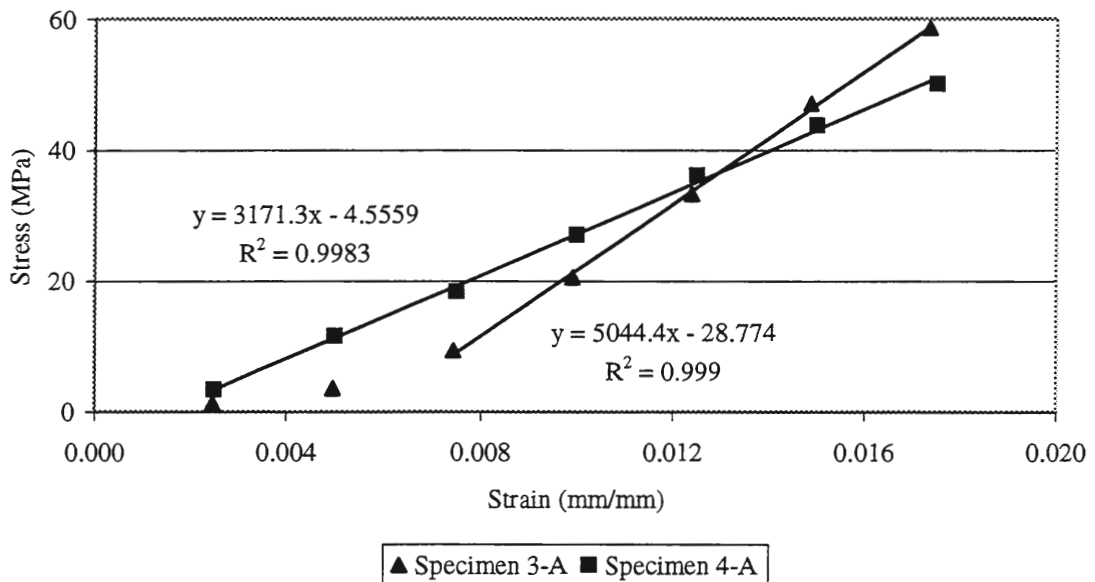


Figure B.2 Stress vs. strain plot for UNI fluidized bed ash, 13 mm long fiberglass fibers, 3% fiberglass by weight with 50/50 PET to filler ratio by weight, largest particle size 2 mm

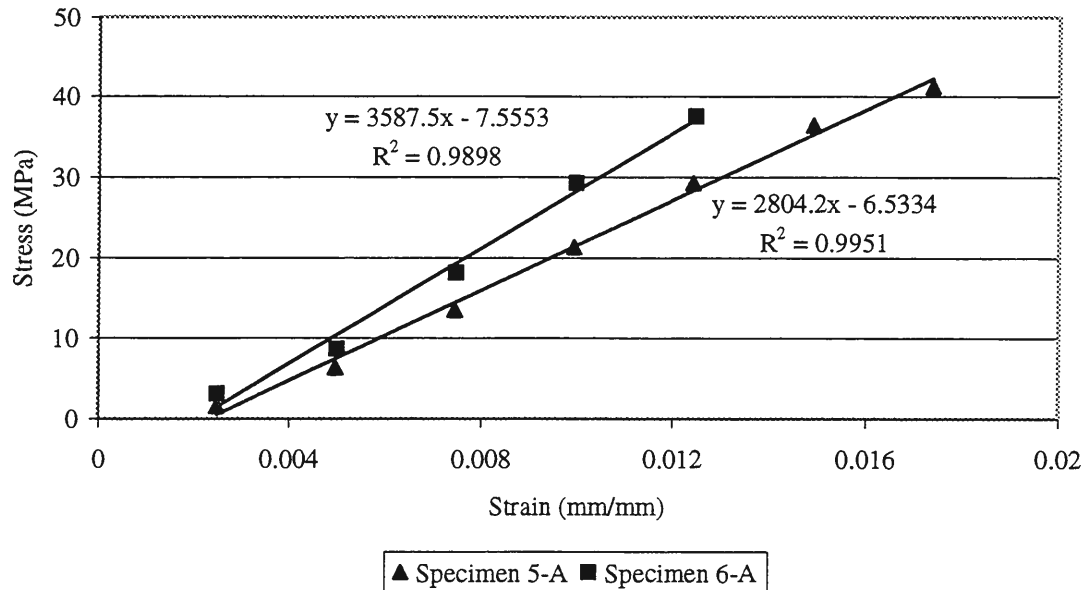


Figure B.3 Stress vs. strain plot for Ames fly ash, 13 mm long fiberglass fibers, no fiberglass, with 50/50 PET to filler ratio by weight

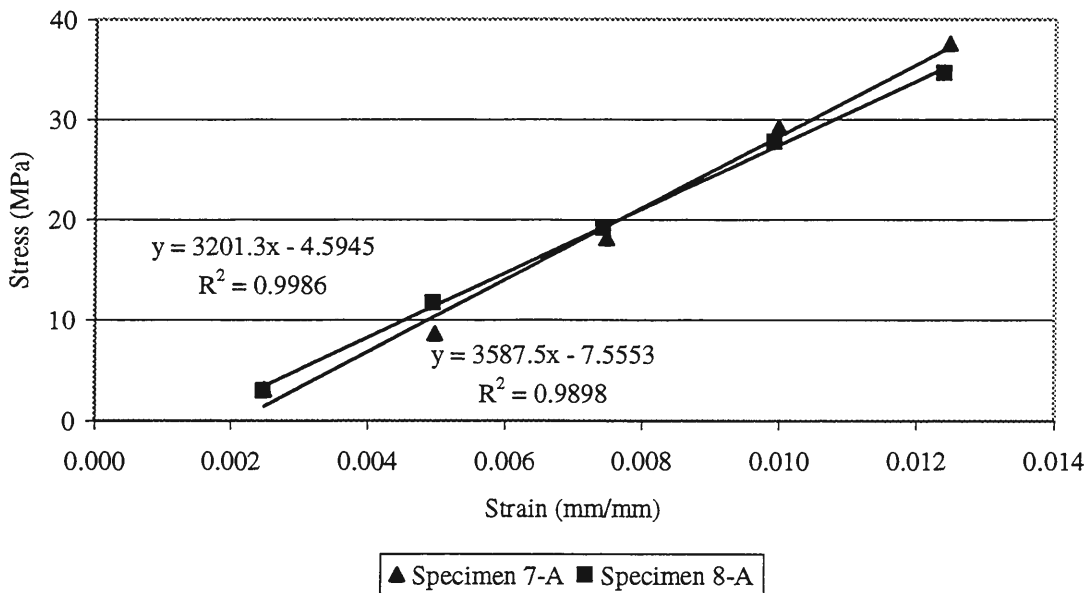


Figure B.4 Stress vs. strain plot for Ames fly ash, 13 mm long fiberglass fibers, 3% fiberglass by weight with 50/50 PET to filler ratio by weight

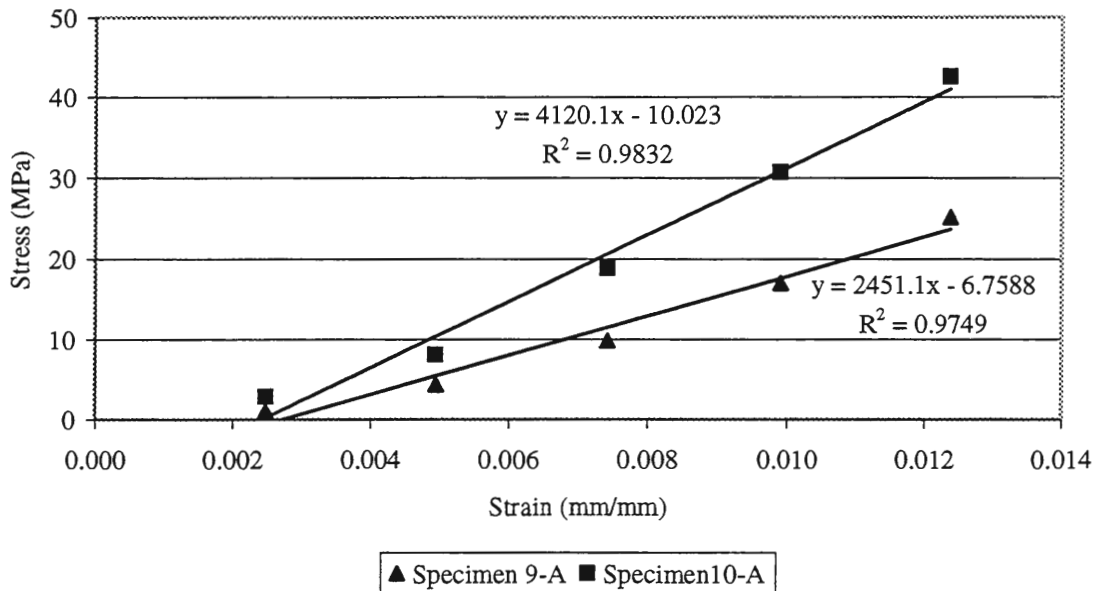


Figure B.5 Stress vs. strain plot for Ames fly ash, 13 mm long fiberglass fibers, 3% fiberglass by weight with 45/55 PET to filler ratio by weight

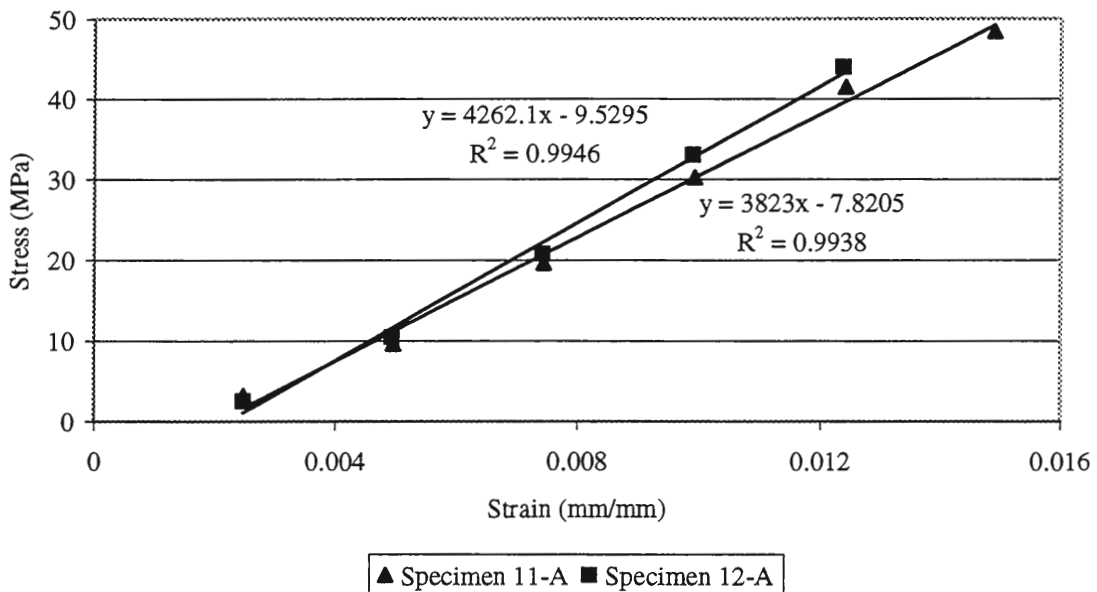


Figure B.6 Stress vs. strain plot for Ames fly ash, 13 mm long fiberglass fibers, 3% fiberglass by weight with 40/60 PET to filler ratio by weight

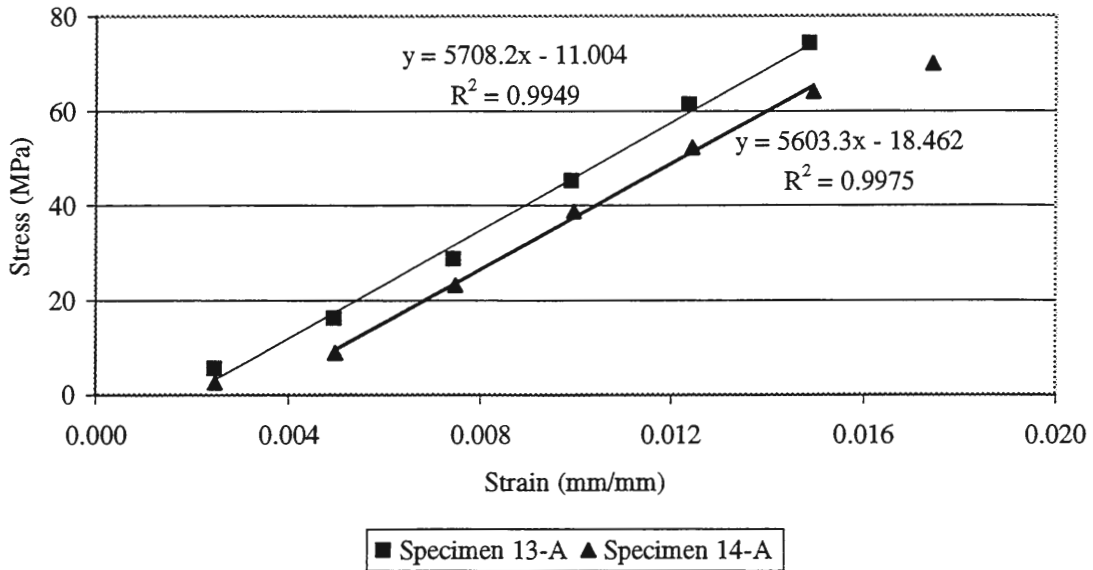


Figure B.7 Stress vs. strain plot for Ames fly ash, 13 mm long fiberglass fibers, 3% fiberglass by weight with 35/65 PET to filler ratio by weight

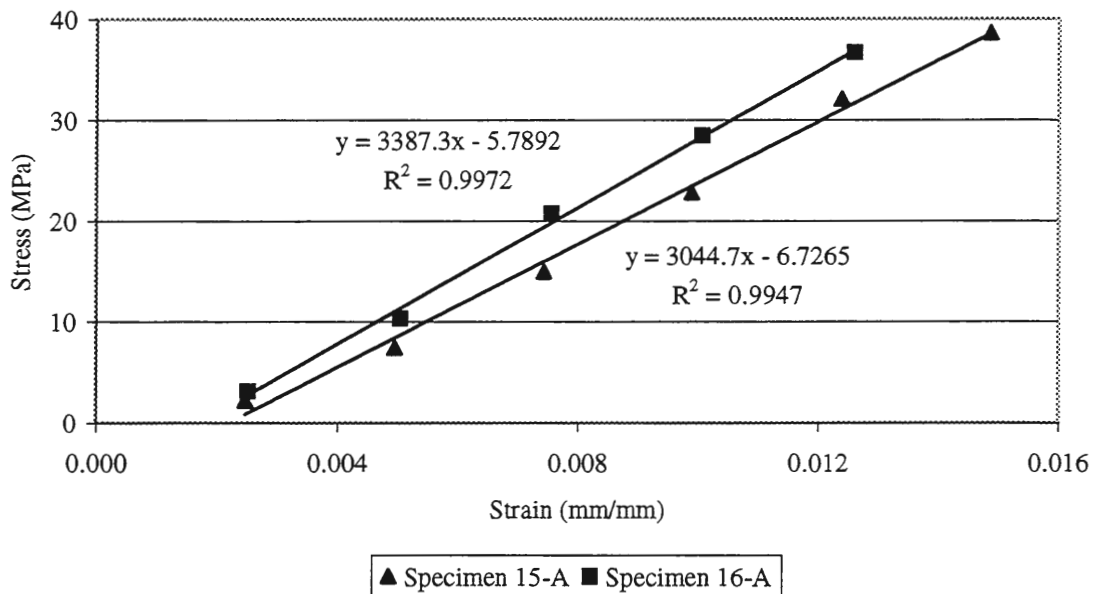


Figure B.8 Stress vs. strain plot for Ames fly ash, 13 mm long fiberglass fibers, 1% fiberglass by weight with 50/50 PET to filler ratio by weight

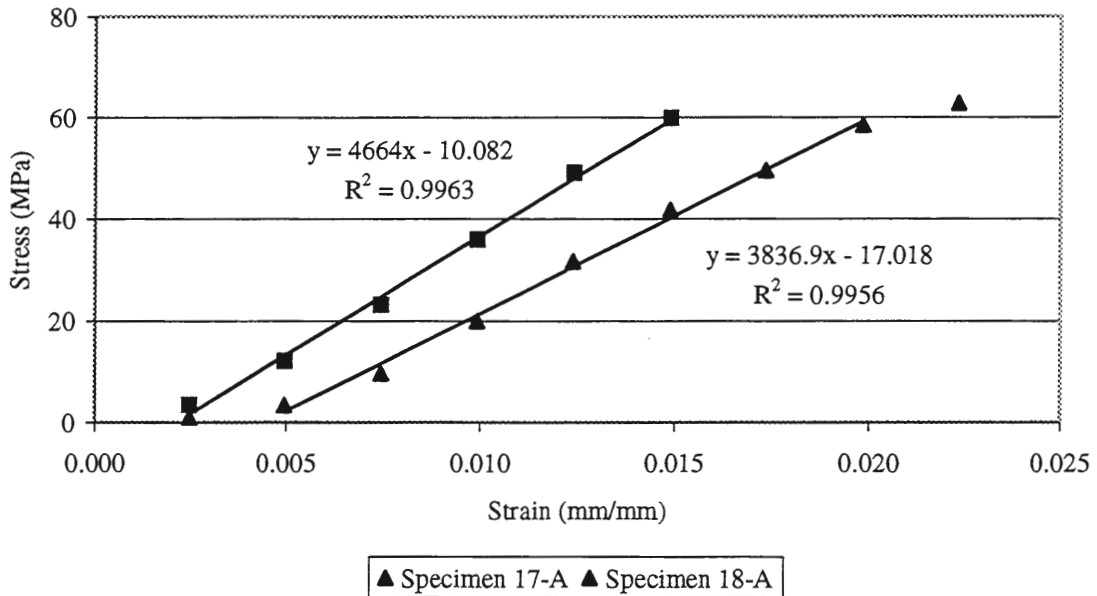


Figure B.9 Stress vs. strain plot for Ames fly ash, 13 mm long fiberglass fibers, 2% fiberglass by weight with 50/50 PET to filler ratio by weight

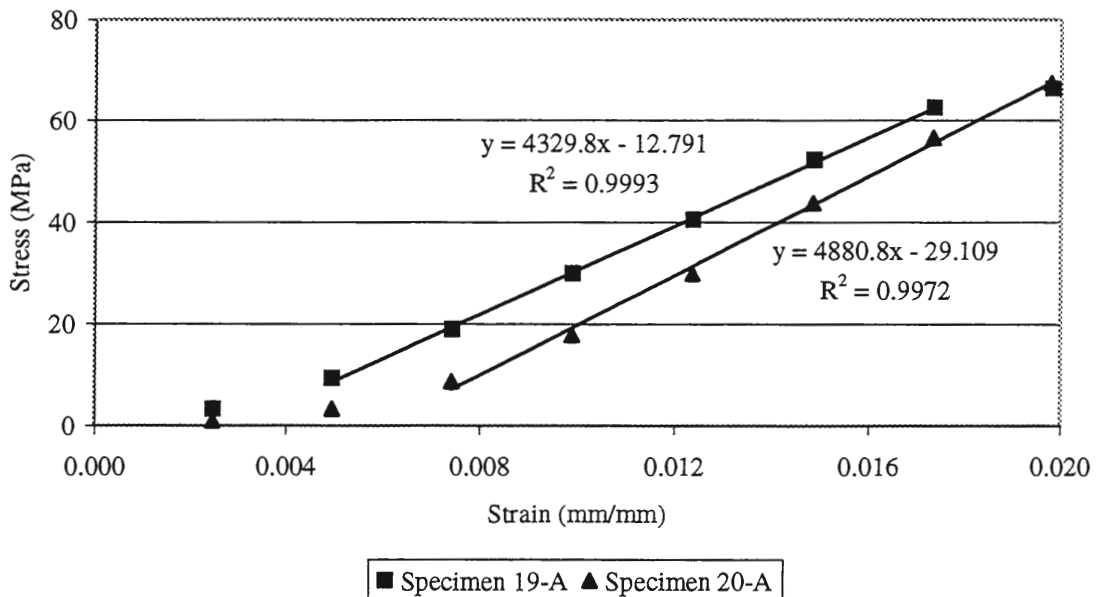


Figure B.10 Stress vs. strain plot for Ames fly ash, 13 mm long fiberglass fibers, 4% fiberglass by weight with 50/50 PET to filler ratio by weight

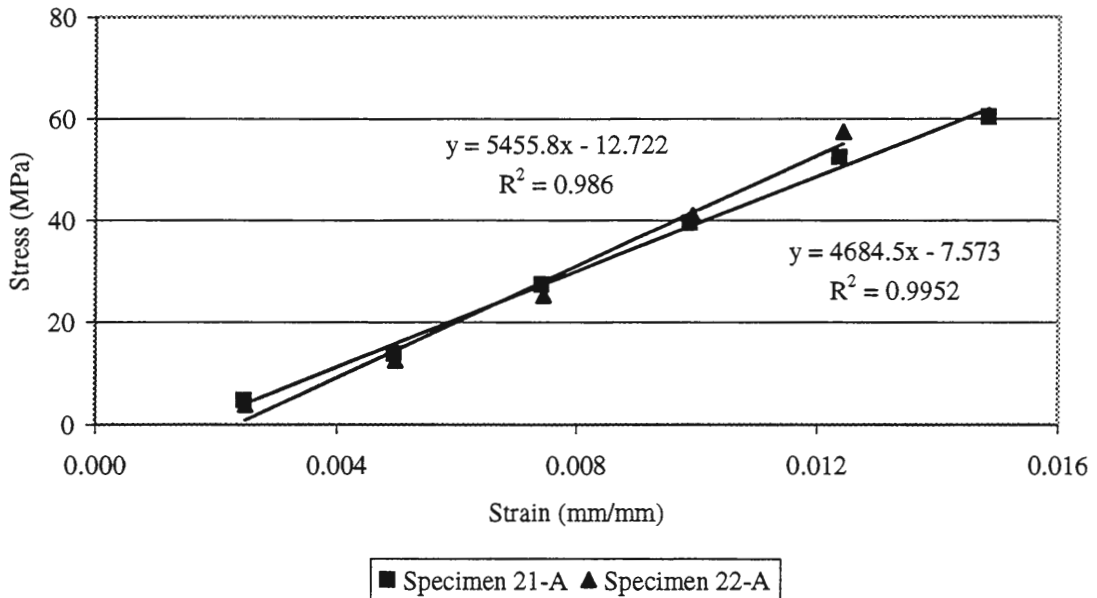


Figure B.11 Stress vs. strain plot for ISU CFB fly ash, 13 mm long fiberglass fibers, 3% fiberglass by weight with 50/50 PET to filler ratio by weight

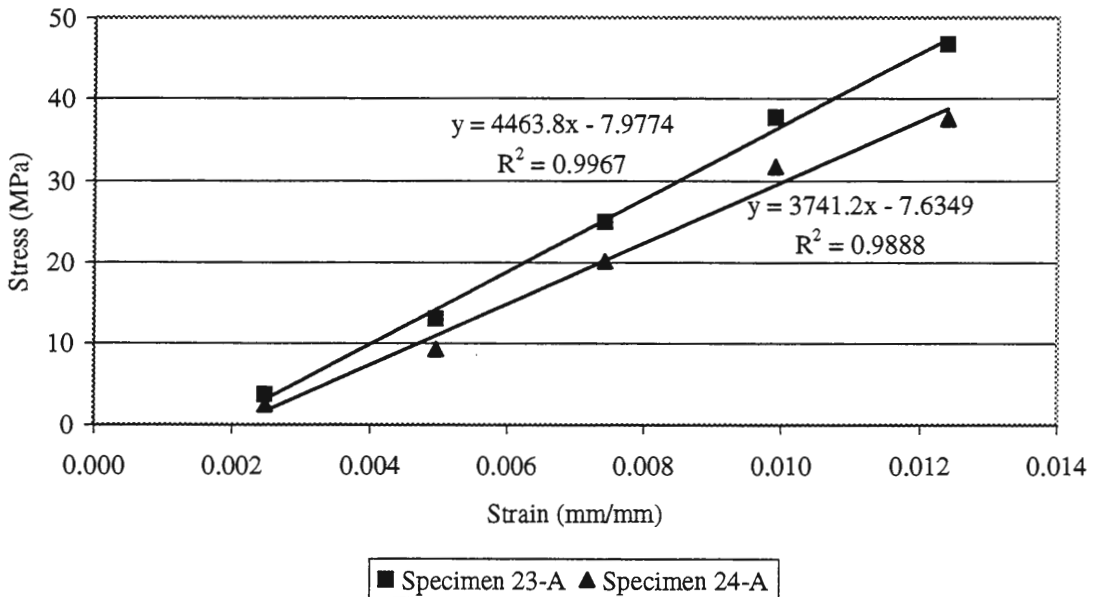


Figure B.12 Stress vs. strain plot for ISU Stoker bottom ash, crushed, 13 mm long fiberglass fibers, 3% fiberglass by weight with 50/50 PET to filler ratio by weight, maximum particle size 2 mm

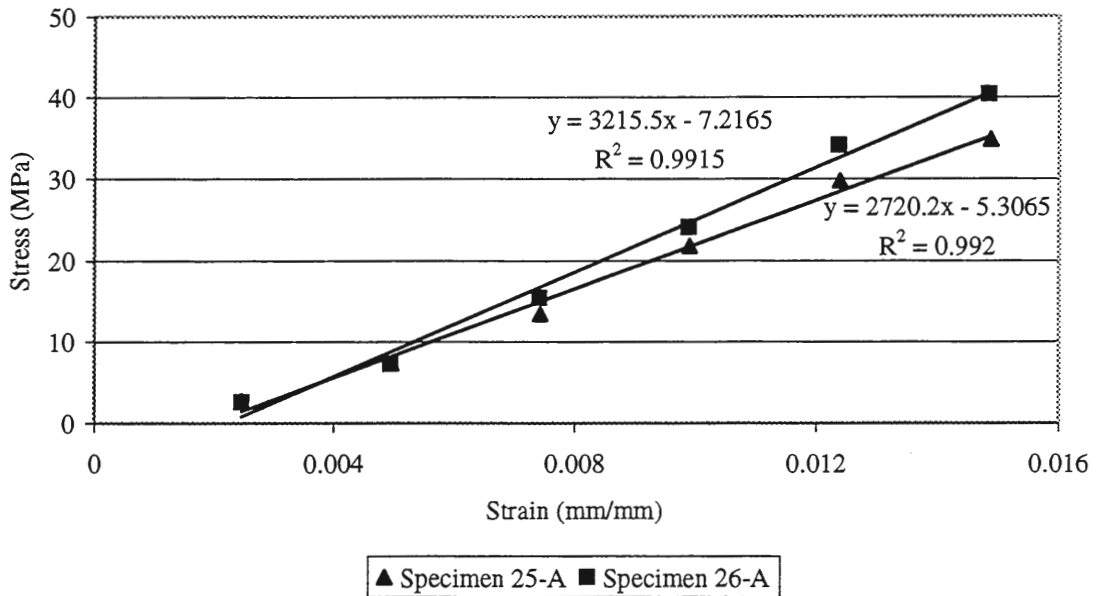


Figure B.13 Stress vs. strain plot for Ames fly ash, 6 mm long fiberglass fibers, 3% fiberglass by weight with 50/50 PET to filler ratio by weight

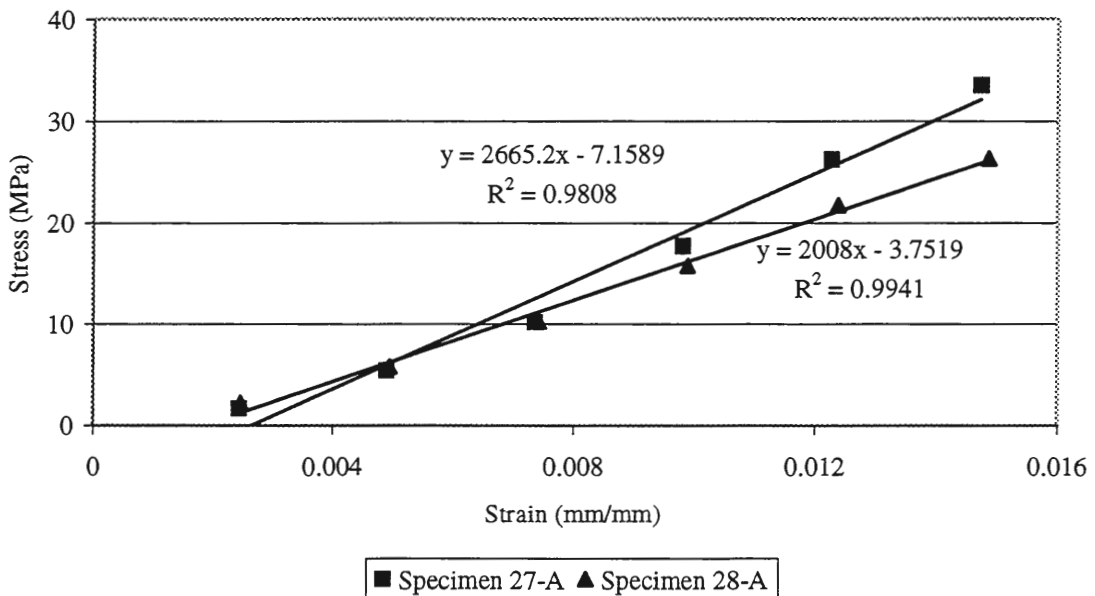


Figure B.14 Stress vs. Strain plot for Ames fly ash, 6 mm long fiberglass fibers, 4% fiberglass by weight with 50/50 PET to filler ratio by weight

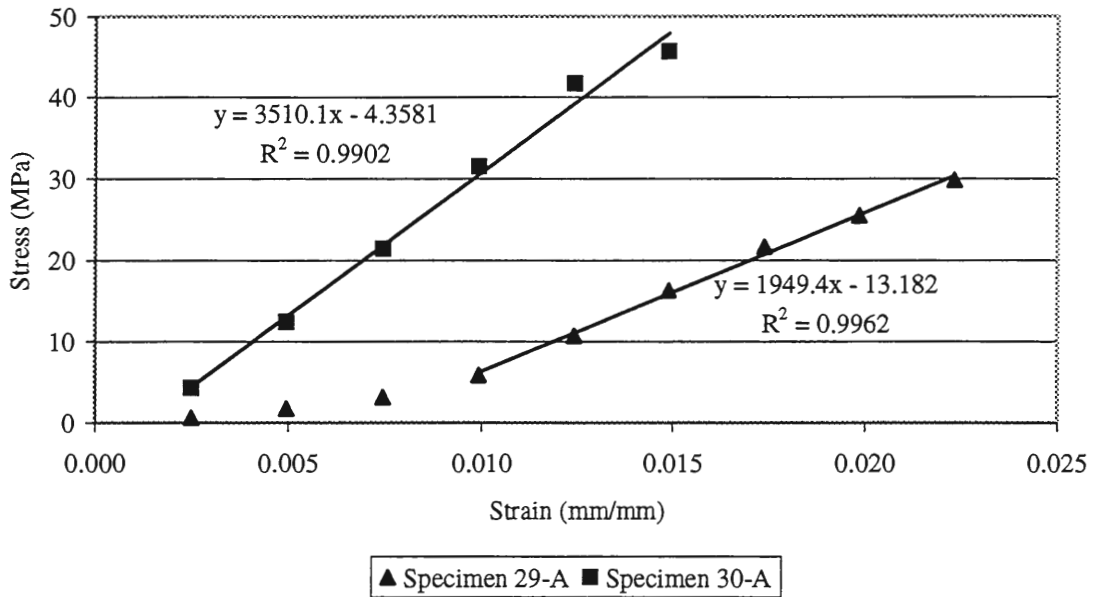


Figure B.15 Stress vs. strain plot for Ames fly ash, 6 mm long fiberglass fibers, 5% fiberglass by weight with 50/50 PET to filler ratio by weight

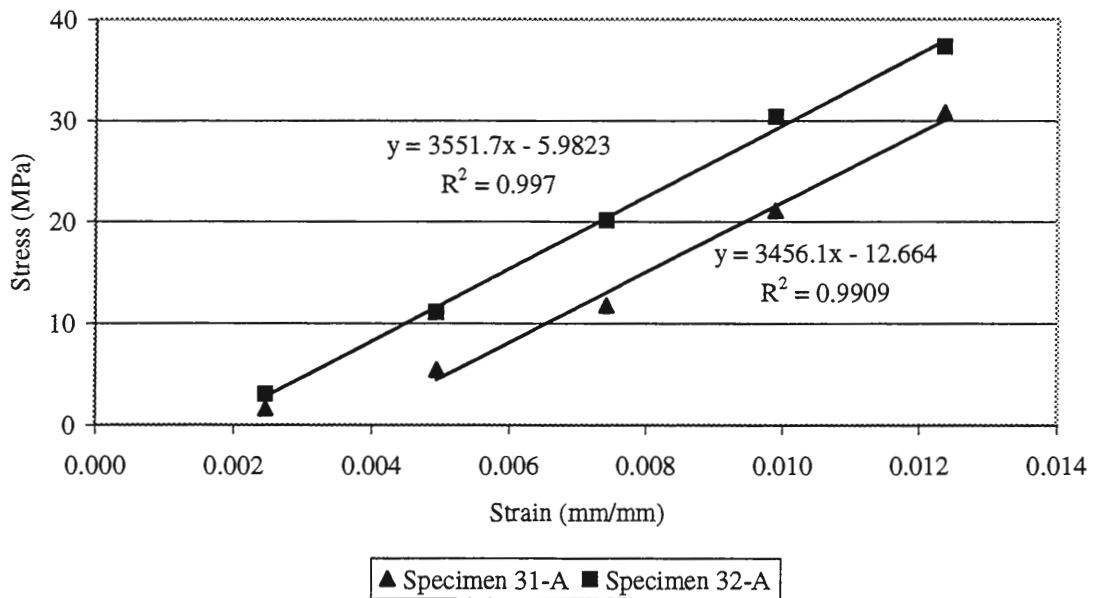


Figure B.16 Stress vs. strain plot for Ames fly ash, 6 mm long fiberglass fibers, 6% fiberglass by weight with 50/50 PET to filler ratio by weight

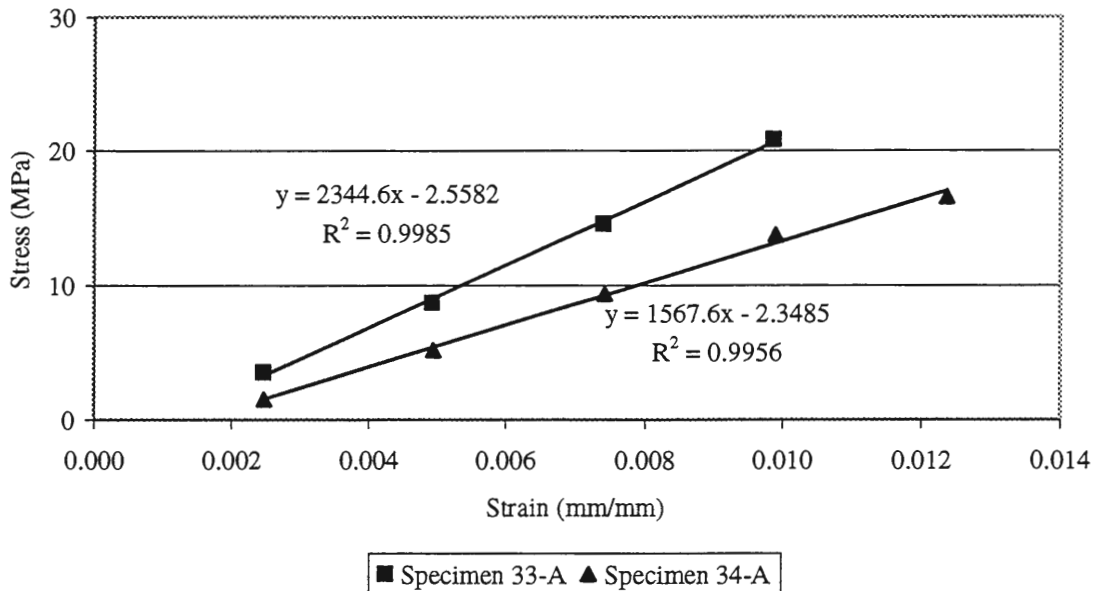


Figure B.17 Stress vs. strain plot for Ames fly ash, 13 mm long fiberglass fibers, 3% fiberglass by weight with 50/50 PET to filler ratio by weight, “dirty” PET

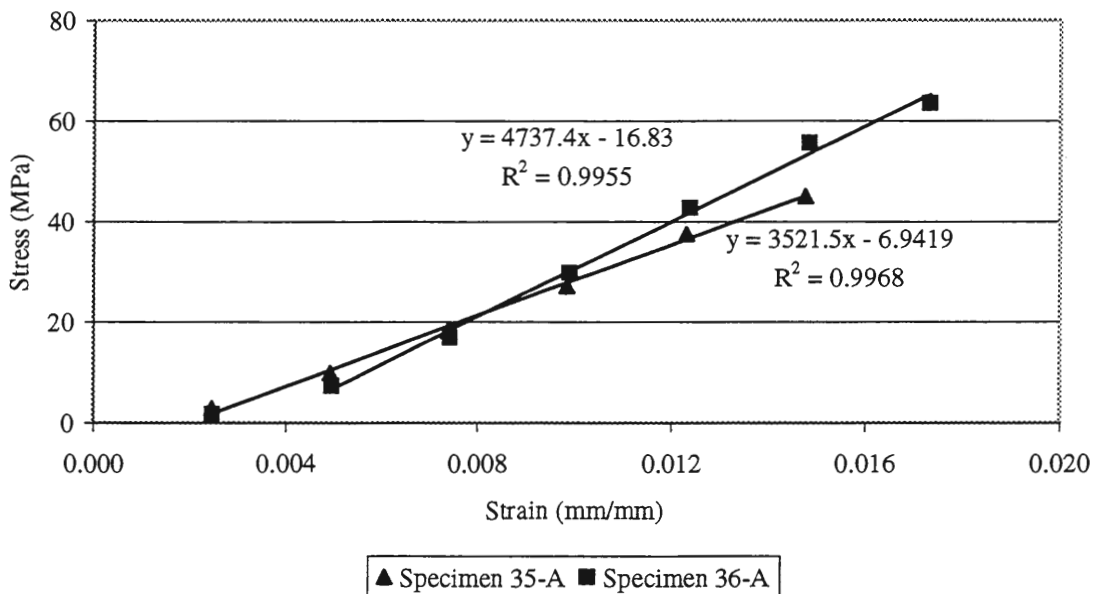


Figure B.18 Stress vs. strain plot for Ames fly ash, 13 mm long fiberglass fibers, 3% fiberglass by weight with 50/50 PET to filler ratio by weight, “clean” PET

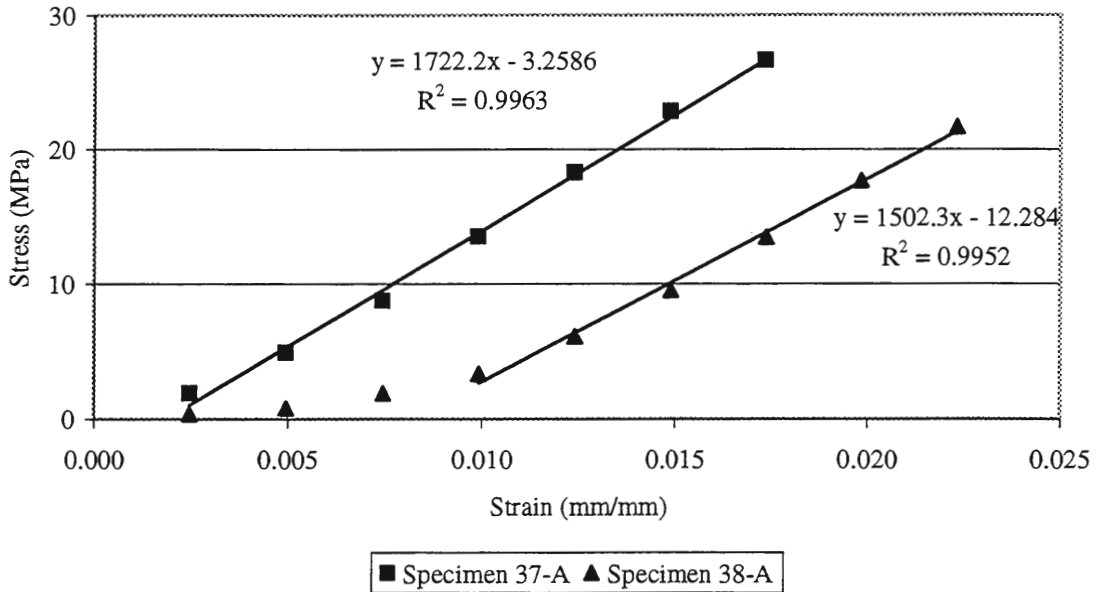


Figure B.19 Stress vs. strain plot for PET plastic, 13 mm long fiberglass fibers, 3% fiberglass by weight with 100/0 PET to filler ratio by weight

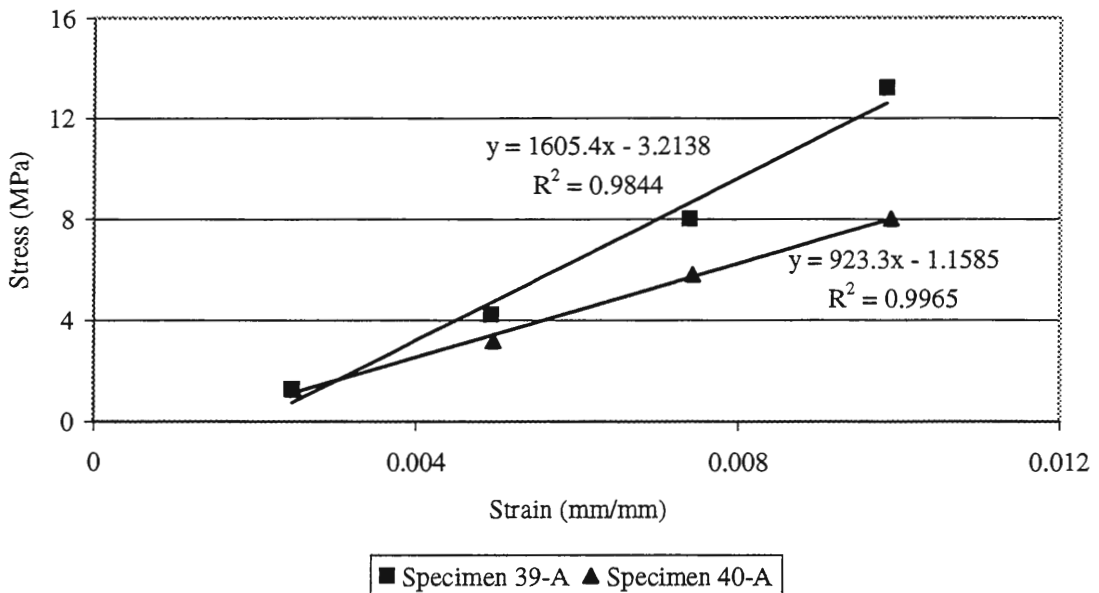


Figure B.20 Stress vs. strain plot for lime, 13 mm long fiberglass fibers, 3% fiberglass by weight with 50/50 PET to filler ratio by weight, largest particle size 2 mm

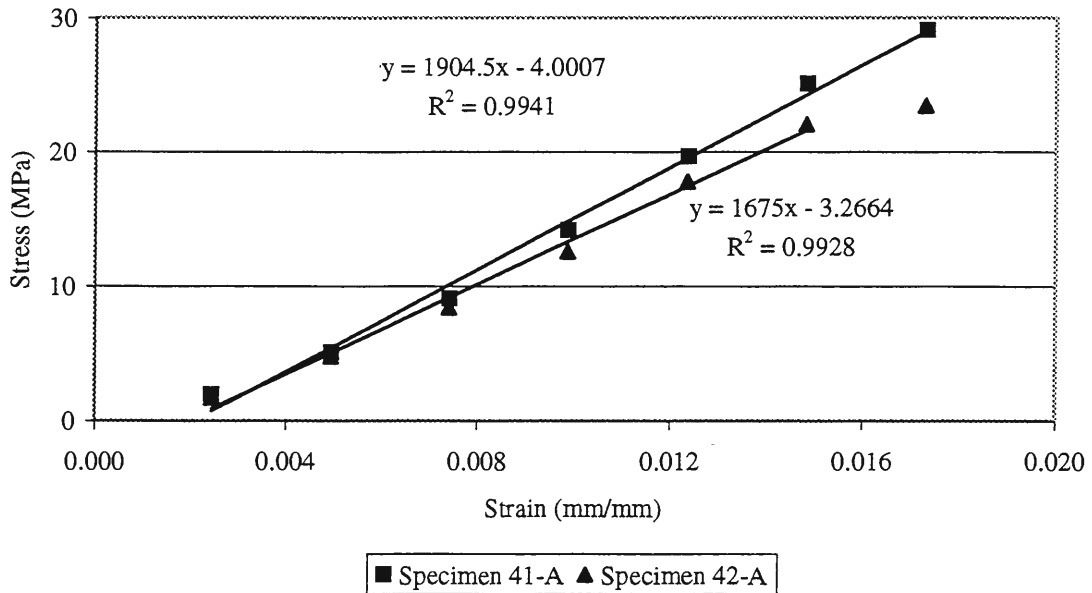


Figure B.21 Stress vs. strain plot for ISU CFB bottom ash, 13 mm long fiberglass fibers, 3% fiberglass by weight with 50/50 PET to filler ratio by weight, maximum particle size 4.75 mm

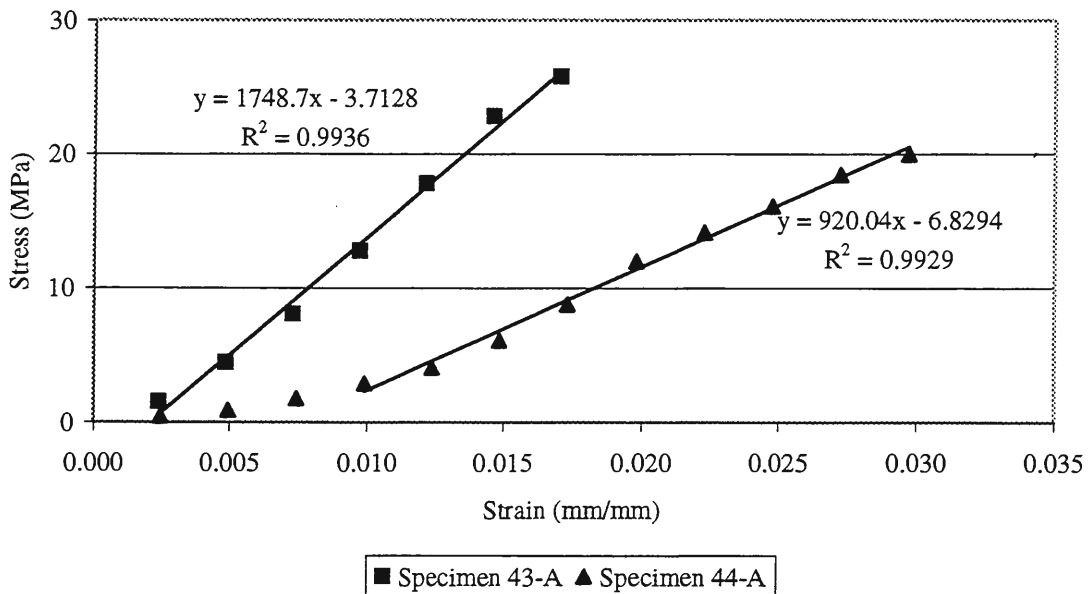


Figure B.22 Stress vs. strain plot for ISU CFB bottom ash, 13 mm long fiberglass fibers, 3% fiberglass by weight with 50/50 PET to filler ratio by weight, maximum particle size 0.425 mm

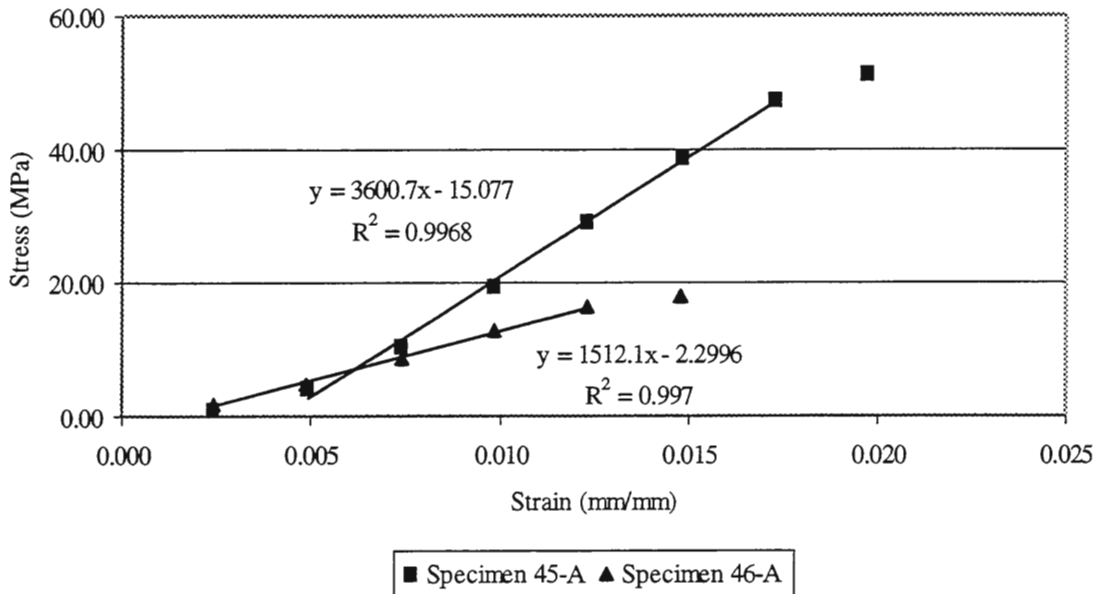


Figure B.23 Stress vs. strain plot for ISU CFB bottom ash, 13 mm long fiberglass fibers, 3% fiberglass by weight with 50/50 PET to filler ratio by weight, maximum particle size 0.150 mm

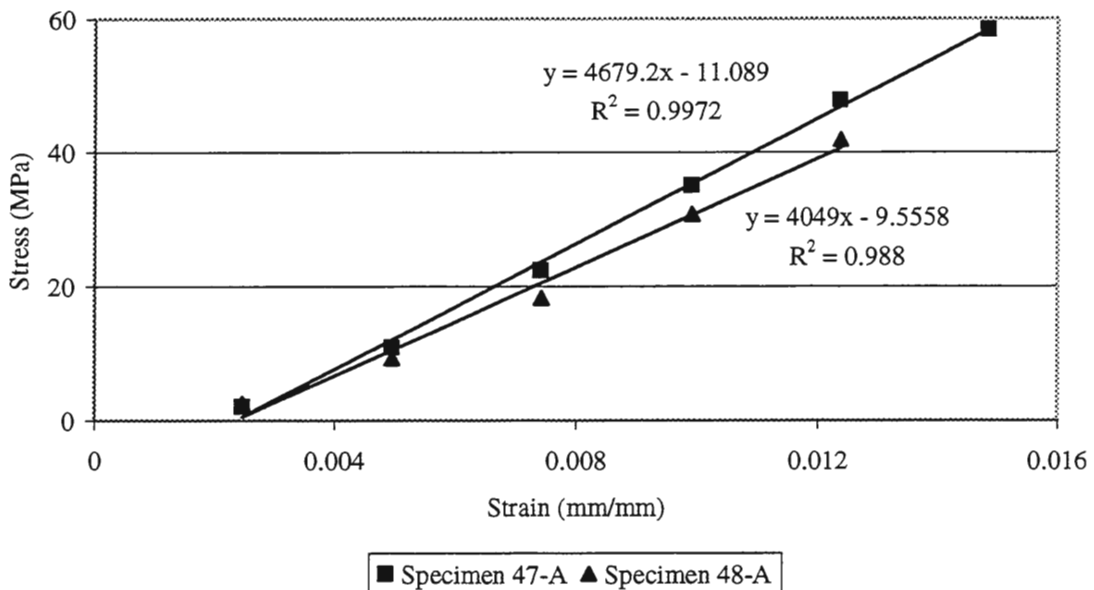


Figure B.24 Stress vs. strain plot for sump, 13 mm long fiberglass fibers, 3% fiberglass by weight with 50/50 PET to filler ratio by weight, maximum particle size 0.150 mm

Table B.3 Cylinder splitting tensile strength data

Sample	Diameter 1 (mm)	Diameter 2 (mm)	Diameter 3 (mm)	Average Diameter (mm)	Length 1 (mm)	Length 2 (mm)	Average Length (mm)	Load Tension (kN)	Splitting Tension (MPa)
1-C	51.31	51.28	51.49	51.36	102.46	102.34	102.40	18.2	2.20
1-D	51.36	51.33	51.31	51.33	101.98	101.88	101.93	16.2	1.97
2-C	51.33	51.51	51.49	51.44	102.16	102.41	102.29	15.6	1.89
2-D	50.90	51.21	51.36	51.16	102.87	102.34	102.60	17.8	2.16
							Average:	17.0	2.06
3-C	51.44	51.18	51.31	51.31	102.97	102.34	102.65	61.6	7.45
3-D	51.26	51.26	51.31	51.27	101.32	101.85	101.59	58.8	7.19
4-C	51.10	51.61	52.07	51.60	102.74	101.98	102.36	26.6	3.21
4-D	51.23	51.21	51.31	51.25	101.52	101.78	101.65	33.4	4.08
							Average:	45.1	5.48
7-C	50.93	50.80	51.03	50.92	103.00	102.54	102.77	35.4	4.31
7-D	50.98	51.08	51.13	51.06	102.87	102.62	102.74	22.2	2.69
8-C	50.67	50.70	50.88	50.75	102.24	102.51	102.37	17.4	2.13
8-D	50.80	50.75	50.93	50.83	103.51	102.87	103.19	17.8	2.16
							Average:	23.2	2.82
9-C	51.69	51.77	51.51	51.66	102.54	102.59	102.57	40.8	4.90
9-D	51.31	51.54	51.61	51.49	102.51	102.34	102.43	23.8	2.87
10-C	51.36	51.00	51.18	51.18	103.00	102.36	102.68	39.8	4.82
10-D	51.23	51.28	51.49	51.33	102.87	103.51	103.19	28.4	3.41
							Average:	33.2	4.00
11-C	51.31	51.31	51.46	51.36	101.85	102.24	102.04	44.4	5.39
11-D	51.26	51.31	51.38	51.32	103.00	102.49	102.74	35.2	4.25
12-C	51.41	51.05	51.05	51.17	102.46	102.26	102.36	20.4	2.48
12-D	51.64	51.41	51.21	51.42	102.54	102.59	102.57	43.4	5.24
							Average:	35.9	4.34
13-C	51.36	51.38	51.44	51.39	101.68	101.85	101.77	64.4	7.84
13-D	51.44	51.46	51.51	51.47	102.36	102.62	102.49	61.0	7.36
14-C	51.56	51.61	51.44	51.54	103.12	102.67	102.90	43.4	5.21
14-D	51.31	51.56	51.51	51.46	102.41	102.16	102.29	57.0	6.89
							Average:	56.5	6.83
15-C	51.00	51.05	51.13	51.06	103.12	102.79	102.96	28.2	3.41
15-D	51.05	50.93	50.90	50.96	103.20	102.62	102.91	19.2	2.33
16-C	50.80	51.28	50.83	50.97	101.60	101.80	101.70	14.6	1.79
16-D	50.80	50.75	50.70	50.75	101.32	101.32	101.32	13.0	1.61
							Average:	18.8	2.29
17-C	50.80	51.03	51.28	51.04	102.46	102.41	102.44	27.6	3.36
17-D	51.05	51.05	51.03	51.05	102.26	102.54	102.40	23.2	2.83
18-C	51.23	51.05	51.16	51.15	102.31	101.88	102.10	29.8	3.63
18-D	50.93	51.00	51.08	51.00	102.54	102.67	102.60	17.0	2.07
							Average:	24.4	2.97

Table B.3 (continued)

Sample	Diameter 1 (mm)	Diameter 2 (mm)	Diameter 3 (mm)	Average Diameter (mm)	Length 1 (mm)	Length 2 (mm)	Average Length (mm)	Load Tension (kN)	Splitting Tension (MPa)
19-C	51.28	51.31	51.05	51.21	102.79	102.34	102.57	26.2	3.18
19-D	51.05	51.08	50.88	51.00	102.74	102.97	102.86	25.4	3.08
20-C	51.21	51.05	50.90	51.05	102.49	102.51	102.50	25.4	3.09
20-D	51.36	51.18	51.03	51.19	102.87	102.82	102.84	25.2	3.05
							Average:	25.6	3.10
21-C	51.05	51.21	51.56	51.27	102.39	102.74	102.57	76.6	9.27
21-D	51.21	51.13	51.31	51.21	102.34	102.97	102.65	79.6	9.64
22-C	50.93	51.13	51.08	51.05	102.39	102.87	102.63	91.0	11.06
22-D	51.23	51.26	51.26	51.25	102.11	102.49	102.30	36.4	4.42
							Average:	70.9	8.60
23-C	51.31	51.18	51.36	51.28	102.97	102.36	102.67	28.4	3.43
23-D	51.36	51.18	51.31	51.28	102.92	103.25	103.09	35.6	4.29
24-C	51.31	51.56	51.26	51.38	102.82	102.46	102.64	40.0	4.83
24-D	51.46	51.31	51.51	51.43	102.77	103.28	103.02	28.6	3.44
							Average:	33.2	4.00
25-C	51.46	51.56	51.18	51.40	102.62	102.64	102.63	38.0	4.59
25-D	51.21	51.31	51.05	51.19	102.16	102.67	102.41	10.6	1.29
26-C	51.16	51.59	51.28	51.34	102.46	103.00	102.73	17.8	2.15
26-D	51.18	51.36	51.23	51.26	102.64	102.72	102.68	40.4	4.89
							Average:	26.7	3.23
27-C	51.44	51.18	51.21	51.27	103.48	102.87	103.17	23.0	2.77
27-D	50.98	50.95	50.80	50.91	102.41	102.95	102.68	13.4	1.63
28-C	50.67	50.93	51.10	50.90	103.00	102.84	102.92	19.2	2.33
28-D	50.95	51.00	50.85	50.94	103.12	103.38	103.25	28.0	3.39
							Average:	20.9	2.53
29-C	51.51	51.18	51.30	51.33	102.36	102.11	102.24	26.2	2.40
29-D	51.56	51.21	51.46	51.41	102.84	102.49	102.67	25.6	3.09
30-C	51.26	51.23	51.31	51.27	103.25	102.74	103.00	23.4	2.82
30-D	51.49	51.05	51.18	51.24	101.75	102.11	101.93	34.2	4.17
							Average:	27.4	3.12
31-C	51.10	51.21	51.18	51.16	102.74	102.57	102.65	28.6	3.47
31-D	51.31	51.16	51.44	51.30	103.28	102.72	103.00	26.0	3.13
32-C	51.08	50.80	51.00	50.96	102.95	103.02	102.98	39.4	4.78
32-D	50.85	50.80	51.18	50.94	103.12	103.76	103.44	37.6	4.54
							Average:	32.9	3.98
33-C	51.10	51.13	51.08	51.10	103.07	103.48	103.28	42.0	5.07
33-D	51.00	51.10	51.10	51.07	102.72	102.87	102.79	24.0	2.91
34-C	51.51	51.08	51.21	51.27	102.31	102.18	102.25	21.0	2.55
34-D	51.38	51.16	51.36	51.30	102.01	102.26	102.13	29.8	3.62
							Average:	29.2	3.54

Table B.3 (continued)

Sample	Diameter 1 (mm)	Diameter 2 (mm)	Diameter 3 (mm)	Average Diameter (mm)	Length 1 (mm)	Length 2 (mm)	Average Length (mm)	Load Tension (kN)	Splitting Tension (MPa)
35-C	51.31	51.18	51.05	51.18	102.79	102.69	102.74	35.8	4.33
35-D	50.98	50.85	51.18	51.00	103.00	102.84	102.92	36.0	4.37
36-C	51.31	51.16	51.05	51.17	102.77	102.29	102.53	45.0	5.46
36-D	51.23	51.08	51.10	51.14	101.88	101.75	101.82	32.0	3.91
							Average:	37.2	4.52
37-C	50.67	50.44	50.62	50.58	102.44	102.84	102.64	19.8	2.43
37-D	50.67	50.57	50.62	50.62	102.21	102.69	102.45	18.2	2.23
38-C	50.70	50.29	50.37	50.45	102.87	102.62	102.74	27.4	3.37
38-D	50.55	50.37	50.37	50.43	101.98	101.85	101.92	26.2	3.25
							Average:	22.9	2.82
39-C	51.92	51.94	52.12	51.99	102.82	103.38	103.10	15.6	1.85
39-D	52.20	51.87	51.89	51.99	102.87	102.82	102.84	21.2	2.52
40-C	51.71	51.79	51.84	51.78	102.62	103.38	103.00	20.4	2.44
40-D	51.79	51.87	51.77	51.81	102.16	102.49	102.32	9.8	1.18
							Average:	16.8	2.00
41-C	51.51	51.44	51.82	51.59	102.24	102.59	102.41	82.2	9.90
41-D	51.82	51.49	51.71	51.67	102.44	102.49	102.46	61.4	7.38
42-C	54.13	51.56	51.74	52.48	103.56	103.35	103.45	47.0	5.51
42-D	53.47	51.31	51.31	52.03	102.92	103.23	103.07	75.2	8.93
							Average:	66.5	7.93
43-C	51.74	51.31	51.49	51.51	103.86	103.30	103.58	49.0	5.85
43-D	51.56	51.31	51.31	51.39	102.54	102.79	102.67	82.8	9.99
44-C	51.18	51.03	51.41	51.21	102.51	102.82	102.67	69.0	8.36
44-D	53.95	51.18	51.71	52.28	103.35	103.28	103.31	64.4	7.59
							Average:	66.3	7.95
45-C	52.71	51.71	51.74	52.05	103.30	103.28	103.29	79.6	9.43
45-D	51.69	51.51	51.66	51.62	102.74	102.69	102.72	71.8	8.62
46-C	52.76	51.56	51.56	51.96	103.58	103.38	103.48	25.0	2.96
46-D	51.51	51.56	52.32	51.80	103.05	102.67	102.86	45.4	5.42
							Average:	55.5	6.61
47-C	51.05	50.88	51.23	51.05	101.90	102.31	102.11	65.8	8.04
47-D	51.56	51.31	51.69	51.52	102.62	102.03	102.32	53.6	6.47
48-C	51.56	51.49	51.51	51.52	101.75	101.85	101.80	44.2	5.36
48-D	51.61	51.64	51.74	51.66	102.03	101.78	101.90	67.0	8.10
							Average:	57.7	6.99
50-A	51.64	52.15	51.51	51.77	103.00	102.24	102.62	13.0	1.56
50-B	51.05	50.95	51.10	51.04	101.73	102.11	101.92	22.2	2.72
50-C	50.34	49.91	50.75	50.33	102.06	102.44	102.25	6.6	0.82
5-B	51.18	51.28	51.21	51.22	101.88	102.13	102.01	16.6	2.02
							Average:	13.9	1.78

Table B.4 Treatments for the statistical analysis

Treatment	Filler Form	PET to Filler Ratio	Form of PET	Length of Fibers (mm)	Percentage of Fibers (%)	Largest particle size (mm)
1	P. C. fly ash	50/50	Processed	13	3	---
3	UNI FB	50/50	Processed	13	3	2
5	Ames	50/50	Processed	13	0	---
7	Ames	50/50	Processed	13	3	---
9	Ames	45/55	Processed	13	3	---
11	Ames	40/60	Processed	13	3	---
13	Ames	35/65	Processed	13	3	---
15	Ames	50/50	Processed	13	1	---
17	Ames	50/50	Processed	13	2	---
19	Ames	50/50	Processed	13	4	---
21	ISU CFB fly ash	50/50	Processed	13	3	---
23	ISU stoker bottom ash	50/50	Processed	13	3	2
25	Ames	50/50	Processed	6	3	---
27	Ames	50/50	Processed	6	4	---
29	Ames	50/50	Processed	6	5	---
31	Ames	50/50	Processed	6	6	---
33	Ames	50/50	Dirty	13	3	---
35	Ames	50/50	Clean	13	3	---
37	Plastic	100/0	Processed	13	3	---
39	Lime	50/50	Processed	13	3	2
41	ISU CFB bottom ash	50/50	Processed	13	3	4.750
43	ISU CFB bottom ash	50/50	Processed	13	3	0.425
45	ISU CFB bottom ash	50/50	Processed	13	3	0.150
47	Sump	50/50	Processed	13	3	0.150

Table B.5 Statistics results for filler material

Treatment	Compressive Strength (MPa)		Splitting Tensile Strength (MPa)	
	Mean Difference	Significance	Mean Difference	Significance
P.C. fly ash - UNI FB	-22.500	0.002	-3.428	0.001
P.C. fly ash - Ames fly ash	Not significant		Not significant	
P.C. fly ash - ISU CFB fly ash	-26.375	0.000	-6.543	0.000
P.C. fly ash - ISU stoker bottom ash	Not significant		-1.943	0.049
P.C. fly ash - No filler	Not significant		Not significant	
P.C. fly ash - Lime	20.000	0.005	Not significant	
P.C. fly ash - CFB bottom ash	Not significant		-5.875	0.000
P.C. fly ash - Sump	-18.000	0.012	-4.938	0.000
UNI FB - Ames fly ash	19.075	0.008	2.660	0.008
UNI FB - ISU CFB fly ash	Not significant		-3.115	0.002
UNI FB - ISU stoker bottom ash	Not significant		Not significant	
UNI FB - No filler	31.150	0.000	2.663	0.008
UNI FB - Lime	42.500	0.000	3.485	0.001
UNI FB - ISU CFB bottom ash	30.750	0.000	-2.448	0.014
UNI FB - Sump	Not significant		Not significant	
Ames fly ash - ISU CFB fly ash	-22.950	0.001	-5.775	0.000
Ames fly ash - ISU stoker bottom ash	Not significant		Not significant	
Ames fly ash - Plastic	Not significant		Not significant	
Ames fly ash - Lime	23.425	0.001	Not significant	
Ames fly ash - ISU CFB bottom ash	Not significant		-5.108	0.000
Ames fly ash - Sump	-14.575	0.039	-4.170	0.000
ISU CFB fly ash - IUS stoker bottom ash	15.900	0.025	4.600	0.000
ISU CFB fly ash - Plastic	35.025	0.000	5.778	0.000
ISU CFB fly ash - Lime	46.375	0.000	6.600	0.000
ISU CFB fly ash - ISU CFB bottom ash	34.625	0.000	Not significant	
ISU CFB fly ash - Sump	Not significant		Not significant	
ISU stoker bottom ash - Plastic	19.125	0.007	Not significant	
ISU stoker bottom ash - Lime	30.475	0.000	2.000	0.043
ISU stoker bottom ash - ISU CFB bottom ash	18.725	0.009	-3.933	0.000
ISU stoker bottom ash - Sump	Not significant		-2.995	0.003
Plastic - Lime	Not significant		Not significant	
Plastic - ISU CFB bottom ash	Not significant		-5.110	0.000
Plastic - Sump	-26.650	0.000	-4.173	0.000
Lime - ISU CFB bottom ash	-11.750	0.095	-5.933	0.000
Lime - Sump	-38.000	0.000	4.995	0.000
ISU CFB bottom ash - Sump	-26.250	0.000	Not significant	

Table B.6 Statistics results for PET to filler ratio

Treatment	Compressive Strength (MPa)		Splitting Tensile Strength (MPa)	
	Mean Difference	Significance	Mean Difference	Significance
100/0 - 50/50	Not significant		Not significant	
100/0 - 45/55	-19.500	0.006	Not significant	
100/0 - 40/60	-22.050	0.002	Not significant	
100/0 - 35/65	-42.425	0.000	-4.005	0.000
50/50 - 45/55	Not significant		Not significant	
50/50 - 40/60	Not significant		Not significant	
50/50 - 35/65	-30.350	0.000	-4.003	0.000
45/55 - 40/60	Not significant		Not significant	
45/55 - 35/65	-22.925	0.002	-2.825	0.005
40/60 - 35/65	-20.375	0.004	-2.485	0.012

Table B.7 Statistics results for form of PET

Treatment	Compressive Strength (MPa)		Splitting Tensile Strength (MPa)	
	Mean Difference	Significance	Mean Difference	Significance
Processed - Dirty	Not significant		Not significant	
Processed - Clean	-14.100	0.046	Not significant	
Dirty - Clean	-23.675	0.001	Not significant	

Table B.8 Statistics results for length of fiberglass fibers

Treatment	Compressive Strength (MPa)		Splitting Tensile Strength (MPa)	
	Mean Difference	Significance	Mean Difference	Significance
13 mm - 6 mm	Not significant		Not significant	

Table B.9 Statistics results for percentage of 6 mm fiberglass fibers

Treatment	Compressive Strength (MPa)		Splitting Tensile Strength (MPa)	
	Mean Difference	Significance	Mean Difference	Significance
0% - 3%	Not significant		Not significant	
0% - 4%	Not significant		Not significant	
0% - 5%	Not significant		Not significant	
0% - 6%	Not significant		-2.200	0.026
3% - 4%	Not significant		Not significant	
3% - 5%	Not significant		Not significant	
3% - 6%	Not significant		Not significant	
4% - 5%	Not significant		Not significant	
4% - 6%	Not significant		Not significant	
5% - 6%	Not significant		Not significant	

Table B.10 Statistics results for percentage of 13 mm fiberglass fibers

Percentage of long fibers	Compressive Strength (MPa)		Splitting Tensile Strength (MPa)	
	Mean Difference	Significance	Mean Difference	Significance
0% - 3%	Not significant		Not significant	
0% - 1%	Not significant		Not significant	
0% - 2%	-21.750	0.000	Not significant	
0% - 4%	-26.900	0.000	Not significant	
3% - 1%	Not significant		Not significant	
3% - 2%	-15.050	0.034	Not significant	
3% - 4%	-20.200	0.005	Not significant	
1% - 2%	Not significant		Not significant	
1% - 4%	-17.275	0.015	Not significant	
2% - 4%	Not significant		Not significant	

Table B.11 Statistics results for largest particle size

Treatment (mm)	Compressive Strength (MPa)		Splitting Tensile Strength (MPa)	
	Mean Difference	Significance	Mean Difference	Significance
2.000 - 0.425	Not significant		Not significant	
2.000 - 0.150	Not significant		Not significant	
0.425 - 0.150	Not significant		Not significant	

APPENDIX C: PIPE SPECIMEN DATA

Table C.1 Pipe specimen design mixes

Pipe	Filler	RPET to Filler Ratio	Form of RPET	Percent of Fiberglass (%)	Maximum Particle Size (mm)	Cooking Time (hours)	Ultimate 3-Edge Bearing Strength (kN/m)
1	Pipe was not tested because of manufacturing problems						
2	Pipe was not tested because of manufacturing problems						
3	P.C. Fly Ash	50/50	Processed	3	---	---	66.86
4	P.C. Fly Ash	50/50	Processed	3	---	6.25	44.73
5	P.C. Fly Ash	50/50	Processed	3	---	5.50	52.75
6	UNI Fluidized Bed Ash	50/50	Processed	3	---	5.75	56.17
7	UNI Fluidized Bed Ash	50/50	Processed	3	2	7.25	54.91
8	UNI Fluidized Bed Ash	50/50	Processed	3	2	4.75	68.30
9	Lime	50/50	Processed	3	2	4.00	42.86
10	Pipe was not tested because of manufacturing problems						
11	Lime	50/50	Processed	3.5	2	4.25	67.24
12	Lime	50/50	Processed	4	2	5.00	50.45
13	Ames Fly Ash	50/50	Dirty	3	---	5.75	53.99
14	Ames Fly Ash	50/50	Processed	3	---	5.50	51.42
15	Ames Fly Ash	50/50	Clean	3	---	5.75	50.23
16	Slump	50/50	Processed	3	0.150	4.00	41.25
17	ISU CFB Fly Ash	50/50	Processed	3	---	5.50	51.27
18	Lime	50/50	Processed	4	2	5.00	55.13
19	UNI Fluidized Bed Ash	40/60	Processed	3	2	4.00	94.65
20	UNI Fluidized Bed Ash	33/67	Processed	3	2	6.50	77.77
21	ISU CFB Bottom Ash	50/50	Processed	3	2	4.75	27.82
22	ISU CFB Bottom Ash	50/50	Processed	3	4.750	5.00	76.84
23	ISU CFB Bottom Ash	50/50	Processed	3	0.425	6.00	50.81
24	ISU CFB Bottom Ash	50/50	Processed	3	0.150	5.00	49.74
25	ISU CFB Stoker Fly Ash	50/50	Processed	3	---	8.50	25.12
26	Scrap Material	3% fiberglass added to the mixture				5.50	72.74
27	Scrap Material	No extra fiberglass was added to the mixture				5.25	38.43
28	ISU Stoker Bottom Ash	50/50	Processed	3	2	6.00	39.46
30	Processed RPET	100/0	Processed	3	---	8.25	21.65

Table C.2 Pipe specimen dimensions

Pipe	Height (m)	Smallest Top Thickness (mm)	Largest Top Thickness (mm)	Smallest Bottom Thickness (mm)	Largest Bottom Thickness (mm)	Average Thickness (mm)	Average Area (m ²)
1	Pipe was not measured due to manufacturing problems						
2	Pipe was not measured due to manufacturing problems						
3	0.2572	37.21	40.03	46.00	46.00	37.71	0.0324
4	0.2572	29.46	43.94	49.40	49.40	37.50	0.0322
5	0.2540	27.89	44.81	44.96	44.96	37.00	0.0319
6	0.2635	35.18	42.55	45.72	45.72	38.86	0.0332
7	0.2604	34.98	44.58	39.32	39.32	38.54	0.0330
8	0.2604	31.62	42.72	42.82	42.82	37.15	0.0320
9	0.2540	30.33	39.37	41.91	41.91	35.90	0.0310
10	Pipe was not measured due to manufacturing problems						
11	0.2572	30.61	38.33	39.50	39.50	35.68	0.0309
12	0.2540	21.79	38.48	41.40	41.40	34.00	0.0296
13	0.2540	33.78	37.72	40.34	40.34	36.79	0.0317
14	0.2572	28.98	38.23	40.74	40.74	35.38	0.0307
15	0.2572	31.67	36.83	41.02	41.02	35.79	0.0310
16	0.2572	32.89	38.05	40.28	40.28	35.95	0.0311
17	0.2540	31.85	37.90	40.01	40.01	36.87	0.0318
18	0.2572	28.60	44.65	47.02	47.02	36.83	0.0317
19	0.2572	32.87	41.25	45.67	45.67	38.30	0.0328
20	0.2572	37.72	41.96	42.24	42.24	39.42	0.0337
21	0.2667	38.46	49.05	43.21	43.21	42.88	0.0361
22	0.2604	31.62	41.17	46.48	46.48	39.08	0.0334
23	0.2604	34.44	39.14	39.32	39.32	36.94	0.0318
24	0.2572	36.88	40.03	43.18	43.18	39.25	0.0335
25	0.2159	33.32	37.69	39.60	39.60	35.88	0.0310
26	0.2572	27.05	38.63	44.45	44.45	35.71	0.0309
27	0.2572	35.00	38.76	39.01	39.01	36.69	0.0316
28	0.2572	32.74	37.13	40.77	40.77	36.55	0.0315
29	0.2572	33.55	36.20	38.53	38.53	35.78	0.0310
30	0.2540	32.94	38.74	43.92	43.92	36.36	0.0314
31	0.2572	33.71	37.13	41.76	41.76	36.33	0.0314

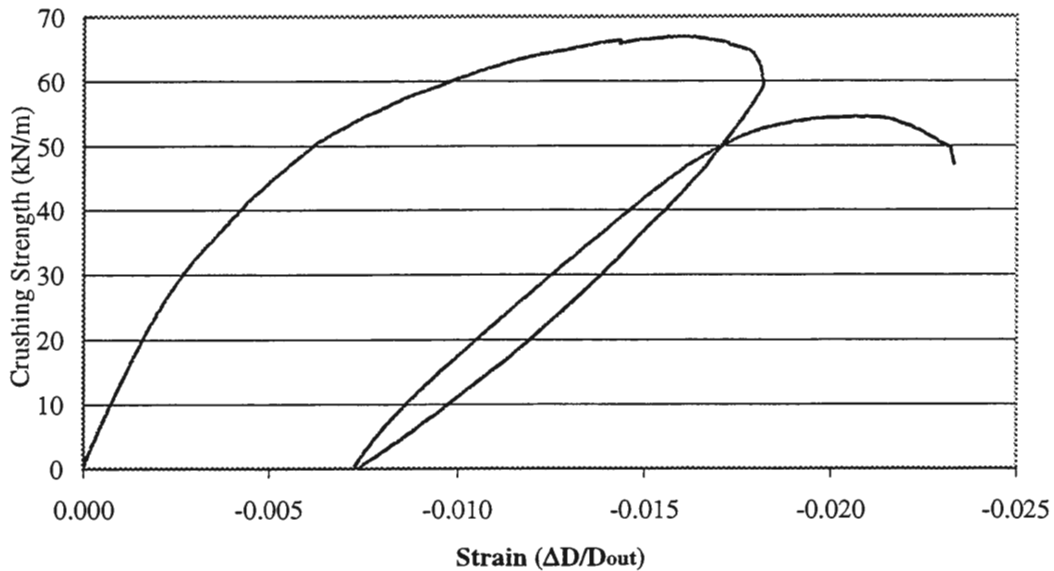


Figure C.1 Pipe specimen # 3, crushing strength vs. strain for P. C. fly ash, 3% fiberglass by weight with 50/50 PET to filler ratio by weight, (load, unload, load to failure)

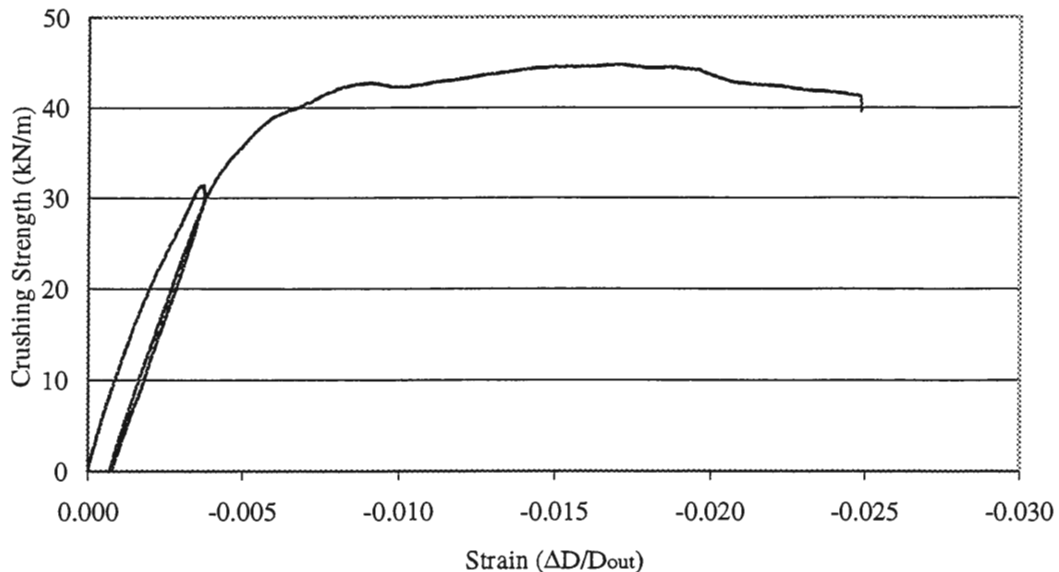


Figure C.2 Pipe specimen # 4, crushing strength vs. strain for P. C. fly ash, 3% fiberglass by weight with 50/50 PET to filler ratio by weight, (load to 75% ultimate strength, unload, load to failure)

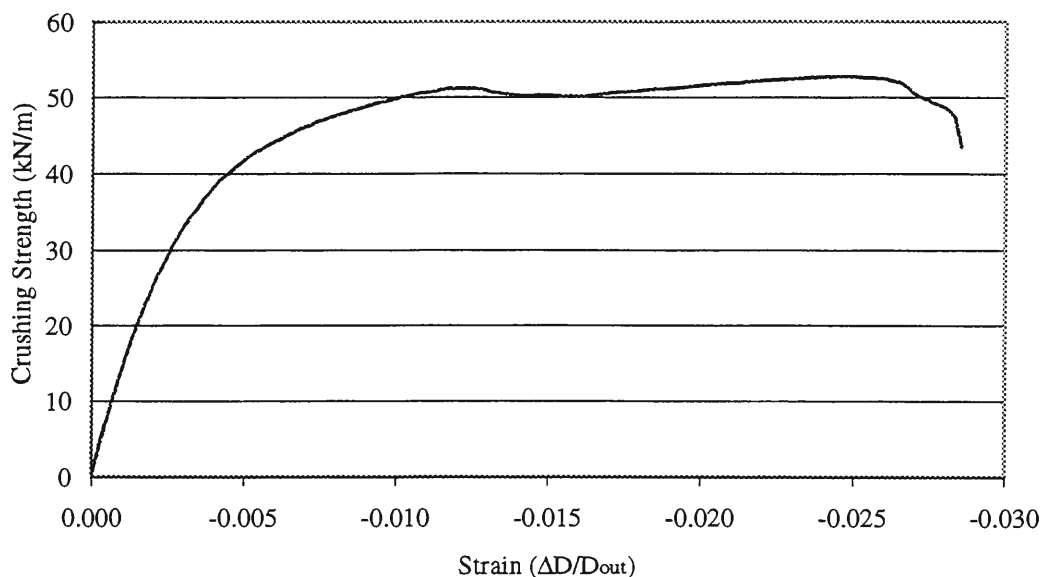


Figure C.3 Pipe specimen # 5, crushing strength vs. strain for P. C. fly ash, and 3% fiberglass by weight with 50/50 PET to filler ratio by weight

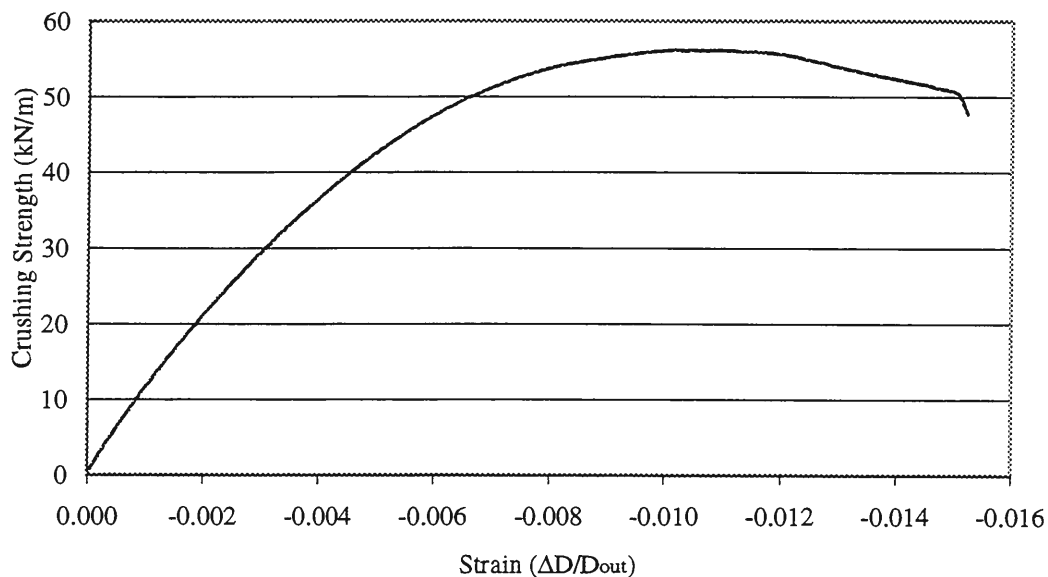


Figure C.4 Pipe specimen # 6, crushing strength vs. strain for UNI fluidized bed ash, and 3% fiberglass by weight with 50/50 PET to filler ratio by weight

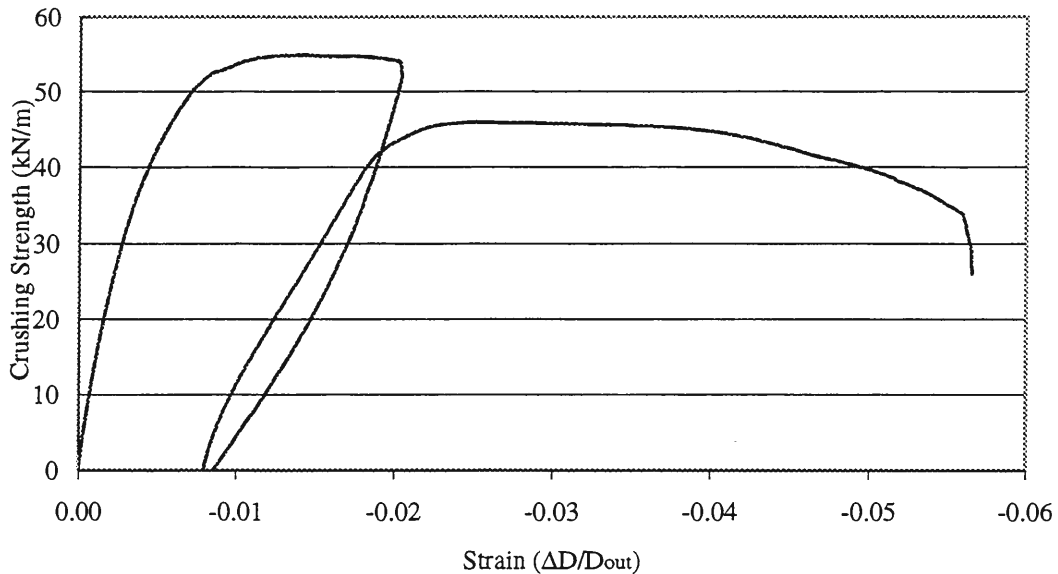


Figure C.5 Pipe specimen # 7, crushing strength vs. strain for UNI fluidized bed ash, 3% fiberglass by weight with 50/50 PET to filler ratio by weight, largest size particles 2 mm, (load, unload, load to failure)

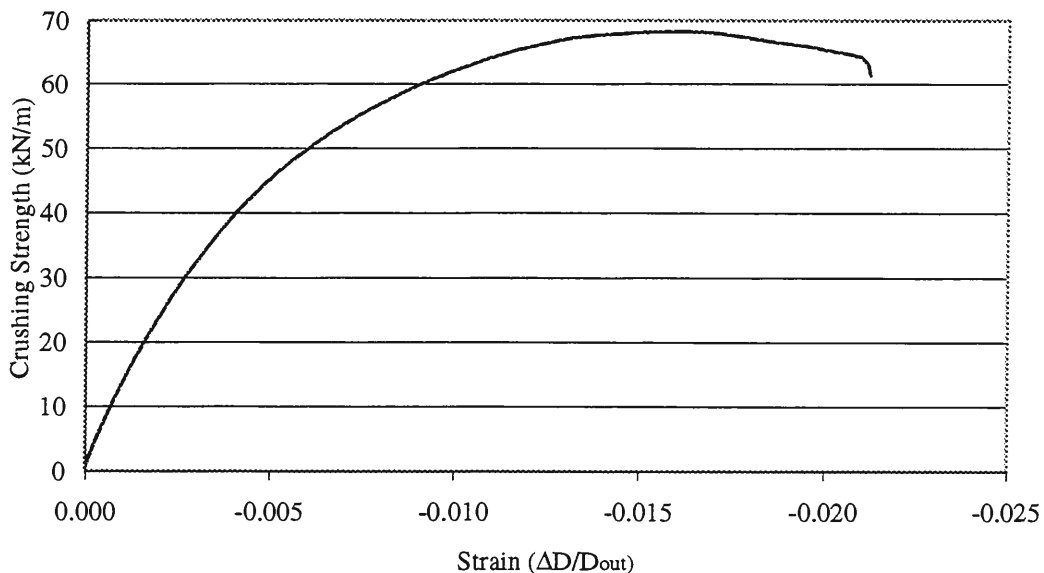


Figure C.6 Pipe specimen # 8, crushing strength vs. strain for UNI fluidized bed ash, and 3% fiberglass by weight with 50/50 PET to filler ratio by weight, largest size particles 2 mm

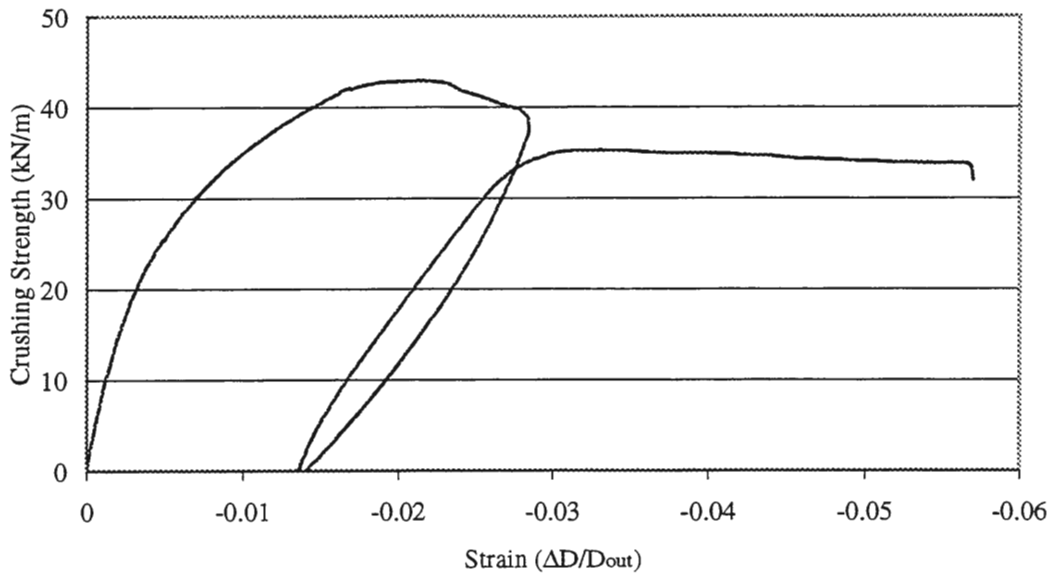


Figure C.7 Pipe specimen # 9, crushing strength vs. strain for lime, and 3% fiberglass by weight with 50/50 PET to filler ratio by weight, largest size particles 2 mm

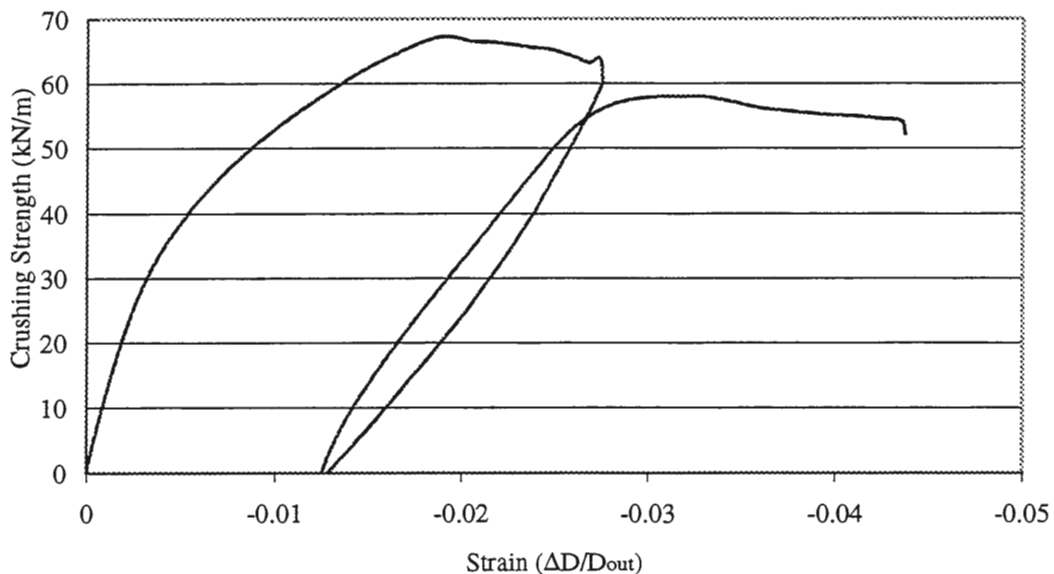


Figure C.8 Pipe specimen # 11, crushing strength vs. strain for lime, and 3.5% fiberglass by weight with 50/50 PET to filler ratio by weight, largest size particles 2 mm, (loading, unloading, and loading to failure)

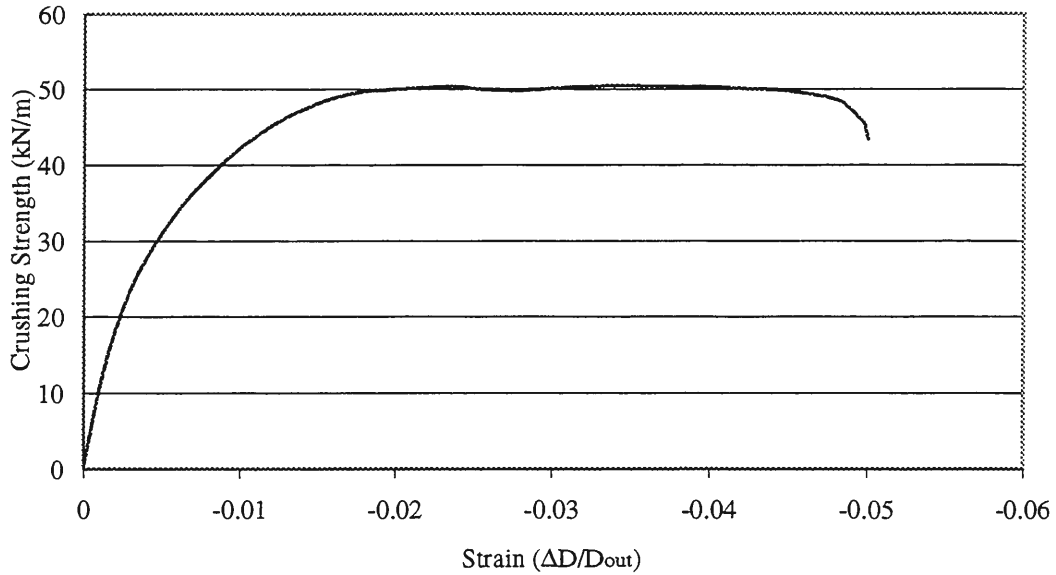


Figure C.9 Pipe specimen # 12, crushing strength vs. strain for lime, and 4% fiberglass by weight with 50/50 PET to filler ratio by weight, largest size particles 2 mm

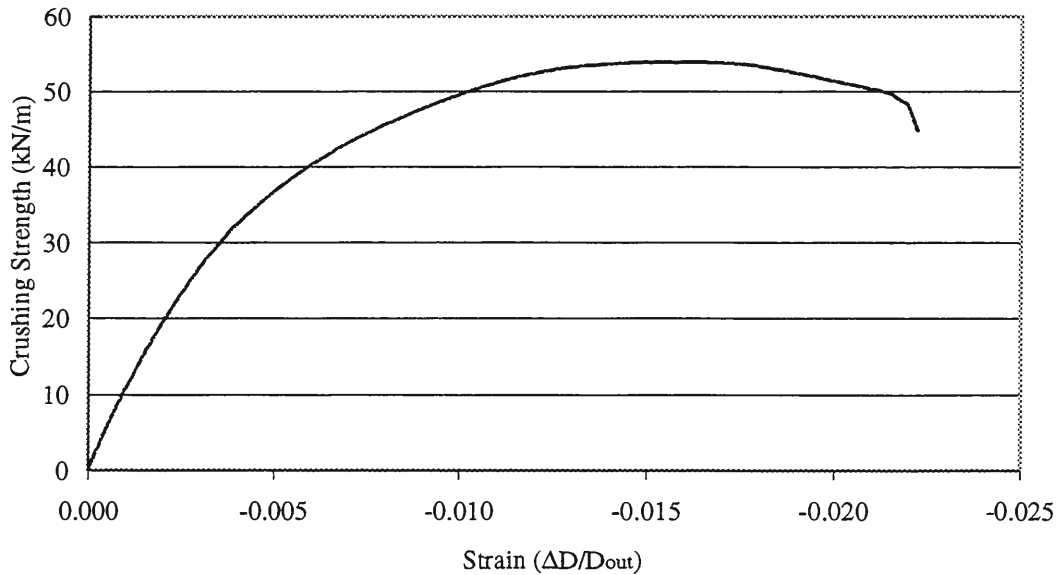


Figure C.10 Pipe specimen # 13, crushing strength vs. strain for Ames fly ash, 3% fiberglass by weight with 50/50 PET to filler ratio by weight, “dirty” PET

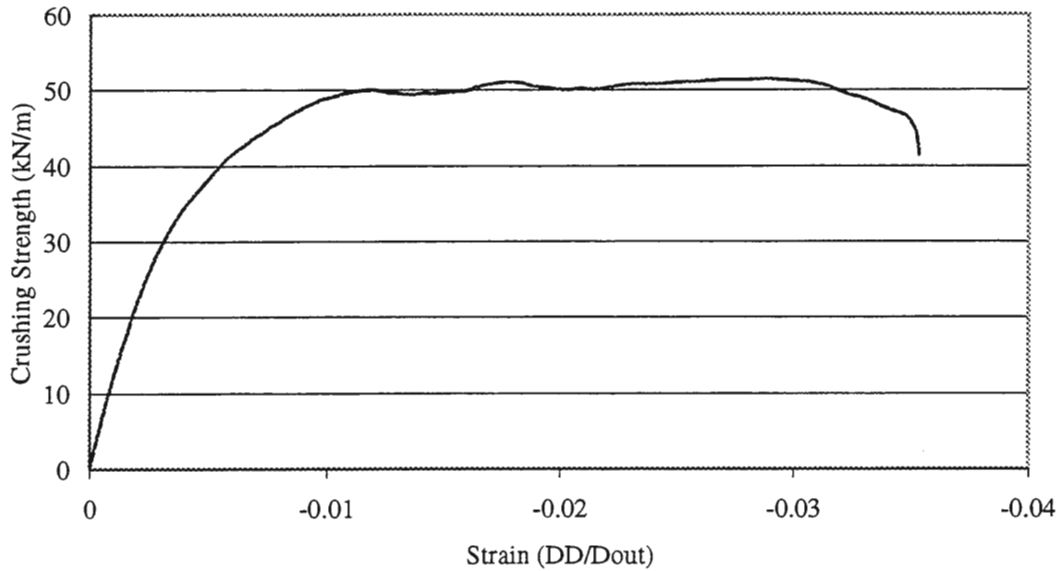


Figure C.11 Pipe specimen # 14, crushing strength vs. strain for Ames fly ash, 3% fiberglass by weight with 50/50 PET to filler ratio by weight, “processed” PET

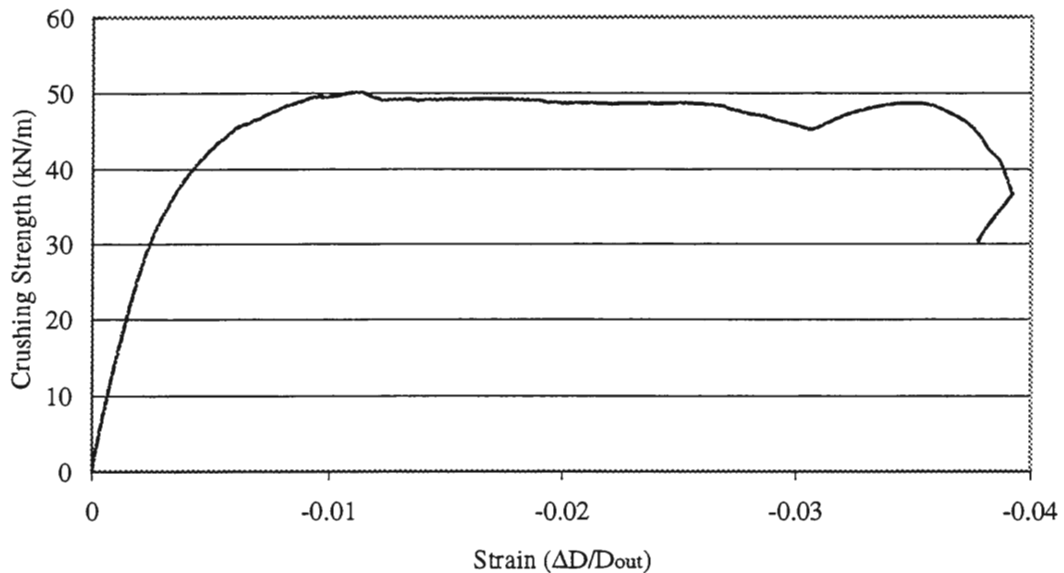


Figure C.12 Pipe specimen # 15, crushing strength vs. strain for Ames fly ash, 3% fiberglass by weight with 50/50 PET to filler ratio by weight, “clean” PET

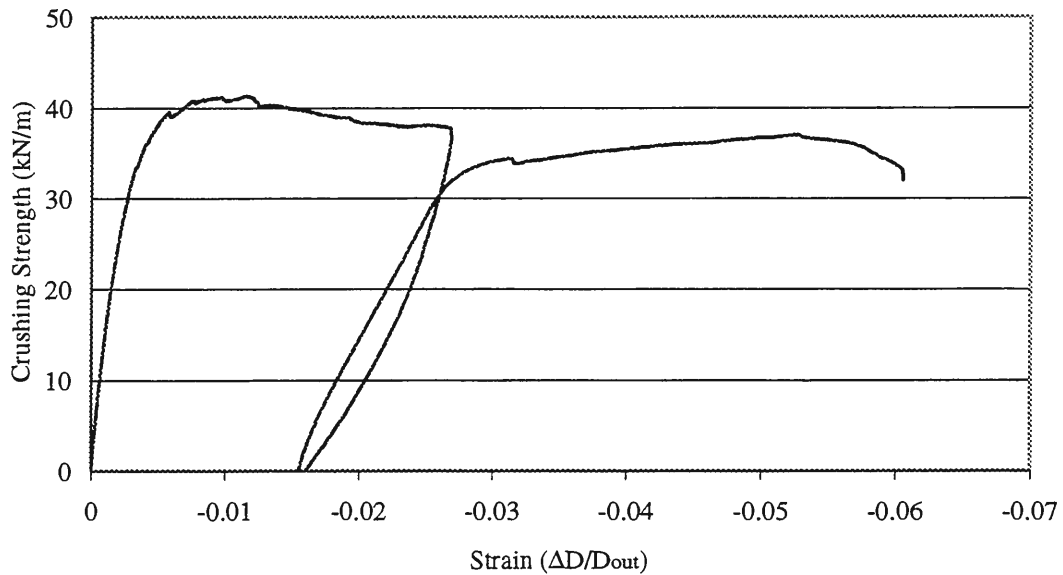


Figure C.13 Pipe specimen # 16, crushing strength vs. strain for sump, and 3% fiberglass by weight with 50/50 PET to filler ratio by weight, largest particle size 0.150 mm

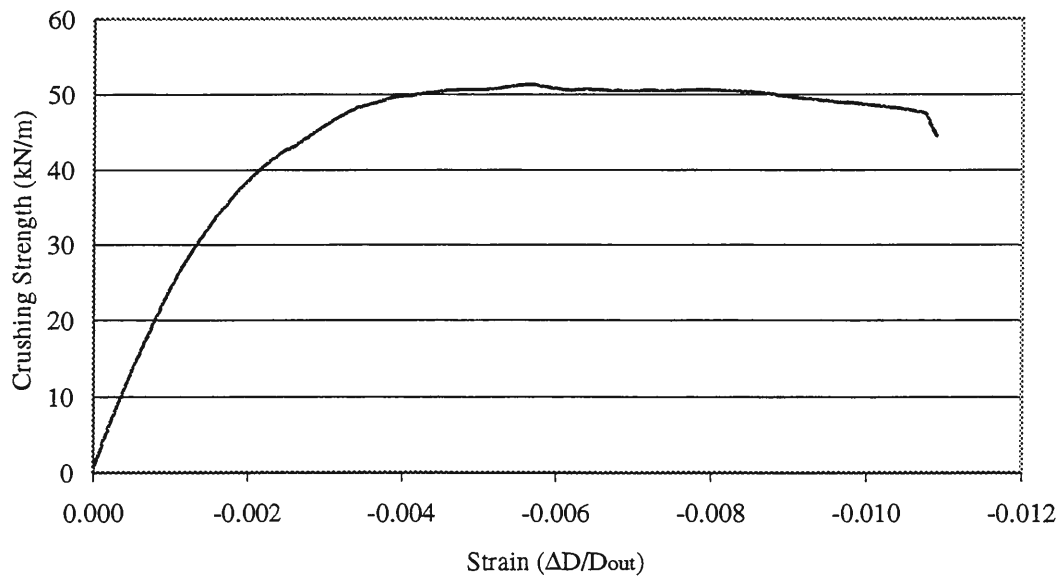


Figure C.14 Pipe specimen # 17, crushing strength vs. strain for ISU CFB fly ash, and 3% fiberglass by weight with 50/50 PET to filler ratio by weight

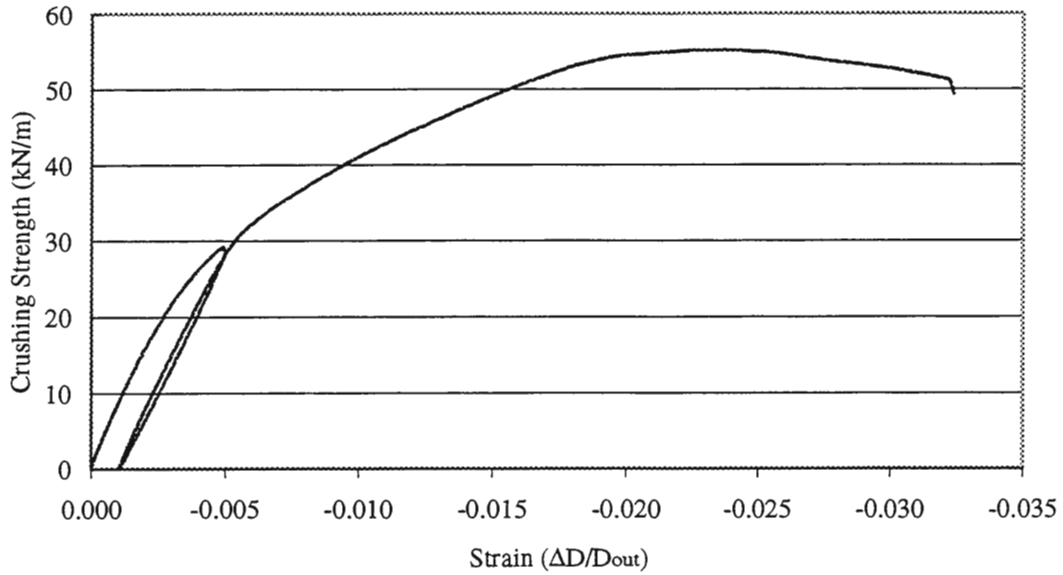


Figure C.15 Pipe specimen # 18, crushing strength vs. strain for lime, 4% fiberglass by weight with 50/50 PET to filler ratio by weight, largest particle size 2 mm, (load to 75% of ultimate strength, unload, load to failure)

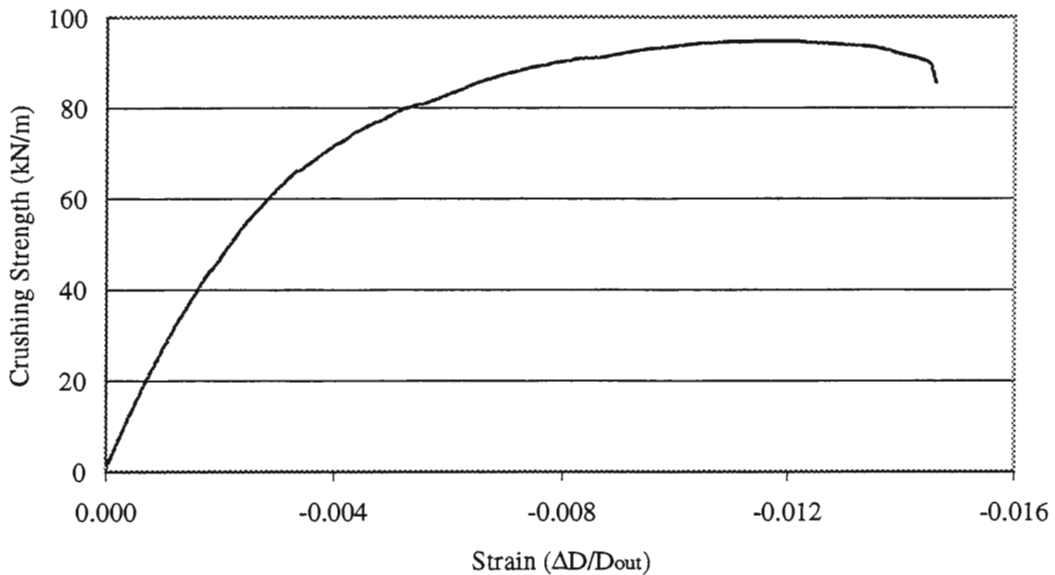


Figure C.16 Pipe specimen # 19, crushing strength vs. strain for UNI fluidized bed ash, and 3% fiberglass by weight with 40/60 PET to filler ratio by weight, largest particle size 2 mm

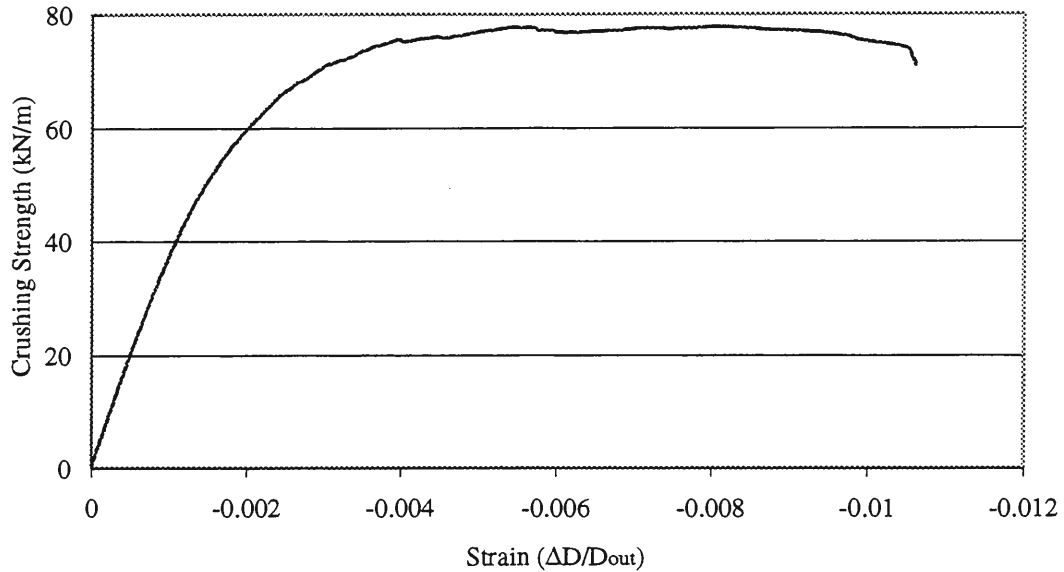


Figure C.17 Pipe specimen # 20, crushing strength vs. strain for UNI fluidized bed ash, and 3% fiberglass by weight with 33/67 PET to filler ratio by weight, largest particle size 2 mm

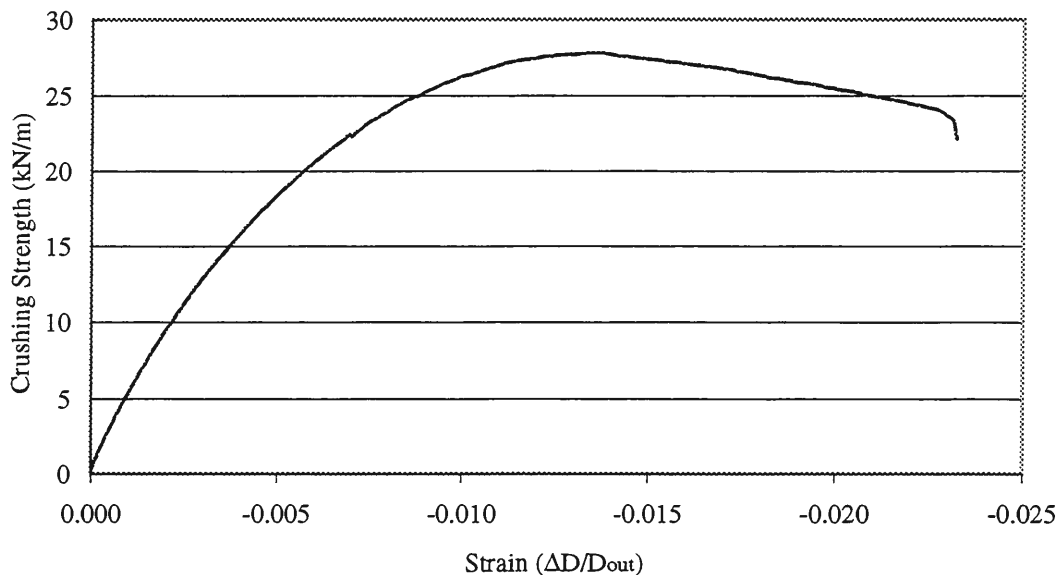


Figure C.18 Pipe specimen # 21, crushing strength vs. strain for ISU CFB bottom ash, and 3% fiberglass by weight with 50/50 PET to filler ratio by weight, largest particle size 2 mm

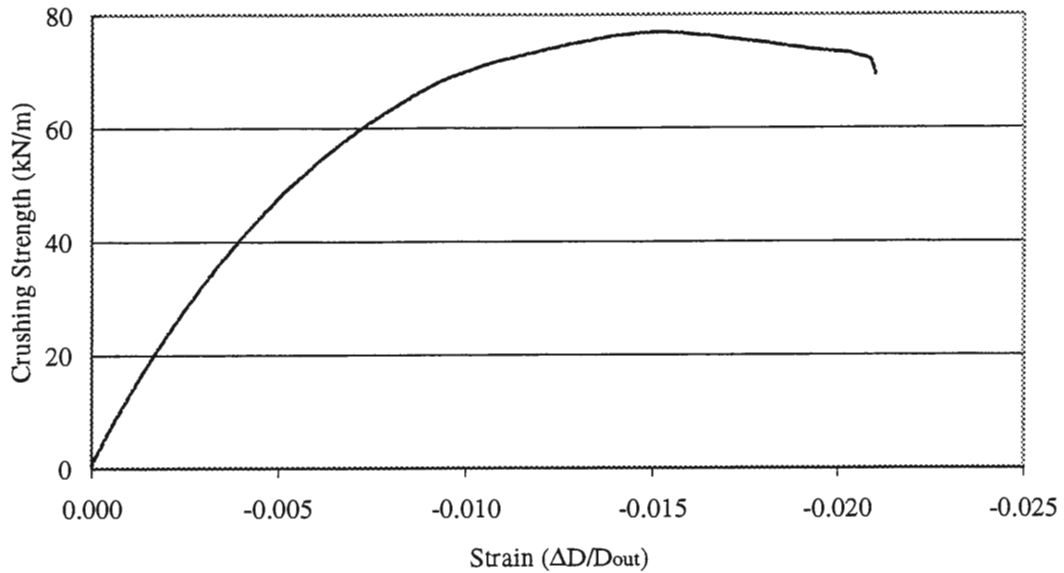


Figure C.19 Pipe specimen # 22, crushing strength vs. strain for ISU CFB bottom ash, and 3% fiberglass by weight with 50/50 PET to filler ratio by weight, largest particle size 4.75 mm

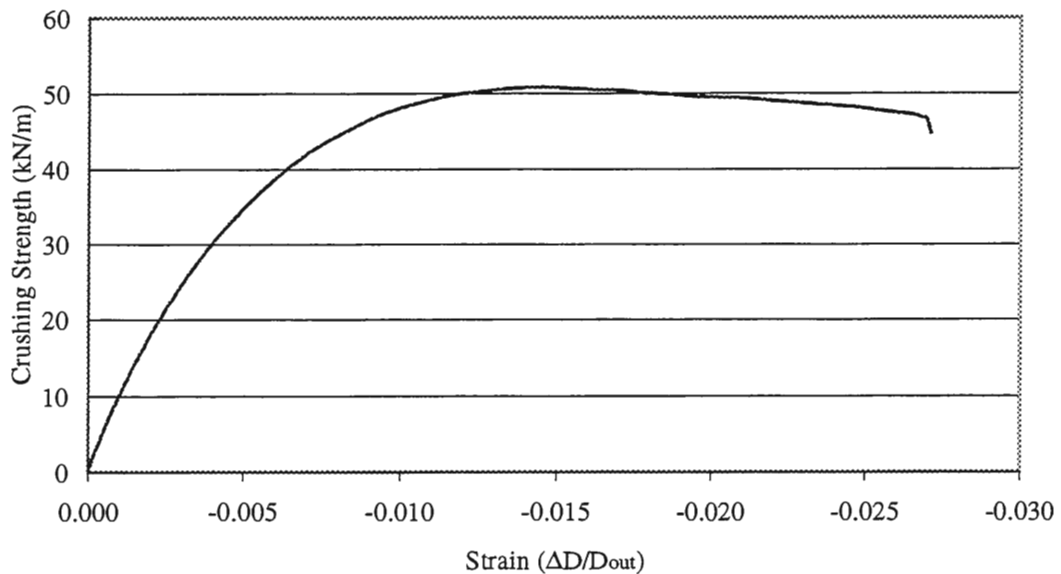


Figure C.20 Pipe specimen # 23, crushing strength vs. strain for ISU CFB bottom ash, and 3% fiberglass by weight with 50/50 PET to filler ratio by weight, largest particle size 0.425 mm

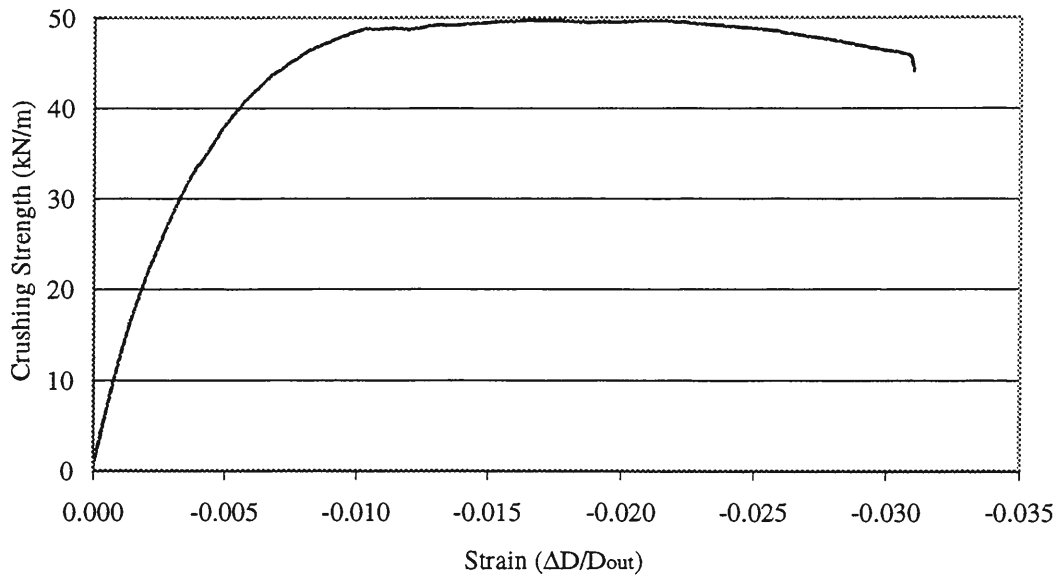


Figure C.21 Pipe specimen # 24, crushing strength vs. strain for ISU CFB bottom ash, and 3% fiberglass by weight with 50/50 PET to filler ratio by weight, largest particle size 0.150 mm

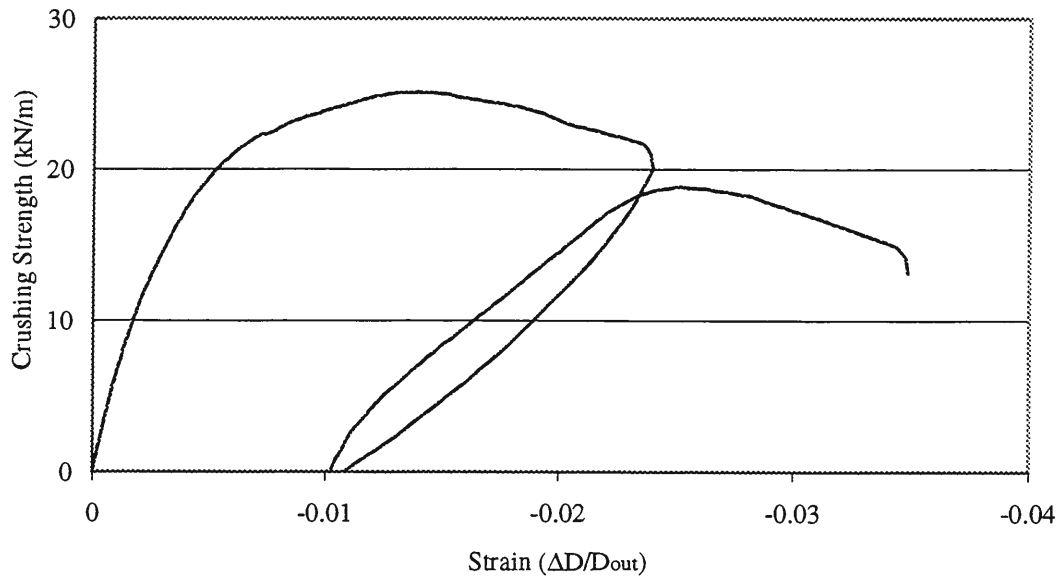


Figure C.22 Pipe specimen # 25, crushing strength vs. strain for ISU stoker fly ash, 3% fiberglass by weight with 50/50 PET to filler ratio by weight, (load, unload, load to failure)

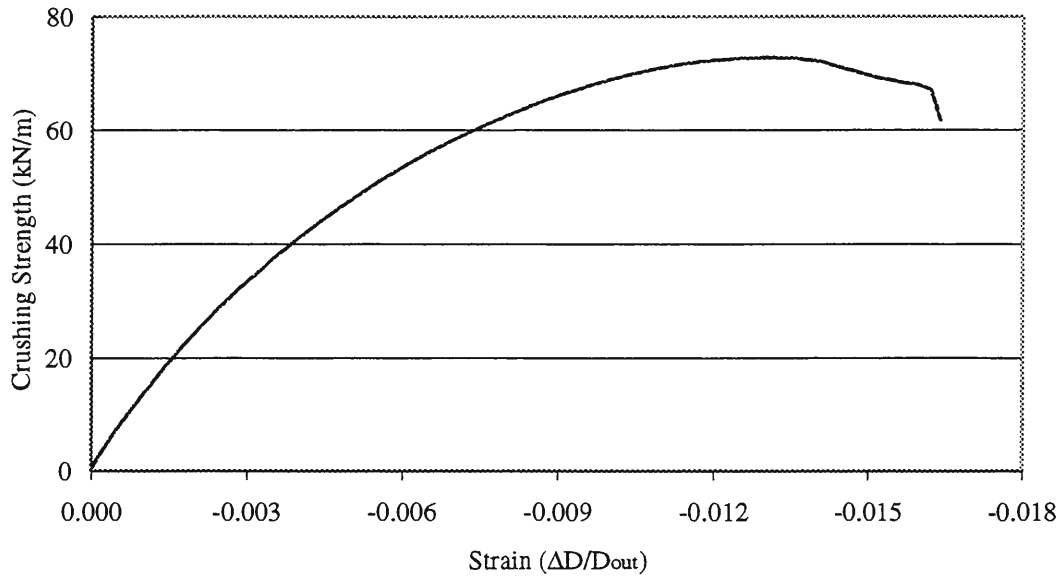


Figure C.23 Pipe specimen # 26 crushing strength vs. strain for crushed material, additional 3% fiberglass added by weight with 50/50 PET to filler ratio by weight

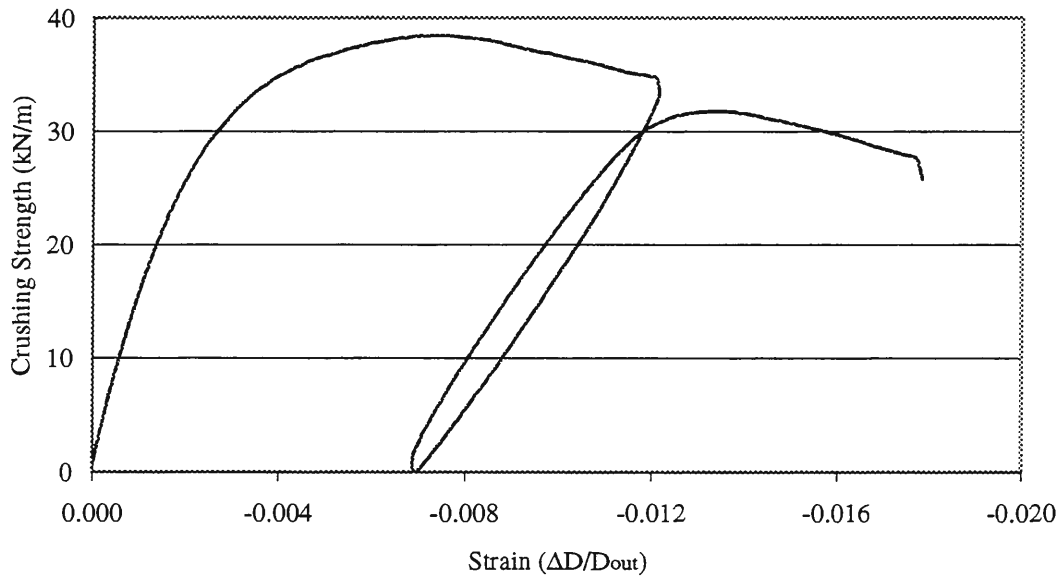


Figure C.24 Pipe specimen # 27 crushing strength vs. strain for crushed material, no additional fiberglass added with 50/50 PET to filler ratio by weight (load, unload, load to failure)

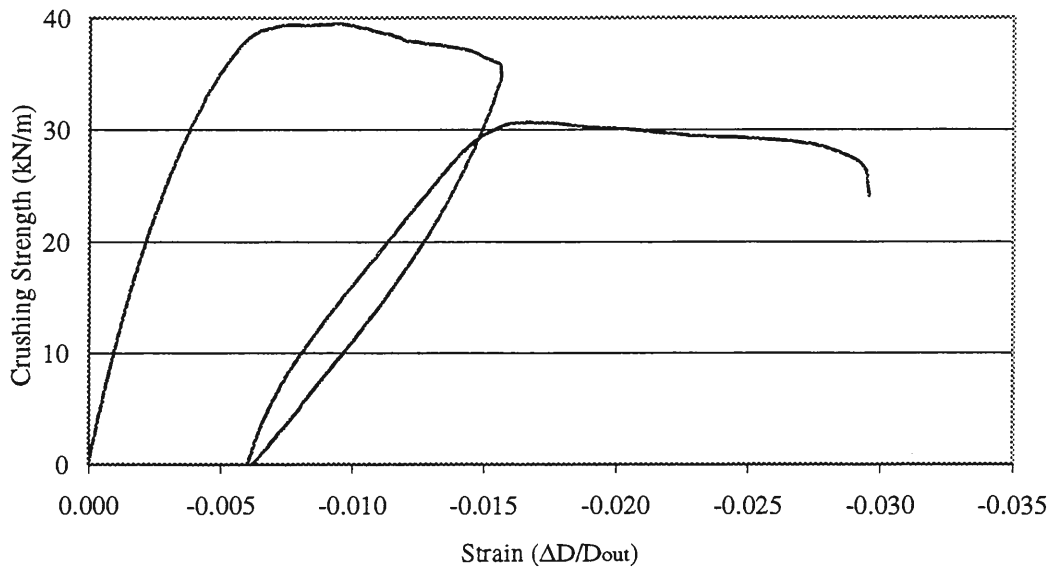


Figure C.25 Pipe specimen # 28 crushing strength vs. strain for ISU stoker bottom ash, crushed, 3% fiberglass by weight with 50/50 PET to filler ratio by weight, largest particle size 2 mm, (load, unload, load to failure)

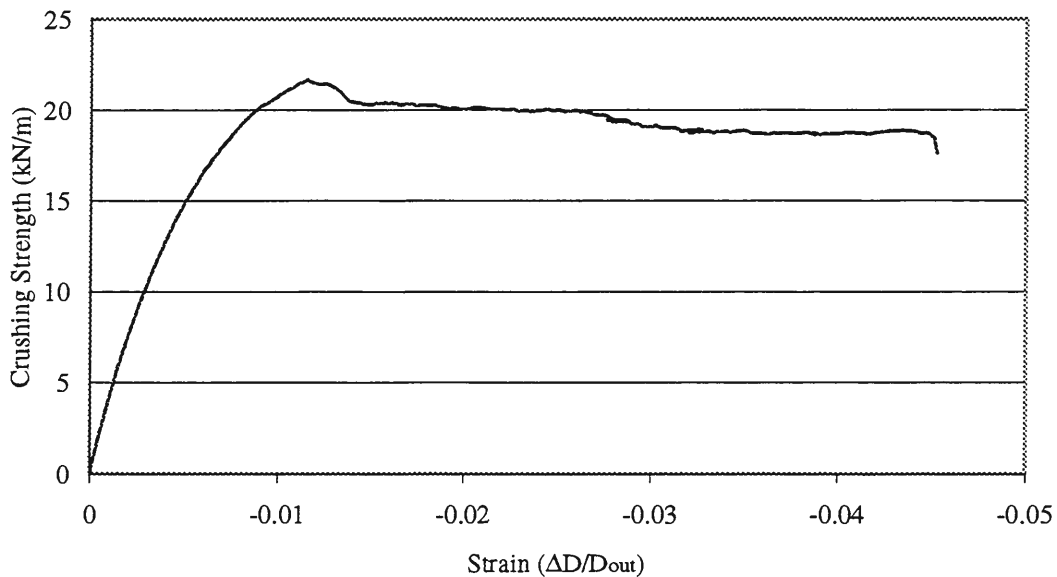
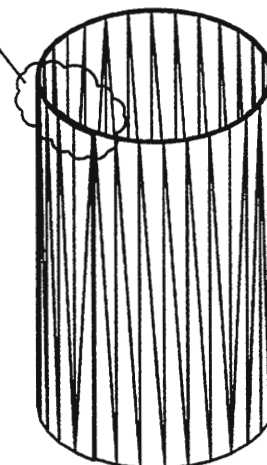
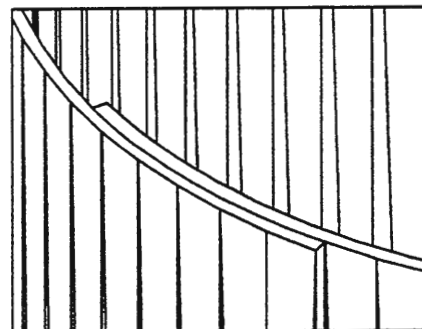
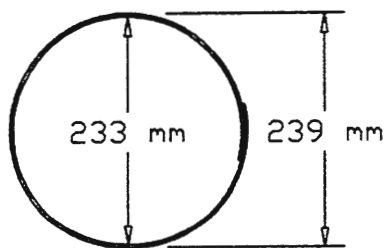
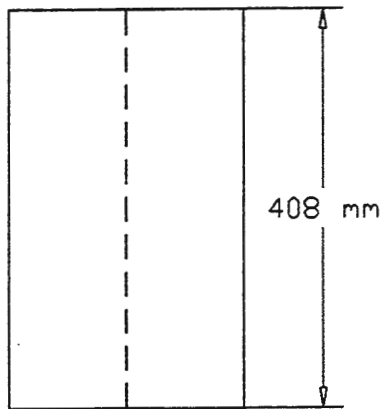
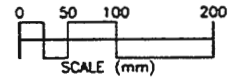
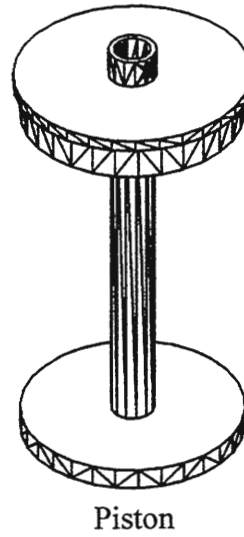
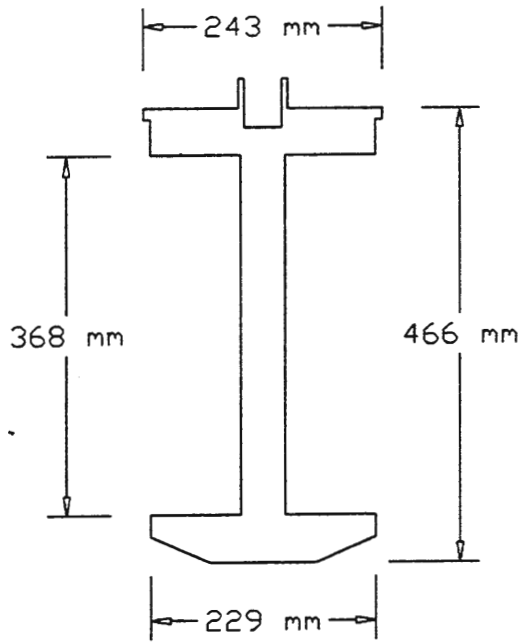
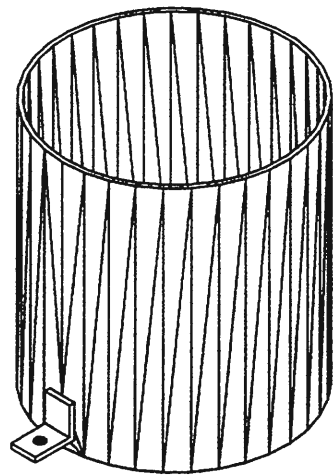
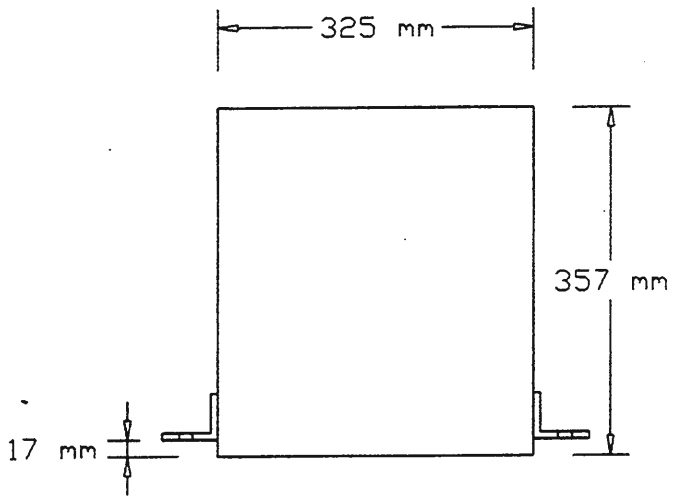


Figure C.26 Pipe specimen # 30 crushing strength vs. strain for “processed PET, 3% fiberglass by weight with 100/0 PET to filler ratio by weight

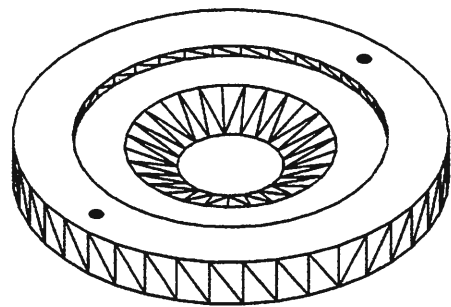
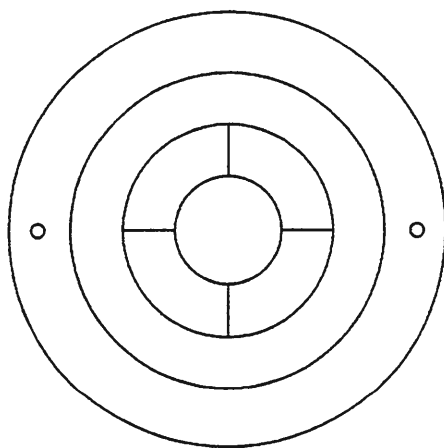
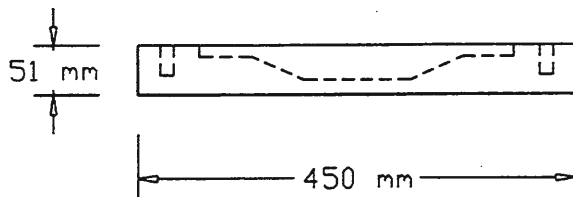
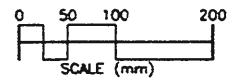


Inner collapsible mold

Figure C.27 Piston and inner collapsible mold



Outer cylinder mold



Bottom plate

Figure C.28 Outer mold and bottom plate

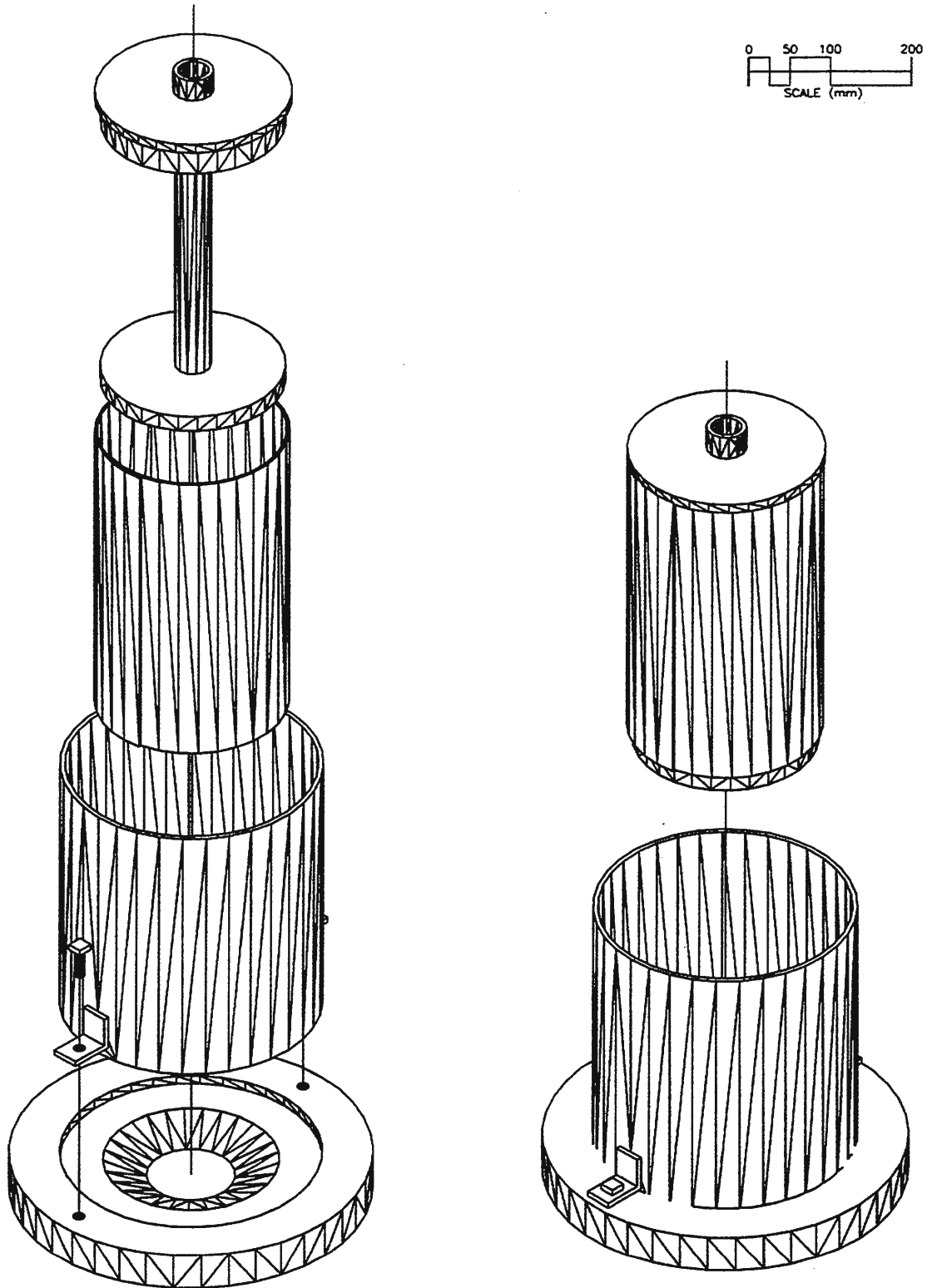


Figure C.29 Mold setup

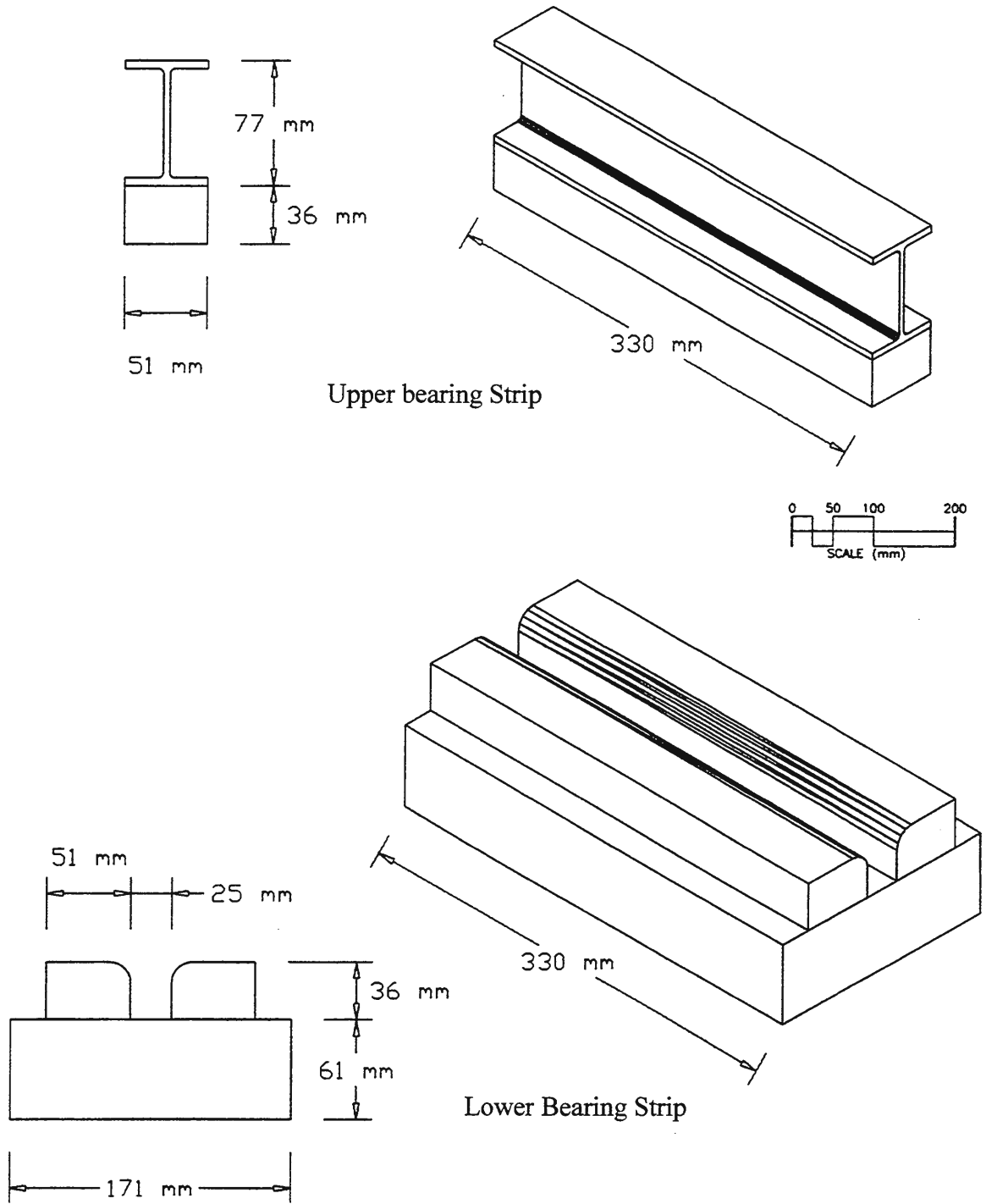


Figure C.30 Upper and lower bearing strips

APPENDIX D: DURABILITY DATA

Table D.1 Water Absorption data

Sample	Mass (g)	Thickness (mm)	Week 1 Adsorption (g)	Week 3 Absorption (g)	Week 5 Absorption (g)	Week 7 Absorption (g)	Water Absorbed (%)
1	24.22	7.366	0.64	0.77	0.96	1.12	4.62
4	27.62	8.458	1.47	2.16	2.40	2.37	8.58
8	25.87	7.747	0.62	0.80	1.01	1.16	4.48
10	24.77	6.985	0.48	0.74	0.94	1.00	4.04
11	23.53	6.401	0.50	0.75	0.89	0.94	3.99
13	24.32	6.452	0.60	0.98	1.29	1.40	5.76
16	27.16	8.103	0.26	0.46	0.77	1.03	3.79
17	24.54	7.087	0.58	0.82	1.01	1.08	4.40
19	20.18	6.248	0.67	0.78	0.99	1.02	5.05
22	23.56	7.188	1.58	2.44	2.47	2.51	10.65
24	22.82	7.137	0.66	0.81	1.11	1.20	5.26
26	29.40	8.306	0.61	0.89	1.05	1.10	3.74
28	23.87	7.239	0.57	0.73	0.80	0.85	3.56
29	24.61	7.137	0.67	0.82	0.91	0.96	3.90
31	24.69	7.036	0.68	0.83	0.99	1.01	4.09
33	25.87	7.442	0.86	1.03	1.14	1.21	4.68
36	23.82	6.706	0.58	0.79	0.93	0.97	4.07
38	12.35	5.131	0.22	0.25	0.44	0.55	4.45
39	17.57	6.071	0.96	0.97	1.17	1.26	7.17
42	22.27	6.807	2.62	2.16	2.57	2.27	11.76
44	26.67	8.026	3.25	2.82	3.07	2.66	12.19
46	25.64	7.417	2.95	2.84	3.17	2.95	12.36
47	26.17	7.442	0.13	0.28	0.38	0.47	1.80

Table D.2 Specimen dimensions prior to acid tests

Sample	Weight (g)	Thickness (mm)	Diameter 1 (mm)	Diameter 2 (mm)
1	27.99	8.179	51.435	51.054
4	22.37	6.756	48.438	51.765
5	25.14	7.671	51.181	51.054
8	26.45	7.823	51.384	51.257
10	23.54	6.985	50.851	50.876
11	27.19	7.315	51.257	51.130
13	28.25	7.391	51.587	51.359
16	22.23	6.502	51.765	51.816
17	23.38	6.528	51.029	51.130
19	27.81	8.103	51.105	51.054
22	23.36	6.934	52.146	51.511
24	24.61	7.671	51.562	52.070
26	26.38	7.518	51.308	51.308
28	28.91	8.001	51.740	51.308
29	22.57	6.477	51.359	51.283
31	25.42	7.036	51.689	51.435
33	23.38	6.858	51.283	51.359
36	24.85	6.934	51.689	51.587
38	16.77	6.782	51.435	51.384
39	22.95	7.391	51.714	51.714
42	22.31	6.401	53.213	53.162
44	19.98	5.182	54.204	53.873
46	20.33	6.350	53.721	54.102
47	28.30	8.433	51.359	51.359

Table D.3 Acid test results for week 1

Sample	Weight (g)	Thickness (mm)	Diameter 1 (mm)	Diameter 2 (mm)	Comments
1	28.44	8.230	51.765	51.740	
4	22.68	6.680	49.022	52.349	Side Chipped
5	25.14	7.366	51.460	51.232	color fading
8	26.68	7.874	51.511	51.079	color fading
10	24.48	7.620	52.070	51.740	color fading
11	27.83	7.798	51.689	51.613	color fading
13	29.20	8.001	51.892	52.019	color fading
16	22.55	6.350	52.019	52.019	color fading
17	23.48	6.756	51.257	52.019	color fading
19	28.16	8.077	51.867	51.257	color fading
22	24.41	6.909	52.451	51.943	
24	24.89	7.518	51.689	52.248	
26	26.89	7.417	51.943	51.613	Dropped and it broke
28	29.24	8.001	52.070	51.689	color fading
29	23.17	6.375	51.791	51.943	color fading
31	25.82	7.391	52.019	51.638	color fading
33	23.86	7.010	51.765	51.892	color fading
36	25.09	6.985	52.146	51.943	color fading
38	16.90	6.731	51.740	51.638	
39	24.48	7.315	52.273	52.553	Growth
42	Specimens degraded to powdery substance				
44	Specimens degraded to powdery substance				
46	Specimens degraded to powdery substance				
47	28.48	8.255	51.562	51.689	

Table D.4 Acid test results for week 3

Sample	Weight (g)	Thickness (mm)	Diameter 1 (mm)	Diameter 2 (mm)	Comments
1	26.31	8.661	43.967	52.527	Falling apart
4	Fell apart cannot measure pieces				
5	25.29	7.468	51.587	51.511	
8	27.63	8.331	52.730	52.578	
10	Fell apart cannot measure pieces				
11	30.21	8.255	54.026	53.619	Falling apart
13	31.63	8.230	53.670	53.797	Side fell off
16	23.22	6.655	52.553	52.781	
17	24.00	6.782	51.562	51.841	
19	29.43	8.382	52.781	52.273	
22	20.00	8.001	53.594	42.570	broken 1/2 left
24	25.13	7.620	51.943	52.502	
26	Specimen was destroyed during the first week of testing				
28	30.42	8.179	52.959	52.451	
29	24.89	7.087	54.483	53.645	flakey, falling apart
31	26.90	7.137	53.010	52.959	
33	17.90	7.468			Falling apart
36	25.67	7.493	52.451	52.299	
38	16.91	6.706	51.664	51.562	
39	24.13	8.077	51.156	53.899	pieces missing
42	Specimen was destroyed during the first week of testing				
44	Specimen was destroyed during the first week of testing				
46	Specimen was destroyed during the first week of testing				
47	28.50	8.230	51.587	51.816	looks best

Table D.5 Acid test results for week 5

Sample	Weight (g)	Thickness (mm)	Diameter 1 (mm)	Diameter 2 (mm)	Comments
1					Fell apart cannot measure pieces
4					Specimen was destroyed during the third week of testing
5	25.53	7.417	51.816	51.460	sides starting to crack
8					Fell apart cannot measure pieces
10					Specimen was destroyed during the third week of testing
11					Fell apart cannot measure pieces
13					Fell apart cannot measure pieces
16	24.09	7.772	53.416	54.737	Starting to crack
17	24.65	5.994	52.172	52.629	sides starting to crack
19					Fell apart cannot measure pieces
22					Fell apart cannot measure pieces
24	25.23	7.620	51.943	52.832	looks good
26					Specimen was destroyed during the first week of testing
28					Fell apart cannot measure pieces
29					Fell apart cannot measure pieces
31					Fell apart cannot measure pieces
33					Fell apart cannot measure pieces
36	26.55	7.087	52.781	52.781	edge coming apart
38	16.99	6.909	51.943	51.816	
39					Fell apart cannot measure pieces
42					Specimen was destroyed during the first week of testing
44					Specimen was destroyed during the first week of testing
46					Specimen was destroyed during the first week of testing
47	28.52	8.433	51.613	51.816	Looks the best

Table D.6 Acid test results for week 7

Sample	Weight (g)	Thickness (mm)	Diameter 1 (mm)	Diameter 2 (mm)	Comments
1					Specimen was destroyed during the fifth week of testing
4					Specimen was destroyed during the third week of testing
5	25.87	7.696	52.121	51.689	sides starting to crack
8					Specimen was destroyed during the fifth week of testing
10					Specimen was destroyed during the third week of testing
11					Specimen was destroyed during the fifth week of testing
13					Specimen was destroyed during the fifth week of testing
16					Specimen was destroyed during the fifth week of testing
17	23.42	7.290	52.934	53.492	pieces fell off while drying
19					Specimen was destroyed during the fifth week of testing
22					Specimen was destroyed during the fifth week of testing
24	25.45	7.696	52.019	52.959	slight crack
26					Specimen was destroyed during the first week of testing
28					Specimen was destroyed during the fifth week of testing
29					Specimen was destroyed during the fifth week of testing
31					Specimen was destroyed during the fifth week of testing
33					Specimen was destroyed during the fifth week of testing
36	27.00	7.366	53.543	54.229	starting to crack
38	16.97	6.833	51.791	51.867	
39					Specimen was destroyed during the fifth week of testing
42					Specimen was destroyed during the first week of testing
44					Specimen was destroyed during the first week of testing
46					Specimen was destroyed during the first week of testing
47	28.53	8.255	51.511	51.714	Looks the best

REFERENCES

1. White, David J., Evaluation of Composite Material from High-Lime Fly Ash and Recycled Polyethylene Terephthalate (PET). Proc. 14th International Symposium on Management and Use of Coal Combustion Products (CCPs), Volume 2, 1998.
2. White, David J. "Microstructure of Composite Material from High-Lime Fly Ash and RPET." Journal of Materials in Civil Engineering Volume 12, No. 1 Feb 2000: 60-65.
3. "Municipal Solid Waste in the United States: 1999 Facts and Figures Executive Summary," online, Environmental Protection Agency. Date accessed July 1, 2002. available: www.epa.gov/epaoswer/non-hm/muncpl/pubs/excsum99.pdf.
4. Ehrig, R. J., ed. Plastics Recycling. Munich Vienna New York: Hanser, 1992.
5. Crawford, R.J. Plastics Engineering, 3rd ed. New York: Oxford, 1998.
6. "Quarterly Report for RMRC Research Project No. #19," online, The Recycled Materials Resource Center. Date accessed Jan. 15, 2002. available: www.rmrc.unh.edu/Research/Rprojects/project19/QReports/Report2/p19q2.pdf.
7. "2000 Recycling Rate Report," online, NAPCOR. Date accessed June 29, 2002. available: www.napcor.com/rate00.html.
8. Pankaj, Varma, E. A. Lofgren, and S. A. Jabarin. "Properties and Kinetics of Thermally Crystallized Oriented Poly(Ethylene Terephthalate) (PET)." Polymer Engineering and Science Volume 38, No. 2, Feb 1998: 237-244.
9. Fann, Daw-Ming, S. K. Huang, and Jiunn-Yih Lee. "Kinetics and Thermal Crystallinity of Recycled PET. I. Dynamic Cooling Crystallization Studies on Blends Recycled with Engineering PET." Journal of Applied Polymer Science Volume 61, 1996: 1375-1385.
10. Rebeiz, K.S. "Strength and Durability Properties of Polyester Concrete Using PET and Fly Ash Wastes." Advanced Performance Materials 1996: 205-214.
11. Miller, Chaz. "PET: #1 is." Waste Age Sept. 1994: 48-61.
12. "CCP Production and Use Survey 2000 (Summary)," online, ACAA. Date accessed: June 29, 2002. available: www.aaa-usa.org/CCP%20Survey/PDF/00SurveyComplete.PDF.

13. American Coal Ash Association. "Fly Ash Facts for Highway Engineers." Report prepared for Federal Highway Administration. Report number FHWA-SA-94-081, August 1995.
14. American Society for Testing and Materials. "Standard Specification for Coal Fly Ash and Raw or Calcined Natural Pozzolan for Use as a Mineral Admixture in Concrete." ASTM C 618, Annual Book of ASTM Standards, Volume 4.02, Philadelphia, 2000: 305-308.
15. Dienhart, G. J., B. R. Stewart, and Tyson S. S, eds. Coal: Innovative Applications of Coal Combustion Products (CCPs). American Coal Ash Association, 1998.
16. "Why Reinforce Plastics with Fiber Glass," online, PPG Fiber Glass. Date accessed: June 29, 2002. available: www.ppg.com/fgs_main/default.htm.
17. Domininghaus, H. Plastic for Engineers. Hanser Publishers. 1993.
18. Chandra, S. and Ohama, Y. Polymers in Concrete. CRC Press, Inc. 1994.
19. Rebeiz, K. S., Banko, A. S., Craft, A. P. "Thermal Properties of Polymer Mortar Using Recycled PET and Fly Ash." Journal of Materials in Civil Engineering. May 1995: 129-133.
20. Rebeiz, K. S., J. W, Rosett, S. M. Nesbit, and A.P. Craft. "Tensile Properties of Polyester Mortar Using PET and Fly Ash Wastes," Chapman & Hall, 1996 1273-1275.
21. Rebeiz, K. S., Fowler, D. W., Paul, D. R. "Materials, Making Polymer Concrete with Recycled PET." Plastic Engineering. February 1991: 33-34.
22. Rebeiz, K. S., "Time-Temperature Properties of Polymer Concrete Using Recycled PET." Cement & Concrete Composites. 17 1995: 119-124.
23. Blaga, A., Beaudoin, J. J., "Canadian Building Digest CBC-242 Polymer Concrete," online. Date accessed: June 29, 2002. available: www.nrc.ca/irc/cbd/cbd242e.html.
24. Moser, A. P. Buried Pipe Design 2nd ed. McGraw-Hill Co. 2001.
25. Rosato, D. V., D. P. DiMattia, and D. V. Rosato. Designing with Plastics and Composites: A Handbook. New York, New York: 1991.
26. Willoughby, D., D. Woodson, and R. Sutherland. Plastic Piping Handbook. New York: New York, 2001.

27. American Society for Testing and Materials. "Standard Specification for Vitrified Clay Pipe, Extra Strength, Standard Strength, and Perforated," ASTM C 700-00, Annual Book of ASTM Standards, Volume 4.05, Philadelphia, 2000: 439-442.
28. "Products," online, Hanson Pipe and Products Inc. Date accessed: June 29, 2002. available: www.hansonconcreteproducts.com/pipe.asp.
29. American Society for Testing and Materials. "Standard Specification for Concrete Sewer, Storm Drain, and Culvert Pipe [Metric]," ASTM C 14M-99, Annual Book of ASTM Standards, Volume 4.05, Philadelphia, 2000: 18-21.
30. American Society for Testing and Materials. "Standard Specification for Reinforced Concrete Culvert, Storm Drain, and Sewer Pipe [Metric]," ASTM C 76M-99a, Annual Book of ASTM Standards, Volume 4.05, Philadelphia, 2000: 65-75.
31. "New environmental bioengineering projects for the undergraduate research course, ChEg 499," online. Date accessed: June 29, 2002. available: www.nd.edu/~ssaddawi/course499.htm.
32. "Designing Concrete for Special Uses," online, Graniterock Products. Date accessed: June 29, 2002. available: www.graniterock.com/products/technotes/tn723.htm.
33. American Society for Testing and Materials. "Standard Test Methods for Compressive Strength of Cylindrical Concrete Specimens," ASTM C 39M-99, Annual Book of ASTM Standards, Volume 4.05, Philadelphia, 2000: 18-22.
34. American Society for Testing and Materials. "Standard Test Methods for Splitting Tensile Strength of Cylindrical Concrete Specimens," ASTM C 496-96, Annual Book of ASTM Standards, Volume 4.05, Philadelphia, 2000: 268-271.
35. American Society for Testing and Materials. "Standard Test Methods for Concrete Pipe, Manhole Sections, or Tile [Metric]," ASTM C 497M-98, Annual Book of ASTM Standards, Volume 4.05, Philadelphia, 2000: 317-325.
36. American Society for Testing and Materials. "Standard Test Methods for Water Absorption of Plastics," ASTM D 570-98, Annual Book of ASTM Standards, Volume 8.01, Philadelphia, 2000: 32-35.
37. American Society for Testing and Materials. "Standard Practices for Evaluating the Resistance of Plastics to Chemical Reagents," ASTM D 543-95, Annual Book of ASTM Standards, Volume 8.01, Philadelphia, 2000: 25-31.